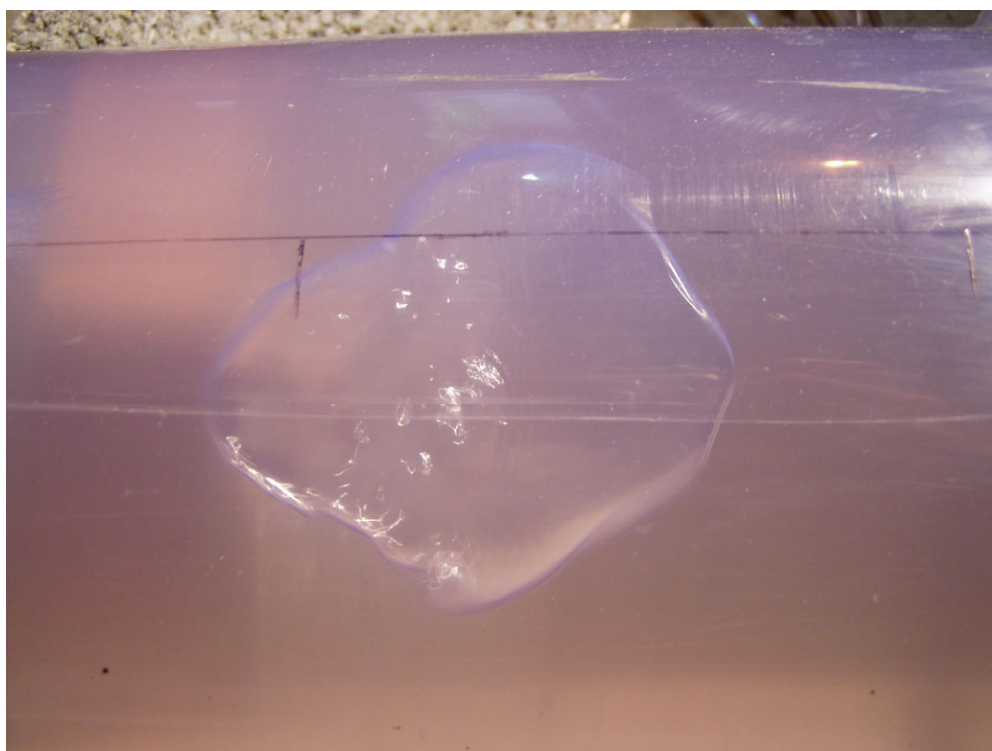


Experimental and numerical studies on movement of air in water pipelines



**M. Escarameia
C. Dabrowski
C. Gahan
C. Lauchlan**

**Report SR 661
Release 2.0
November 2004**

Document Information

Project	Guidance Manual for prevention of air problems in water pipelines
Report title	Experimental and numerical studies on movement of air in water pipelines
Client	DTI
Client Representative	Mr M Roe
Project No.	MAS 0440
Report No.	SR 661
Doc. ref.	SR661 Exp and num studies of air in water pipelines ver2.0.doc
Project Manager	M. Escameia
Project Sponsor	P Besley

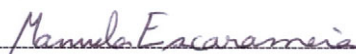
Document History

Date	Release	Prepared	Approved	Authorised	Notes
22/10/04	1.0	csl			Draft sent to S Group members for comment
29/11/04	2.0	mme	mme	pb	Includes comments from S Group members

Prepared



Approved



Authorised



© HR Wallingford Limited

This report is a contribution to research generally and it would be imprudent for third parties to rely on it in specific applications without first checking its suitability. Various sections of this report rely on data supplied by or drawn from third party sources. HR Wallingford accepts no liability for loss or damage suffered by the client or third parties as a result of errors or inaccuracies in such third party data. HR Wallingford will only accept responsibility for the use of its material in specific projects where it has been engaged to advise upon a specific commission and given the opportunity to express a view on the reliability of the material for the particular applications.

Summary

Experimental and numerical studies on movement of air in water pipelines

M. Escarameia
C. Dabrowski
C. Gahan
C. Lauchlan

Report SR 661
November 2004

This report is the second output on research into air problems in pipelines and follows a comprehensive literature review (Lauchlan et al, 2004). It describes experimental and numerical studies that were conducted to enable the development of design guidance on how to minimise the negative effects of the presence of air pockets in pipes, particularly for mild slopes.

The report describes the design of a test facility, its operation, tests carried out and the development of design formulae on critical flow velocity for air pocket movement and on the rate of expulsion of air through hydraulic jumps. Findings are also described on air pocket velocity, bubble velocity downstream of hydraulic jumps and on other characteristics associated with hydraulic jumps, and on the effect of air pockets on the hydraulic gradient. The tests were carried out in a 150mm internal diameter pipe at slopes varying between 0 and 22.5 degrees but, in view of past research findings, the present results can be taken as generally valid for slopes up to about 40 degrees.

In the numerical study, air pockets of varying size and their location within a pipeline profile were investigated to determine their effects on hydraulic transients. The pipeline tested was based on a real sewerage pipeline in the UK, consisting of a sewer rising main connected to a downstream gravity sewer. Air pockets of various volumes (0.001m^3 to 1.0m^3) were placed at sequential junctions along the pipeline profile. It was found that, in certain circumstances, the presence of air pockets can cause both high and low pressure fluctuations which are sufficiently large to potentially cause pipeline failure. Suggestions are made as to the critical conditions in a pipeline for adverse air pocket effects on hydraulic transients.

Acknowledgements

The authors are very grateful for the valuable comments received from the members of the Steering Group. Acknowledgement is also due to Mr Richard May, recently retired from HR Wallingford for his general guidance during the design of the test rig, to Mr Phil Hollinrake for his role in the practical aspects of design of the experimental facility and supervision of its construction, and to Mr Kasay Asmeron for his help with the testing.

Contents

<i>Title page</i>	<i>i</i>
<i>Document Information</i>	<i>ii</i>
<i>Summary</i>	<i>iii</i>
<i>Acknowledgements</i>	<i>v</i>
<i>Contents</i>	<i>vii</i>
1. Background	1
2. Design of test facility	1
3. Description of test facility	3
4. Instrumentation	6
5. Laboratory tests	8
5.1 Test procedure	8
5.2 Test data	9
5.2.1 Downward slopes	9
5.2.2 Upward slopes	12
5.3 Data analysis	12
6. Analysis of results	13
6.1 Critical flow velocity	13
6.2 Air pocket velocity	17
6.3 Head loss	19
6.4 Hydraulic jumps	20
7. Numerical studies	21
7.1 Background	22
7.1.1 Pressure transients	22
7.1.2 Entrapped air	22
7.2 Computational model	23
7.3 Simulation procedure	24
7.3.1 Background	24
7.3.2 Model Description	25
7.3.3 Model validation	26
7.4 Analysis of simulation results	26
7.4.1 Series One – total head vs. time; for specific volumes of air	27
7.4.2 Series Two – total head vs. time; surges at specific junctions	39
7.4.3 Series Three – total head vs. distance; for specific volumes of air	39
7.4.4 Series Four – total head vs. distance; for specific air pocket locations	47
7.4.5 Series Five – total head vs. time; for specific air pocket locations	53
8. Evaluation of numerical study results	54
8.1 Introduction	54
8.2 Observations	54
8.3 Pressure enhancement factor	55
8.3.1 Case study simulations for ‘realistic’ profile and horizontal profile	56
8.3.2 Summary	69

Contents continued

9.	Conclusions	69
9.1	Laboratory experiments	69
9.2	Numerical study	71
10.	References	73

Tables

Table 1	Test data for 0 degree downward slope (horizontal); critical flow velocity
Table 2	Test data for 0.8 degree downward slope (1 in 72); critical flow velocity
Table 3	Test data for 2.5 degree downward slope (1 in 23); critical flow velocity
Table 4	Test data for 3.4 degree downward slope; critical flow velocity
Table 5	Test data for 6 degree downward slope (1 in 9.5); critical flow velocity
Table 6	Test data for 11.5 degree downward slope (1 in 5); critical flow velocity
Table 7	Test data for 16.5 degree downward slope (1 in 3.4); critical flow velocity
Table 8	Test data for 22.5 degree downward slope (1 in 2.4); critical flow velocity
Table 9	Test data on air pocket velocity for downward slopes
Table 10	Test data for 2.5 degree downward slope (1 in 23); hydraulic gradients with and without air pocket
Table 11	Test data for 3.4 degree downward slope (1 in 17); hydraulic gradients with and without air pocket
Table 12	Hydraulic jump lengths
Table 13	Hydraulic jump tests; tests on exhaustion of air cavity
Table 14	Hydraulic jump tests; duration of air circulation period
Table 15	Average air pocket velocities measured in the tests
Table 16	Details of the Pipeline Profile – CASES 13 & 15
Table 17	Characteristic pump curve data
Table 18	Critical Locations for Various Volumes of Air Pocket – Showing Overall Maximum Total Head Values (At Pump Exit)
Table 19	Air Pocket Volumes & Locations to give Peak Surges at Sequential Locations along the Pipeline Profile
Table 20	Locations of Air Pocket to give Peak Surges at Sequential Locations along the Pipeline Profile
Table 21	CASE 13 - Peak Pressure Enhancement Factors at Sequential Locations along the Pipeline Profile
Table 22	CASE 15 - Peak Pressure Enhancement Factors at Sequential Locations along the Pipeline Profile
Table 23	CASE 1 - Peak Pressure Enhancement Factors at Sequential Locations along the Pipeline Profile
Table 24	CASE 2 - Peak Pressure Enhancement Factors at Sequential Locations along the Pipeline Profile
Table 25	CASE 3 - Peak Pressure Enhancement Factors at Sequential Locations along the Pipeline Profile
Table 26	Summary of Peak Pressure Enhancement Factors

Figures

Figure 1	Schematic plan view of test facility (dimensions in mm).....	4
Figure 2	Minimisation of steps between bends and straight pipe sections (dimensions in mm).....	5
Figure 3	Test section showing location of tapping points (dimensions in mm).....	7

Contents continued

Figure 4	Types of air pocket shape	10
Figure 5	Schematic of hydraulic jump in pipe	11
Figure 6	Comparison of experimental results with previous research	13
Figure 7	Relationship between critical flow velocity and pipe slope.....	14
Figure 8	Relationship between Froude number and slope parameter for different air pocket classes.....	15
Figure 9	Comparison between Froude number calculated from test data and numerically using Equation (15).....	16
Figure 10	Variation of coefficient a with volume parameter n	16
Figure 11	Comparison of HRW equation and work by previous researchers.....	17
Figure 12	Relationship between critical flow velocity and air pocket velocity	18
Figure 13	Dependency of the ratio air pocket velocity/critical flow velocity on pipe slope....	19
Figure 14	Comparison of hydraulic gradients with and without air pockets	20
Figure 15	Rate of air entrained at hydraulic jumps taken from Chanson and Qiao (1994) and test results.....	21
Figure 16	Pipeline profile.....	25
Figure 17	Comparison of the Effects of Differing Air Pocket Sizes showing Total Head with Time for no air pocket	28
Figure 18	Comparison of the Effects of Differing Air Pocket Sizes when placed at Junction 2 showing Total Head with Time for Volume of Air = 0.001 m ³	29
Figure 19	Comparison of the Effects of Differing Air Pocket Sizes when placed at Junction 1 showing Total Head with Time for Volume of Air = 0.001 m ³	30
Figure 20	Comparison of the Effects of Differing Air Pocket Sizes when placed at Junction 1 showing Total Head with Time for Volume of Air = 0.010 m ³	31
Figure 21	Comparison of the Effects of Differing Air Pocket Sizes when placed at Junction 1 showing Total Head with Time for Volume of Air = 0.025 m ³	33
Figure 22	Comparison of the Effects of Differing Air Pocket Sizes when placed at Junction 1 showing Total Head with Time for Volume of Air = 0.05 m ³	35
Figure 23	Comparison of the Effects of Differing Air Pocket Sizes when placed at Junction 1 showing Total Head with Time for Volume of Air = 0.1 m ³	37
Figure 24	Comparison of the Effects of Differing Air Pocket Sizes when placed at Junction 6 showing Total Head with Time for Volume of Air = 1.0 m ³	38
Figure 25	Comparison of the Effects of Differing Air Pocket Sizes when placed at Junction 1 showing Total Head with Time for Volume of Air = 1.0 m ³	39
Figure 26	Comparison of the Effects of Differing Air Pocket Sizes when placed at Junction 1 showing Max/Min Head with Time	41
Figure 27	Comparison of the Effects of Differing Air Pocket Sizes when placed at Junction 2 showing Max/Min Head with Time	42
Figure 28	Comparison of the Effects of Differing Air Pocket Sizes when placed at Junction 3 showing Max/Min Head with Time	43
Figure 29	Comparison of the Effects of Differing Air Pocket Sizes when placed at Junction 4 showing Max/Min Head with Time	44
Figure 30	Comparison of the Effects of Differing Air Pocket Sizes when placed at Junction 5 showing Max/Min Head with Time	45
Figure 31	Comparison of the Effects of Differing Air Pocket Sizes when placed at Junction 6 showing Max/Min Head with Time	46
Figure 32	Comparison of the Effects of an Air Pocket of 0.001m ³ when placed at Differing Junctions showing Max/Min Head with Time.....	48
Figure 33	Comparison of the Effects of an Air Pocket of 0.01m ³ when placed at Differing Junctions showing Max/Min Head with Time.....	49

Contents continued

Figure 34	Comparison of the Effects of an Air Pocket of 0.025m ³ when placed at Differing Junctions showing Max/Min Head with Time	50
Figure 35	Comparison of the Effects of an Air Pocket of 0.05m ³ when placed at Differing Junctions showing Max/Min Head with Time	51
Figure 36	Comparison of Effects of an Air Pocket of 0.1m ³ when placed at Differing Junctions showing Max/Min Head with Time	52
Figure 37	Comparison of the Effects of an Air Pocket of 1.0m ³ when placed at Differing Junctions showing Max/Min Head with Time	53
Figure 38	CASE 13 - Pressure Enhancement Factors at Pump Exit	56
Figure 39	CASE 13 - Pressure Enhancement Factors at Junction 1	56
Figure 40	CASE 13 - Pressure Enhancement Factors at Junction 2	57
Figure 41	CASE 13 - Pressure Enhancement Factors at Junction 3	57
Figure 42	CASE 13 - Pressure Enhancement Factors at Junction 4	58
Figure 43	CASE 13 - Pressure Enhancement Factors at Junction 5	58
Figure 44	CASE 15 - Pressure Enhancement Factors at Pump Exit	59
Figure 45	CASE 15 - Pressure Enhancement Factors at Junction 1	59
Figure 46	CASE 15 - Pressure Enhancement Factors at Junction 2	60
Figure 47	CASE 15 - Pressure Enhancement Factors at Junction 3	60
Figure 48	CASE 15 - Pressure Enhancement Factors at Junction 4	61
Figure 49	CASE 15 - Pressure Enhancement Factors at Junction 5	61
Figure 50	CASE 1 - Pressure Enhancement Factors at Pump Exit	62
Figure 51	CASE 1 - Pressure Enhancement Factors at Junction 1	63
Figure 52	CASE 1 - Pressure Enhancement Factors at Junction 2	63
Figure 53	CASE 2 - Pressure Enhancement Factors at Pump Exit	64
Figure 54	CASE 2 - Pressure Enhancement Factors at Junction 1	64
Figure 55	CASE 2 - Pressure Enhancement Factors at Junction 2	65
Figure 56	CASE 2 - Pressure Enhancement Factors at Junction 3	65
Figure 57	CASE 3 - Pressure Enhancement Factors at Pump Exit	66
Figure 58	CASE 3 - Pressure Enhancement Factors at Junction 1	66
Figure 59	CASE 3 - Pressure Enhancement Factors at Junction 2	67
Figure 60	CASE 3 - Pressure Enhancement Factors at Junction 3	67
Figure 61	CASE 3 - Pressure Enhancement Factors at Junction 4	68
Figure 62	CASE 3 - Pressure Enhancement Factors at Junction 5	68
Figure 63	CASE 3 - Pressure Enhancement Factors at Junction 6	69

Plates

Plate 1	Test section with a flat set-up viewed from downstream
Plate 2	Test section at a 22.5 degree slope
Plate 3	Air injection system
Plate 4	Injecting air into the test section
Plate 5	Example of elongated air pocket on flat slope
Plate 6	Example of wedge-like air pocket
Plate 7	Flat slope; upstream end of air pocket; top view
Plate 8	Flat slope; downstream end; top view
Plate 9	Flat slope; air pocket at increasing velocity; top view
Plate 10	Flat slope; breaking of air pocket; top view
Plate 11	6 degree slope; wedge-shape pocket; top view
Plate 12	6 degree slope; air pocket; top view
Plate 13	6 degree slope; air pocket increasing flow

Contents continued

Plate 14	22.5 degree slope; air pocket
Plate 15	22.5 degree slope; air pocket breaking
Plate 16	Test HJ6, 2.5 degrees, side view
Plate 17	Test HJ6, 2.5 degrees, bubbles coalescing; view from top
Plate 18	Test HJ, 6 degrees; flow 6 l per sec
Plate 19	Test HJ, 6 degrees; flow 15 l per sec
Plate 20	Hydraulic jump; 11 degree slope; 18 l per sec

1. *Background*

This report is the second output of a research study commissioned by the Department of Trade and Industry (DTI), to be carried out between October 2003 and November 2005 (the first output was a review of existing literature and practical experience – see Lauchlan et al, 2004). The study is aimed at producing a guidance manual for designers and operators of pipelines in order to reduce the number and cost of problems caused by air in water and wastewater pipelines. The detailed objectives of the study can be summarised as follows:

- To collect and review existing knowledge and experience relating to air problems in pipelines.
- To carry out targeted experimental and numerical studies to obtain information necessary for the preparation of the guidance manual.
- To combine information from the knowledge review with results from the experimental and numerical studies to produce practical design guidelines for use in the manual.
- To produce a guidance manual for designers and operators of water and waste water pipelines on how to avoid or eliminate problems due to air.

A Steering Group was formed for the project involving the following partners:

Black & Veatch Consulting (BVCs)
BP, British Petroleum
Dean & Dyball
MWH
Ove Arup & Partners
Thames Water Utilities
United Utilities
University of Liverpool, Department of Civil Engineering

The present report describes work carried out under Stage 3 of the project which was concerned with experimental and numerical studies to collect necessary additional data on the factors affecting the movement of air pockets in pipelines and the effect of air on surge pressures.

Following information on the project background in Chapter 1, Chapters 2, 3 and 4 describe the design, characteristics and instrumentation used in the test facility. The laboratory tests are described in Chapter 5 and the analysis of results is presented in Chapter 6. Chapters 7 and 8 deal with the numerical simulations of pressure transients that were undertaken to assess how air pockets may affect pressure transients. The conclusions from the laboratory and numerical studies are presented in Chapter 9.

2. *Design of test facility*

The design of the test facility was strongly influenced by the findings of the literature review (Lauchlan et al, 2004). The purpose of the laboratory tests was in effect to allow the collection of data that was identified as missing or in need of confirmation by the literature review. The main conclusions from the review and from consultation with the

Steering Group members that directly impacted on the design of the test rig can be summarised as follows:

- Most formulae suggested by the various researchers relate the critical velocity of the flow, V (i.e. the velocity of the flow that produces movement of air pockets or bubbles) with the pipe diameter D and slope S , as well as with the acceleration due to gravity. It should be noted however that much of this work was carried out using a single pipe diameter and therefore dependence on D could not be established from the experiments.
- The laboratory investigation should concentrate on air pocket movement as opposed to bubble movement given that bubbles will tend to coalesce into air pockets and these present generally more critical conditions for the design and operation of pipelines.
- The most critical (and therefore interesting) case to study for the movement of air pockets concerns downward pipes (as opposed to upward pipes where air is more easily moved by the flow).
- With regard to the scale of models used for investigative studies, the published literature sheds little light on this matter. The work by Zukoski (1966) and by Viana et al (2003) appear to suggest that, for turbulent flow conditions, viscosity and surface tension effects will be minimal in pipes of diameter 175mm or larger. For practical reasons it was decided that pipe diameters of 160mm od (or 150mm id) would be acceptable for the test rig.
- No useful information was identified regarding the effect of different pipe materials on the transport of bubbles or pockets in prototype or laboratory pipes but for ease of observation of air pocket movement transparent pipe materials are preferred.
- Plotting of various researchers' results indicated that there is a need to clarify the relationship between $V/(gD)^{0.5}$ and the pipe gradient, particularly for very shallow gradients. It was also decided to extend tests to cover some steeper slopes up to 22.5 degrees to establish whether the curve is convex (as suggested by Gandenberger, 1957 and Bendiksen, 1984) or concave (as suggested by Falvey, 1980 and Kalinske and Bliss, 1943) – see Lauchlan et al (2004).

The above conclusions led to the following design criteria for the test rig:

- Use of pipe diameters as large as practical, i.e. 150mm id
- Ability to observe flow of water and air, i.e. include transparent sections
- Ability to change the pipe slope with relative ease
- Study movement of air pockets in downward slopes but if possible allow for measurements in upward slopes
- Design for maximum slope of 22.5 degrees
- Need to achieve maximum flow velocities of the order of 1.5m/s
- Minimise number of joints and bends in test section as fittings cause head losses and air to be trapped
- Use minimum length of test section of 3m.

In addition to the above, the design of the test facility had to take into account some other practical aspects such as the available laboratory space and allocated budget.

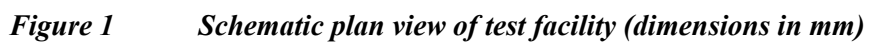
3. *Description of test facility*

The test rig was approximately 13m in length by 5m in width (see a schematic plan view in Figure 1). It was designed as an open circuit re-circulating facility whereby the flow was pumped from a supply sump into a constant head tank, conveyed through pipework and then discharged back into the sump. The pipework used in the test rig had 150mm internal diameter and consisted of two types of PVC: grey PVC in most of the rig and clear PVC in the test section. This transparent test section was formed by a 1.5m long leg followed by a 22.5 degrees sloping section of pipe with a length of 3m and by another pipe section 1m in length. A further transparent section was introduced at the downstream end of the test rig, before the pipe discharged the flow into the sump. Two 22.5 degree bends were used in the test section: these were carefully specified as large radius bends in order to introduce as small as possible a disturbance to the flow.

Before assembling, the internal and external diameters of the bends were measured and compared with the diameters of the adjacent straight sections. Where the differences in the internal diameters indicated that air could potentially be caught in the passage between the bends and the straight sections, these differences were minimised by adding filling to create ramps as opposed to steps (see Figure 2).

The main feature of the experimental facility was the ability to rotate the whole of the test section in smooth steps from the horizontal position to the required maximum angle of 22.5 degrees. A support frame was used to hold the test section in position. The test section in a flat position is shown in Plate 1 whereas Plate 2 shows the test section set up at a 22.5 degree slope.

Valves were introduced upstream and downstream of the test section to allow accurate control of the flow rate and of the flow depth conditions required in the tests.



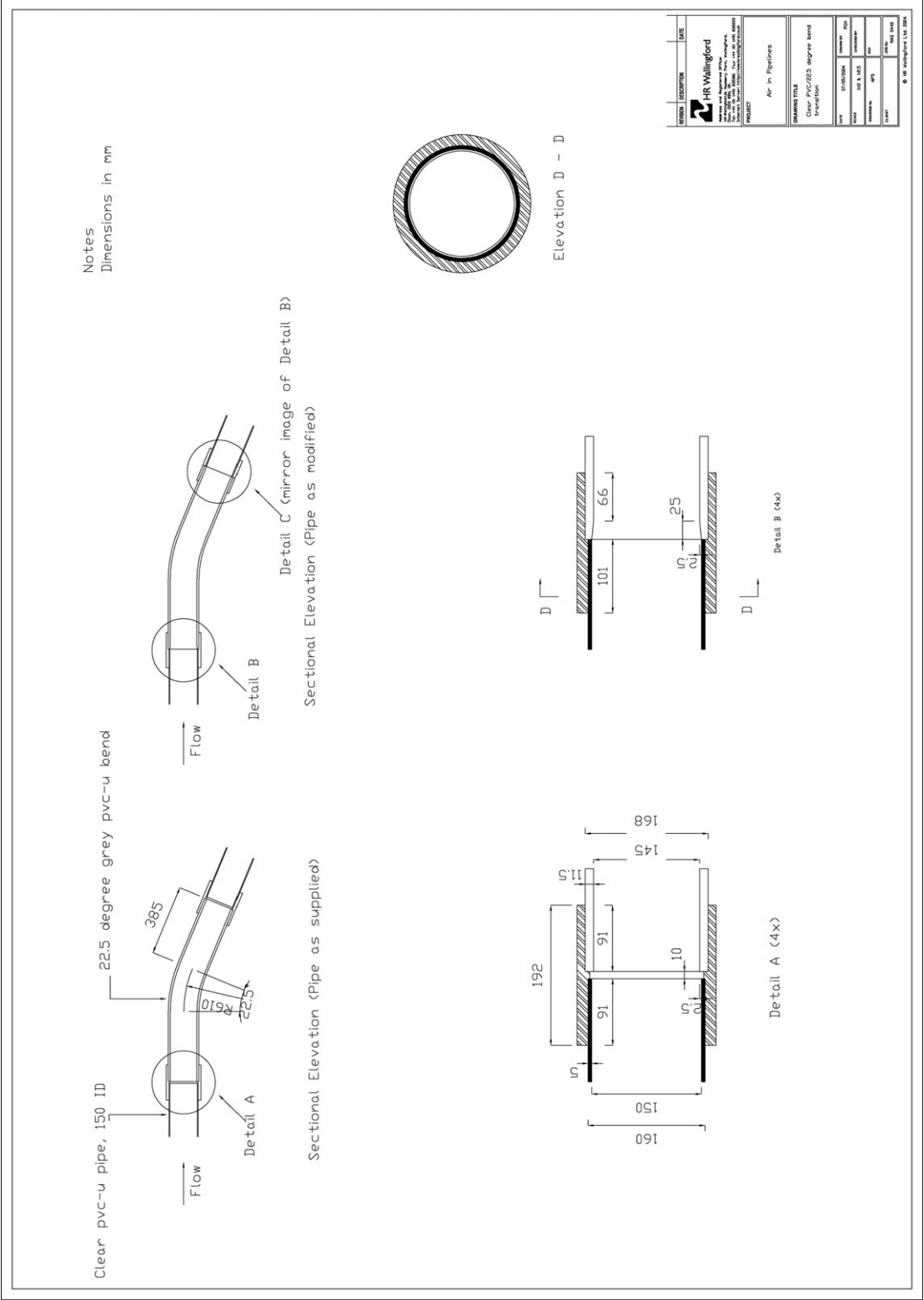


Figure 2 *Minimisation of steps between bends and straight pipe sections (dimensions in mm)*

4. *Instrumentation*

The flow rate was measured by an electromagnetic flow meter (Krohne IFC 010D) 150mm in diameter. The accuracy of this type of flow meter is $\pm 2\%$.

Tapping points and a manometer board were used for the measurement of head losses. Several tapping points were introduced in the test section as shown in Figure 3. As well as tapping points, quick release pneumatic fittings (8mm od/6mm id) were also installed to allow the withdrawal of water and injection of air, as described later in this section.

The atmospheric pressure was measured using a calibrated barometer (type Fischer 104).

Air and water temperatures were monitored using a digital thermometer of make Comark.

Measurement of the travel velocity of air bubbles and pockets was made by timing the air bubble/pocket trajectory using a stopwatch.

For the setting of the pipe angle, an inclinometer was used to give the general slope, which was then accurately determined by means of an engineering level.

A purpose-built Air Injection System (Plate 3), with graduated scale was made to allow the introduction of air bubbles/pockets into the pipe section. This device was designed for a maximum air capacity of 2 litres. The principle of operation is as follows: water is drawn from the test pipe at an upstream section, air inside the cylinder is compressed and then the amount required is carefully released into the test section (Plate 4). The injection of air could be done either under static conditions or with a small flow in the test pipe. By using water from the test section to dislodge the air inside the cylinder the pressure of the water transferred to the cylinder is the same as that inside the test section and therefore the volume of the air pocket is accurately determined. The 255mm long cylinder was made of 100mm ID perspex tube covered at the top and base by perspex plates. Quick release pneumatic fittings (8mm od/6mm id) connected to flexible tubing were installed at the base, to allow the flow of water into the cylinder, and at the top to allow the release of air into the test section. A tap was also installed at the base to enable the cylinder to be drained.



5. *Laboratory tests*

5.1 TEST PROCEDURE

Preliminary tests were carried at the start of the experimental work for the operator to familiarise himself with the test rig and with the air/water flow processes involved. Initially, the facility was set with a flat test section; this was then changed to the maximum slope that could be achieved with the test rig, 22.5 degrees, so that the full range of conditions could be observed.

At the start of the tests it was immediately apparent that the shape of the air pockets varied dramatically with the pipe slope, the pocket being very elongated and thin for flat slope and taking a wedge-like shape for the steeper slope (compare Plates 5 and 6). The shape of the pockets also influenced the way in which the tests were conducted, namely the introduction of air into the pipe section. It was originally thought that the air could be injected in the 1.5m long horizontal reach following the 90° bend under static conditions (see Figure 1) and that the air pocket could be made to move downstream by an increase in the flow. The minimum flow velocity at which it would move would correspond to the critical flow velocity. However, it was found that the air pocket generated with horizontal pipes was so elongated that parts of the pocket would be caught at the 22.5 degree bends and break up into smaller bubbles, thus affecting the measured volume. It was noted in Section 3 that care had been taken to minimise any steps between the bends and the straight sections of pipe but this was apparently not sufficient and strongly indicates that the presence of pipe fittings will have a marked effect on the tendency for air accumulation. For the steeper slope this was a lesser problem but still there was some risk of the air pocket being affected by the bends. Under static water conditions it was also observed that the air would tend to move upstream too easily.

For these reasons, an alternative test procedure was followed: the air was injected in the 3m long section of pipe under a low flow velocity, which allowed the air to move upstream in the pipe and become stable before the flow rate was increased to the critical velocity that made the air pocket move downstream. An exception to this were the tests at 0° slope, where the air was introduced under static flow conditions.

During the test programme it was also realised that injecting the air with the Air Injection System would not produce large air pockets and therefore the air was injected by means of a simple bicycle pump. This method had the disadvantage that the air injected was compressed and therefore its volume could not be measured prior to injection. The volume of the resulting air pocket had to be determined from measurement of its dimensions once the pocket was formed in the test section.

During the tests to study air pocket movement the flow rate associated with the critical flow velocity was measured. Head losses in the test section with and without the air pocket were also measured by means of tapping points connected to a manometer board. The travel velocity of the air pocket was also recorded.

The tests of air movement in hydraulic jumps were carried out in the following way. The flow conditions in the test rig were set up by adjusting the valves upstream and downstream of the test section so that a stable jump was formed in the transparent test section. Once the jump was formed, measurements were taken of the flow rate, jump length and travel velocity of the air bubbles entrained by the jump. Most tests were

carried out with the open surface section upstream of the jump closed to the atmosphere, but in order to investigate the effect of a constant air supply, some tests were performed with the tapping points open upstream of the jump. In these tests it was observed that the air volume upstream of the jump remained constant, i.e. it could not be expelled by the jump.

5.2 TEST DATA

5.2.1 Downward slopes

Two main types of test were carried out. In the first group of tests (Group A) the main focus was on finding the critical flow velocity necessary to remove air pockets from the pipe section set at different slopes. As a side investigation, the air pocket velocities were measured and analysed, as well as the head losses in the test section with and without the air pocket. The second group of tests (Group HJ) included tests performed to investigate the removal of air at hydraulic jumps and observe the flow conditions associated with this phenomenon.

As mentioned in 5.1, the Group A tests enabled the observation of the shape and size of air pockets associated with the various slopes tested. A summary description of the air pocket shapes observed is shown in Figure 4 and illustrates the variation from elongated shape to wedge-shape as the slope increased from 0 to 22.5 degrees. The breaking up of the air pocket with increasing velocity for the case of flat slope is illustrated in Plates 7 to 10. In all the plates the flow is from the left. Examples of wedge-shape air pockets are given in Plates 11, 12 and 13 (slope of 6 degrees) and Plates 14 and 15 (slope of 22.5 degrees).

The results of the Group A tests, that were concerned with the measurement of critical flow velocity for air pocket movement, are presented in Tables 1 to 8 for all the eight slopes tested. In these tables the volume of air injected using the Air Injection System and the ambient conditions are also recorded, namely the atmospheric pressure and the air and water temperatures. In these tables there is also a column for the “estimated air volume” which corresponds to conditions where, in order to achieve larger air pockets, the air was not injected with the Air Injection System but by other means and the volume had to be calculated. This is explained in Section 5.3.

The results of the Group A tests, that were concerned with the measurement of the speed of movement of the air pockets once the threshold of movement was achieved, are summarised in Table 9. This table shows data from tests carried out at 0, 2.5 and 6 degree slopes; further, sporadic, data was collected at other slopes but only for some flow rates and is not presented in this table. As can be seen from Table 9, the velocity of air pockets, which was measured in relation to two fixed positions on the pipe wall, ranged from 0.02 to 0.56m/s.

The results of the Group A tests, that were concerned with the measurement of head losses in the pipes due to the presence of air pockets, are summarised in Tables 10 and 11. As can be seen from these tables, the hydraulic gradients for flow with air pocket and without the air pocket were calculated for a range of flow rates. The head measurements were taken along the downward length of pipe at tapping points situated 1.8m apart. Usable data, i.e. data that provided reliable estimates of the hydraulic gradient, was only obtained for two slopes: 2.5 and 3.4 degrees, as explained in Section 6.3.

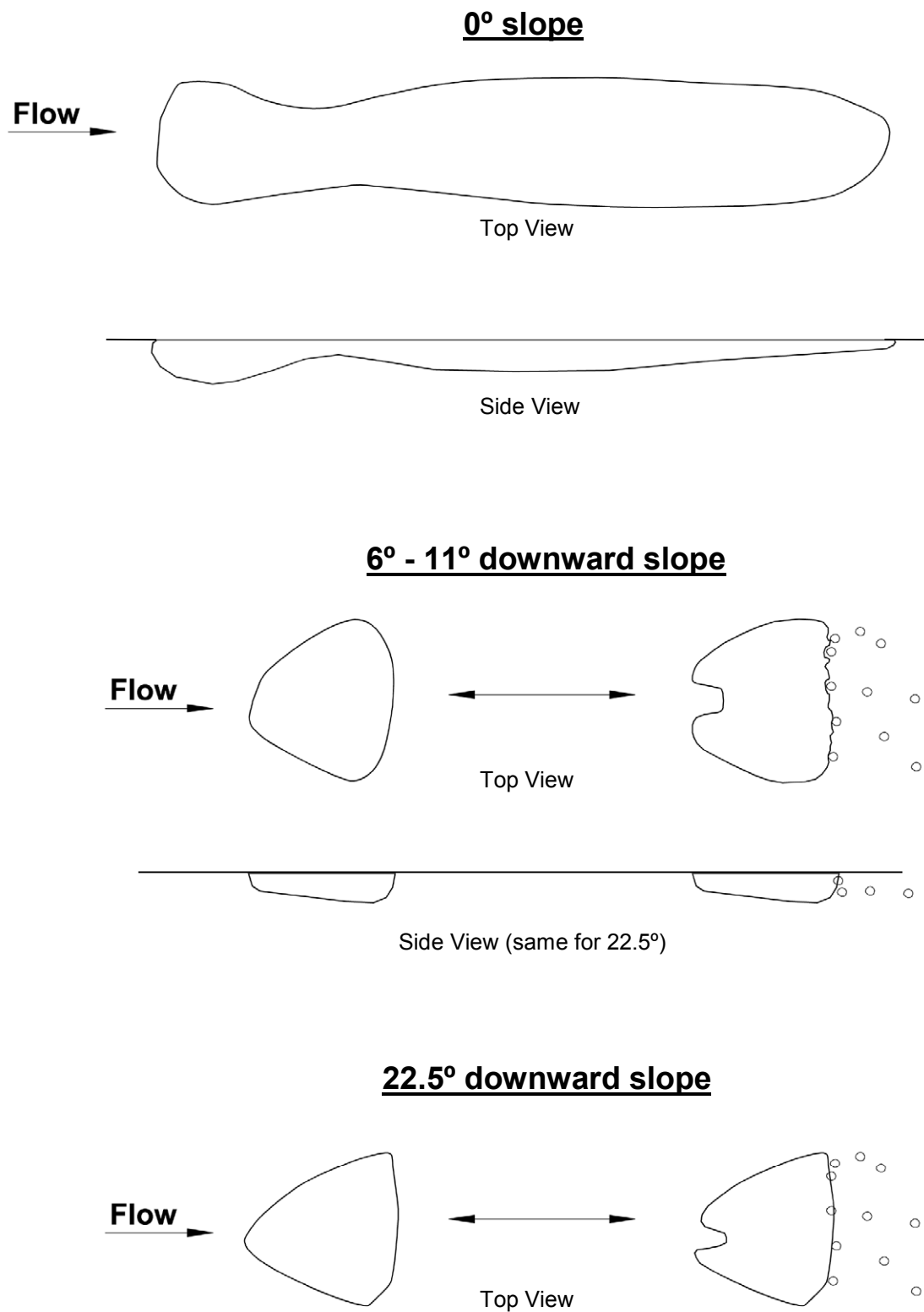


Figure 4 *Types of air pocket shape*

The Group HJ tests involved the following: observation of the flow conditions at hydraulic jumps formed in downward sloping pipes and the measurement of: the hydraulic jump length; the velocity of air bubbles downstream of the jump; and the time required to exhaust the air above the jump and the corresponding change in air volume. Approximate measurements of the bubble sizes released by the jump and moved downstream were also taken using a ruler. It was found that the bubble size was typically in the range 3-5mm. The speed of movement of these bubbles varied between 0.4 and 0.7m/s; the ratio bubble vel. /flow vel. varied between 0.6 and 1.5.

With regard to the jump length (see Figure 5), two lengths were considered (results are presented in Table 12):

- Jump front length (JFL), which was defined as the length of the steep face of the jump; and
- Overall jump length (OJL).

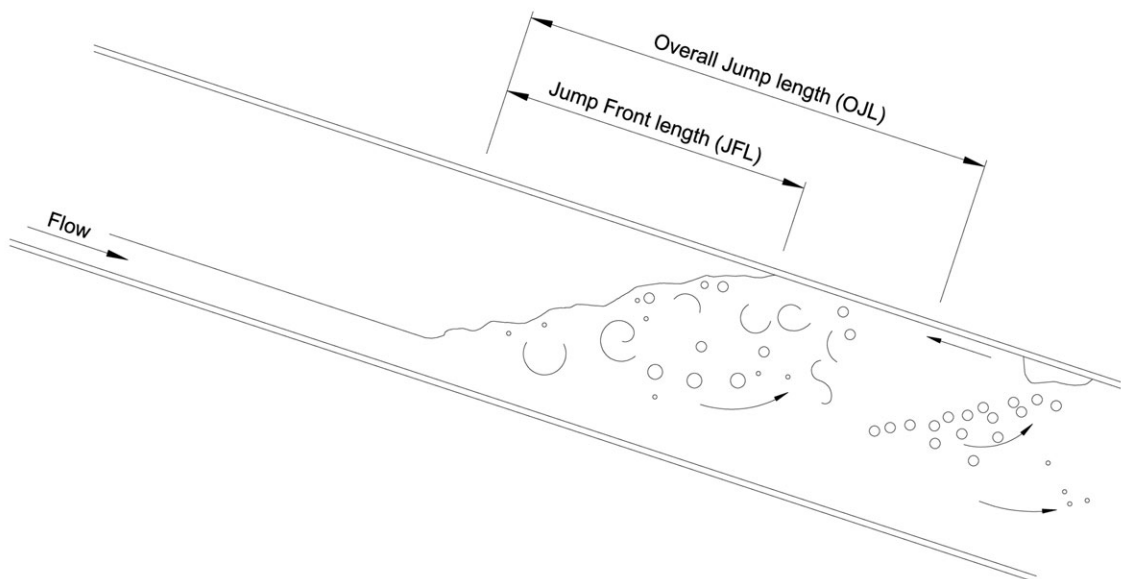


Figure 5 *Schematic of hydraulic jump in pipe*

It was found that typically JFL/D varied between 1.3 and 5 and OJL/D varied between 2 and 11, where D is the pipe diameter.

The results of the other measurements are summarised in Table 13. The flow conditions associated with hydraulic jumps at 2.5, 6 and 11 degrees for various flow rates are illustrated in Plates 16 to 20. During the tests the following phenomenon was observed. The air was entrained by the jump in the form of bubbles, typically 3 to 5mm in diameter; a proportion of these bubbles was carried downstream by the flow but a certain amount coalesced as they moved downstream, increasing in size. Due to this increase in size and therefore in buoyancy, the bubbles would rise to the top of the pipe where they coalesced further into air pockets of several tens of millimetres in size (see

Plate 17). These then moved upstream towards the front of the hydraulic jump and the air was engulfed back into the air cavity upstream of the jump. As this phenomenon appeared to be periodic, the duration of a complete cycle was measured in the tests (see Table 14). This behaviour has been reported before, for example by Kalinske and Bliss (1943).

5.2.2 Upward slopes

Additional tests were performed with negative slopes (upward slopes) to determine critical flow conditions for air pocket movement. The slopes tested were -1.02 and -1.9 degrees and the air pocket sizes varied between 135 mm³ and 1300000 mm³ (or 1.3 litres) and between 262 mm³ and 11225 mm³ respectively for the two slopes. At both slopes it was found that no flow was necessary to transport the air pockets. Even very small pockets around 250 mm³ (-1.02 degrees) and 140 mm³ (-1.9 degrees) in volume moved upwards due to buoyancy forces. Depending on the size of the pocket, they moved at pocket velocities between 0.12 m/s and 0.18 m/s (-1.02 degrees) and between 0.06 m/s and 0.63 m/s (-1.9 degrees). These values are comparable with the air pocket velocities obtained for downward slopes (see Section 5.2.1).

5.3 DATA ANALYSIS

For several tests the analysis of the data required the calculation of air volumes since the use of the Air Injection System was confined to a certain range of air pocket volumes (see Section 5.1). For very small air pockets the water level in the cylinder did not change significantly and therefore the accuracy of reading was low. On the other hand, creating very large pockets was not possible due to insufficient air pressure in the cylinder. At the start of the test programme considerable effort was spent on establishing the most appropriate way of estimating the air pocket volumes. The width of the air pocket at the top of the pipe was measured along the pipe perimeter and corrected for the thickness of the pipe. By applying trigonometric relationships the area, A_{air} , defined by the cord and the internal perimeter of the pipe occupied by the air pocket was calculated. Knowing the length of the air pocket, L_{air} , which was also measured during the tests, the air volume could then be calculated. As the air pocket shape varied depending on the size, slope and flow velocity (see Figure 4), several alternative ways were tried to approximate the air pocket to a regular geometric shape (e.g. cylindrical, conical, etc). Some comparisons were made between measured air volumes and the volumes resulting from the various possible assumptions for the air pocket shape. It was found that although the air pocket shape varied significantly, the equation below provided a good method for estimating the air pocket volume, V_{air} :

$$V_{\text{air}} = A_{\text{air}} L_{\text{air}} \quad (1)$$

where A_{air} is the cross-sectional area occupied by the air and L_{air} is the length of the air pocket.

The determination of the volume of the air cavity upstream of hydraulic jumps was also carried out using Equation (1).

Previous researchers such as Kent (1952) have used a non-dimensional parameter to characterise the size of air bubbles or pockets. In order to facilitate comparisons of the test results with former results, it was decided to adopt Kent's parameter in the present study which is given as follows:

$$n = 4V_{\text{air}} / (\pi D^3) \quad (2)$$

where V_{air} is the volume of the air pocket and D is the pipe diameter.

This parameter includes the pipe diameter and therefore allows the transfer of results from model to pipe systems with different pipe diameters.

6. Analysis of results

All the data analysis reported in Section 6 refers to downward sloping pipes.

6.1 CRITICAL FLOW VELOCITY

The literature review carried out in the first stage of this study showed a very wide range in the values quoted by the different researchers for the critical flow velocity that is required to move air pockets downstream along a downward sloping pipe. It was mentioned in Section 2 that one of the main aims of the experimental work was to clarify the relationship between $V/(gD)^{0.5}$ and the pipe gradient, particularly for very shallow gradients and to establish whether the curve is convex (as suggested by Gandenberger, 1957 and Bendiksen, 1984) or concave (as suggested by Falvey, 1980 and Kalinske and Bliss, 1943) – see Lauchlan et al (2004). In order to ascertain this, the data collected in the tests was therefore superimposed on a graph where the results of a number of researchers were also plotted (Figure 6 – for detailed information on work referred to in the legend see Lauchlan et al, 2004).

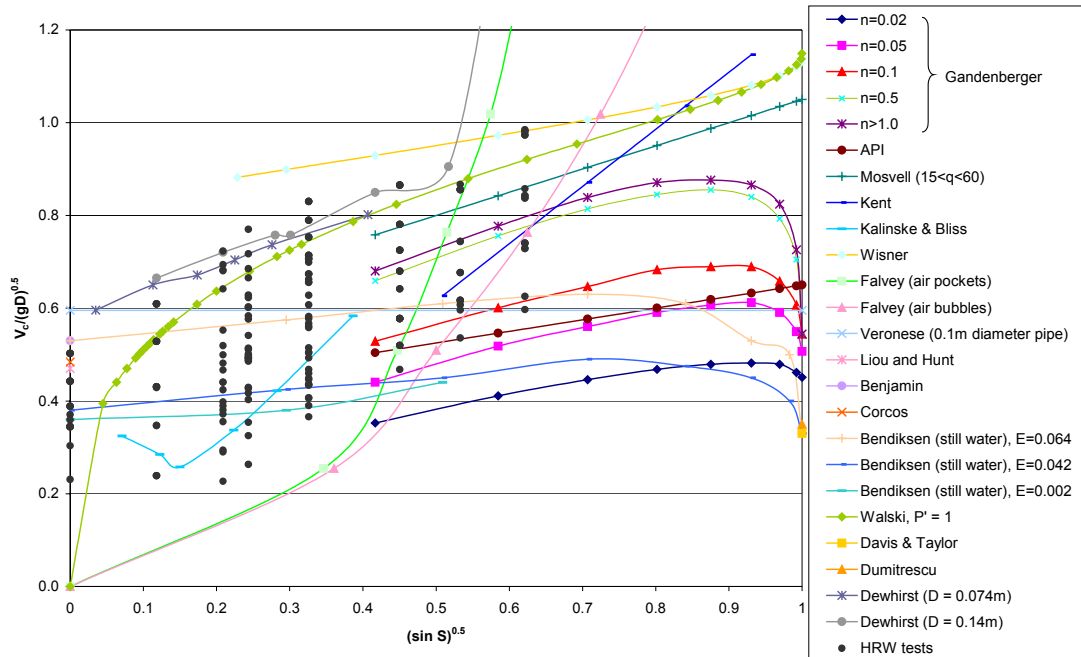


Figure 6 Comparison of experimental results with previous research

It is apparent from this Figure that the experimental data fitted well within the other researchers range of results. However the large scatter in the present experimental data indicates that the critical velocity is dependent not only on the pipe slope, S , but is also

affected by another parameter(s) not represented in the graph. As the tests were carried out with various sizes of air pocket, this was a parameter that could well explain the scatter. The experimental data was checked to investigate whether there was a correlation between air pocket size and critical velocity and, as expected, it was found that, for the same pipe slope, the larger pockets were associated with higher critical velocities. It was therefore decided to take account of pocket size by grouping the air pocket sizes in classes, making a total of 6 classes. Due to the variation in pocket size within each class, the critical flow velocity for air pocket movement covered a range of values and it was decided to use the average value as the representative value for each class. Figure 7 shows the experimental results based on the critical average flow velocity required to move a stationary air pocket in a downward sloping pipe for different air pocket volumes, defined by the parameter n (see Equation 2).

Thus for each class of air pocket different equations for the critical flow velocity as a function of slope were found. The following equations can be used to estimate the critical flow velocity having the values for n and the downward slope:

$$V = 0.030 S^{0.8} + 0.44 \quad \text{for} \quad n < 0.06 \quad (3)$$

$$V = 0.096 S^{0.5} + 0.60 \quad \text{for} \quad 0.06 \leq n < 0.12 \quad (4)$$

$$V = 0.069 S^{0.62} + 0.68 \quad \text{for} \quad 0.12 \leq n < 0.18 \quad (5)$$

$$V = 0.14 S^{0.35} + 0.70 \quad \text{for} \quad 0.18 \leq n < 0.24 \quad (6)$$

$$V = 0.037 S^{0.87} + 0.72 \quad \text{for} \quad 0.24 \leq n < 0.30 \quad (7)$$

$$V = 0.053 S^{0.75} + 0.74 \quad \text{for} \quad 0.30 \leq n < 2 \quad (8)$$

where V is the minimum flow velocity required for movement of an air pocket of size defined by the parameter $n (= 4V_{\text{air}} / (\pi D^3))$ in a downward pipe of slope S and diameter D . V_{air} is the volume of the air pocket.

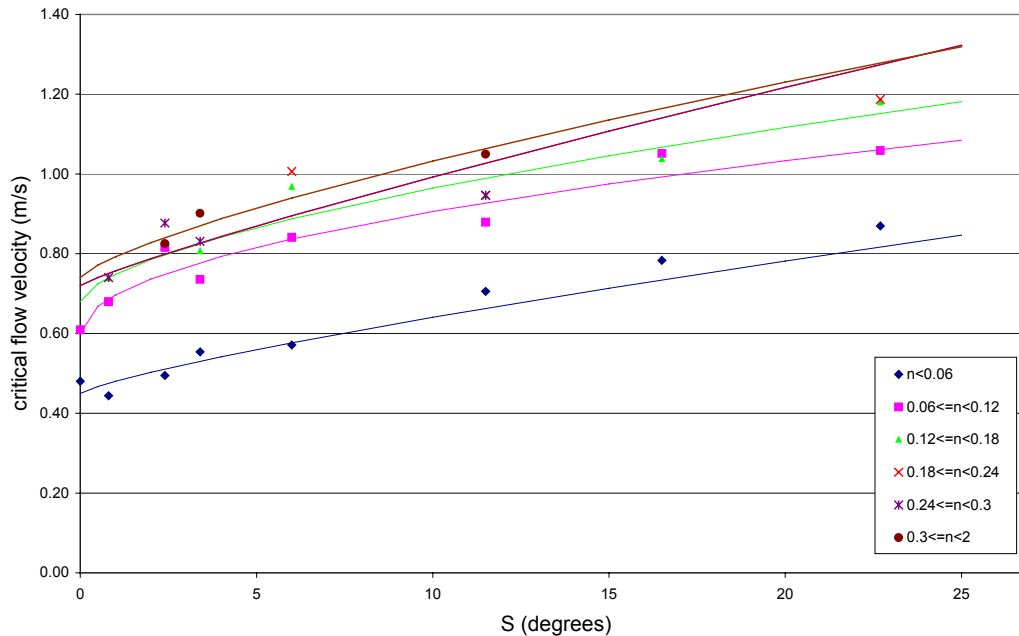


Figure 7 Relationship between critical flow velocity and pipe slope

As in many other investigations (see Figure 6) it is advantageous also here to plot the results in non-dimensional form, i.e. the Froude number ($V/(gD^{0.5})$) as a function of (\sin

angle)^{0.5} – see Figure 7. Using the root of the sine of the angle, the curves become straight lines, which makes the analysis easier. For this analysis, which was aimed at providing conservative values for design purposes, the critical flow velocities used to calculate the Froude number were the maximum values in each of the air pocket classes for each slope. The following best-fit equations were obtained for each class:

$$V/(gD)^{0.5} = 0.5599 (\sin S)^{0.5} + 0.4526 \quad \text{for} \quad n < 0.06 \quad (9)$$

$$V/(gD)^{0.5} = 0.6129 (\sin S)^{0.5} + 0.4868 \quad \text{for} \quad 0.06 \leq n < 0.12 \quad (10)$$

$$V/(gD)^{0.5} = 0.6569 (\sin S)^{0.5} + 0.5351 \quad \text{for} \quad 0.12 \leq n < 0.18 \quad (11)$$

$$V/(gD)^{0.5} = 0.5573 (\sin S)^{0.5} + 0.6050 \quad \text{for} \quad 0.18 \leq n < 0.24 \quad (12)$$

$$V/(gD)^{0.5} = 0.4607 (\sin S)^{0.5} + 0.8030 \quad \text{for} \quad 0.24 \leq n < 0.30 \quad (13)$$

$$V/(gD)^{0.5} = 0.6676 (\sin S)^{0.5} + 0.5730 \quad \text{for} \quad 0.30 \leq n < 2 \quad (14)$$

A general equation to predict the dimensionless flow velocity parameter (Froude number) based on the above equations is given below. Note that for simplicity the number of classes defining the air pocket size was reduced from six to four:

$$V/(gD)^{0.5} = 0.5599 (\sin S)^{0.5} + a \quad (15)$$

where a equals:

0.4526	for	$n < 0.06$
0.5033	for	$0.06 \leq n < 0.12$
0.5739	for	$0.12 \leq n < 0.30$
0.6065	for	$0.30 \leq n < 2$

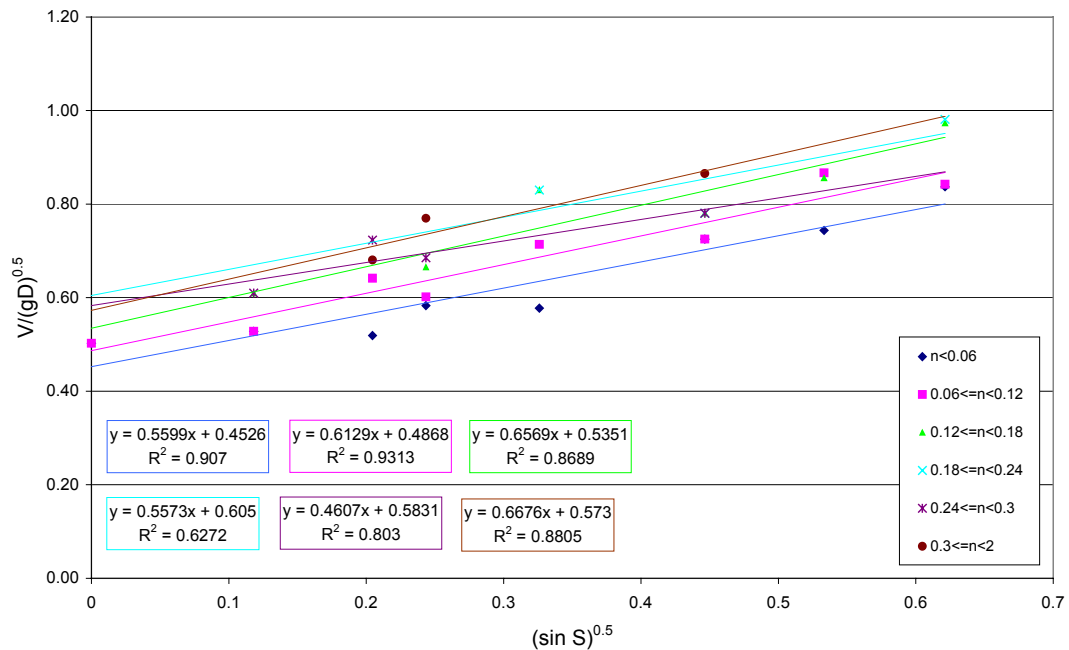


Figure 8 Relationship between Froude number and slope parameter for different air pocket classes

The values of the Froude number obtained using Equation (15) were plotted against the experimental values in Figure 9 to verify the validity of the Equation. It can be seen that the agreement is very good.

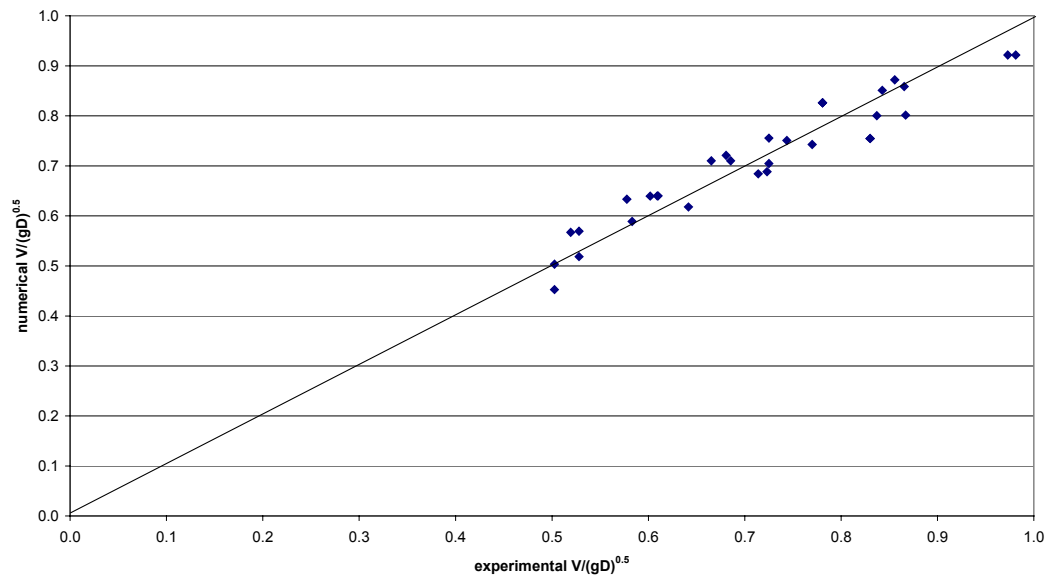


Figure 9 Comparison between Froude number calculated from test data and numerically using Equation (15)

Equation (15) indicates that for increasing values of n , the Froude number would also increase but it is unclear at what rate. In order to assess the variation of a with n , these two parameters were plotted in Figure 10 (in the x-axis n_{mid} denotes the middle value with the range). It can be seen that the increase in a is not linear with n and therefore it is expected that the value of a (and therefore the critical velocity) would not increase significantly with larger air pocket sizes.

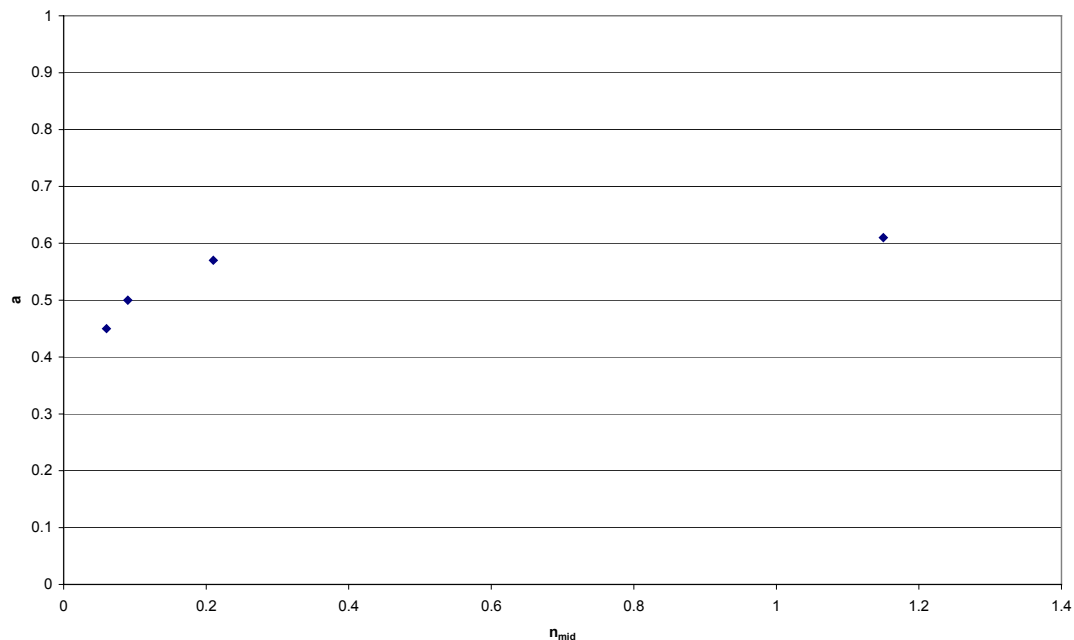


Figure 10 Variation of coefficient a with volume parameter n

An envelope of HRW's results (i.e. Equation (15)) for the smallest and the highest air pocket classes) is given in Figure 11 and is compared with the work of previous researchers (refer to Lauchlan et al, 2004). In the range of slopes tested, the present results showed a linear increase of the Froude number with the slope factor, at a similar rate as suggested by Gandenberger, Mosvell, and, except for smaller slopes, also by Walski, for example. Contrary to the present results, which are more in accordance with Dewhirst, Veronese, Corcos, Benjamin and Liou and Hunt, Walski suggests zero critical velocities at zero slope. However, in the present study detailed tests at very mild slopes showed that this appears not to be the case.

6.2 AIR POCKET VELOCITY

It was expected that, after establishing the critical flow velocity for movement, the air pocket would move slowly down the slope, for all slopes and pocket sizes. This is because the critical flow velocity is defined as the velocity that just makes the air pocket move. In reality this simple scenario was not achieved because air pockets change shape during movement and the degree of change depends on their size, the flow velocity and the pipe slope. Moreover, at certain combinations of flow velocity and slope, larger pockets become unstable and break up. Consequently, the various forces acting on the air pocket (for example friction and buoyancy forces) are affected and so is the air pocket velocity.

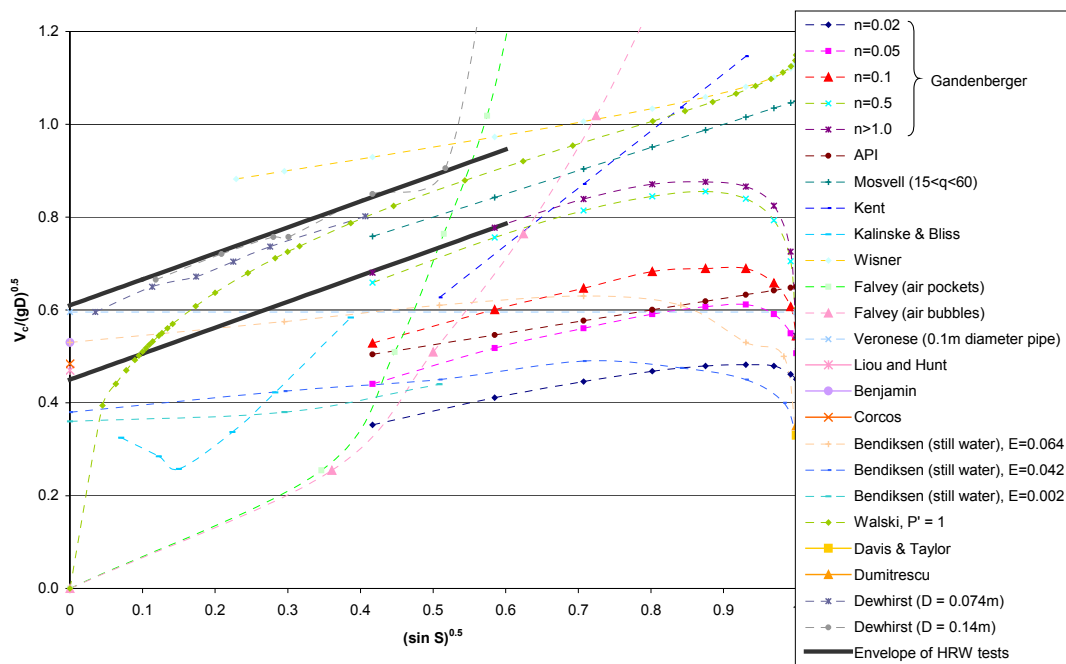


Figure 11 Comparison of HRW equation and work by previous researchers

Of all the test data collected it was only possible to establish reasonable correlations between the critical flow velocity and the corresponding air pocket velocity for three series of tests (see Table 9). These relationships are shown in Figure 12.

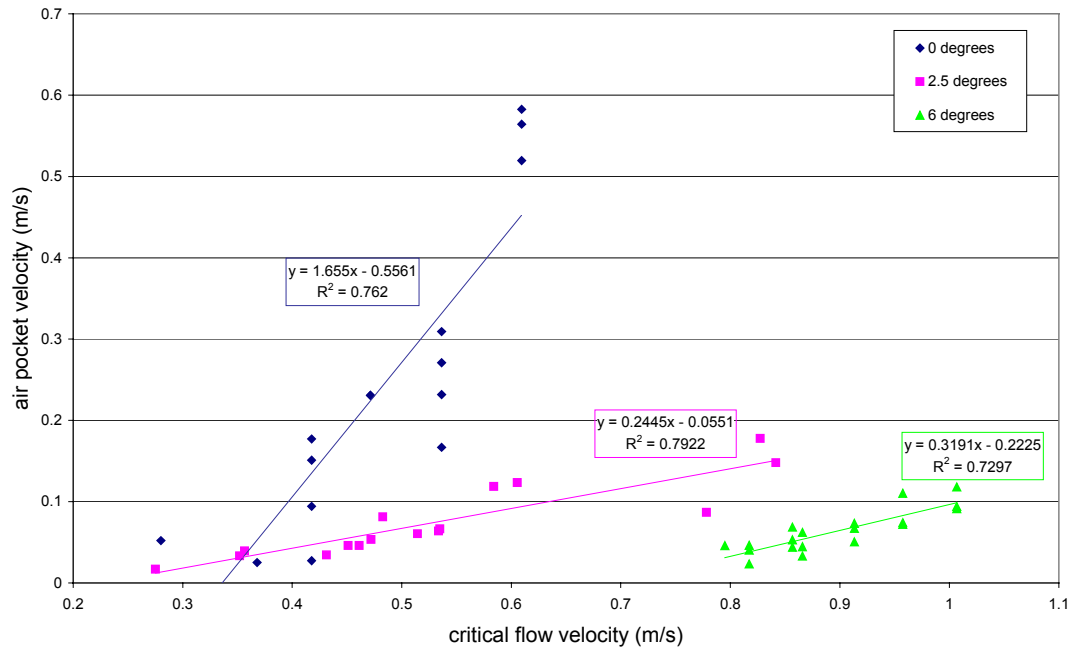


Figure 12 Relationship between critical flow velocity and air pocket velocity

It is apparent in Figure 12 that for a certain slope, the air pocket velocity (measured in relation to two fixed positions on the pipe wall) increases with the critical flow velocity, i.e. with increasing slope. However, it is also apparent that the rate of this increase slows down with steeper slopes. Table 15 gives the ratios of the average air pocket velocities and critical flow velocities obtained for all the tests carried out (both for tests where good and where weak correlations were established between air pocket velocity and critical velocity). The exponential reduction in these ratios with the pipe slope is clearly seen in Figure 13: air pockets tend to slow down the steeper the pipe slope. This appears to indicate that once the frictional resistance between the air pocket and the pipe material at low slopes is overcome, the air pocket will move relatively quickly. At steeper slopes a stabilised air pocket reacts much faster to increasing water flow rate possibly because its shape is less elongated than in milder slopes and therefore less affected by frictional resistance. However, once in movement, its speed is relatively lower. This implies that expelling the same volume of air from a steep pipe will take longer than from a pipe at a milder slope. For the same pipe diameter, the time required to move an air pocket in a pipe at 11 degrees can be 15 times greater than in a horizontal pipe.

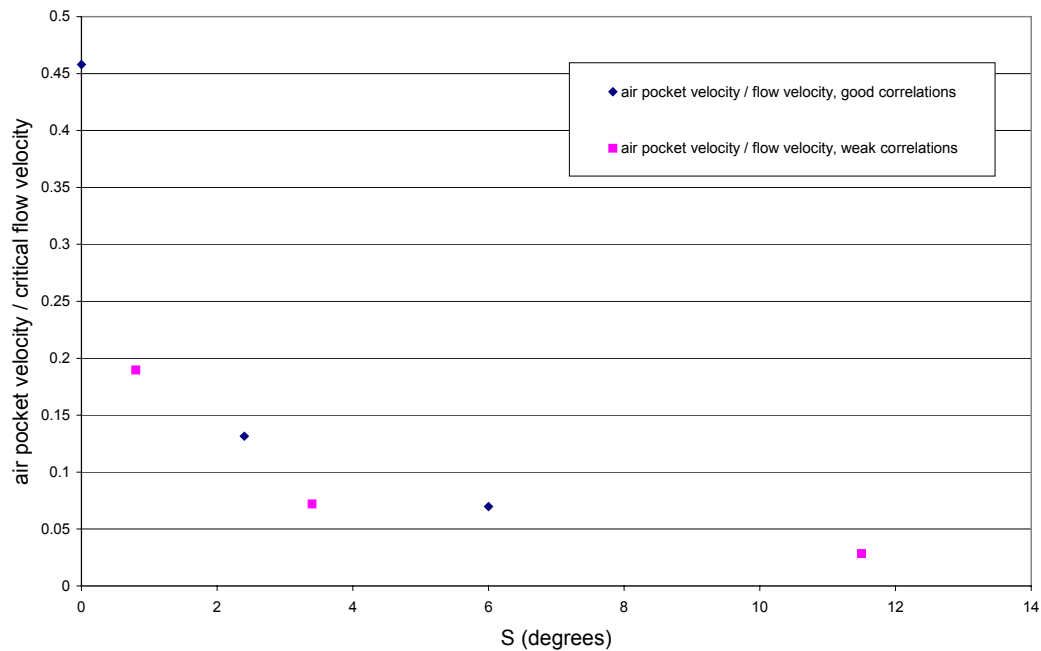


Figure 13 *Dependency of the ratio air pocket velocity/critical flow velocity on pipe slope*

6.3 HEAD LOSS

Although most of the tests gave a large scatter in results, for two test series (at 2.5 degrees and 3.4 degrees) there was a clear difference in head losses with and without air pockets. The test results and the obtained correlation lines are shown in Figure 14. As expected, the hydraulic gradient between two tapping points (distance 1.8 m) generally increased with increasing flow velocity. It was found that for the same flow conditions hydraulic gradients with air pocket were generally higher than for full water flow in the pipe. Within the range tested the hydraulic gradients with air pocket were generally about 25 to 35% higher than those measured without an air pocket. This difference appeared to increase with increasing hydraulic gradient. This can be explained by the fact that at higher flow velocities it was possible to move larger air pockets down the slope and this influenced the flow behaviour more strongly than small pockets at small flow velocities.

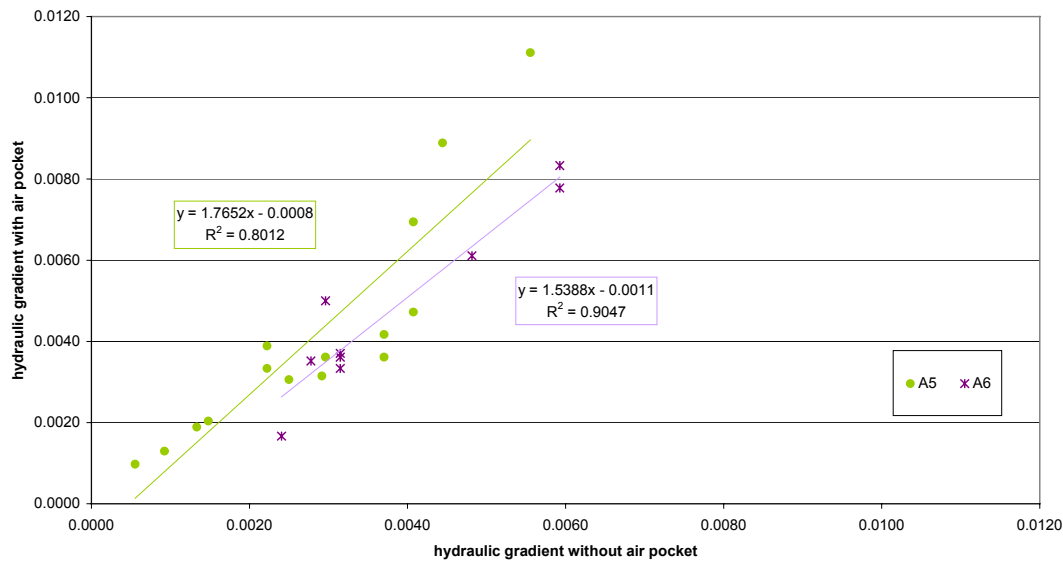


Figure 14 Comparison of hydraulic gradients with and without air pockets

Various researchers have obtained contradictory results with regard to head losses associated with air pockets. Some have obtained lower friction factors for air/water flows than for water flows while James and Silberman (1958) for example found equal or slightly higher factors. Despite the difficulty in obtaining accurate results, the present tests do indicate that the friction factor for flows with air pockets is higher than that for liquid flow alone.

6.4 HYDRAULIC JUMPS

Although several tests were carried out to investigate the rate of expulsion of air through hydraulic jumps, it was found that if the flow velocities were small or/and the initial air volumes upstream of the jump were large, it was not possible to remove the air. In several tests, however, the right conditions were met and it was possible to relate the flow of air with the water flow. The test results were plotted in Figure 15, together with results from other studies (refer to Lauchlan et al, 2004). In this Figure the Froude number corresponds to the flow upstream of the jump and was defined as:

$$F_r = QB^{0.5} / (A^{1.5} g^{0.5}) \quad (16)$$

where Q is the water flow, B and A are respectively the surface width and area of the flow and g is the acceleration due to gravity.

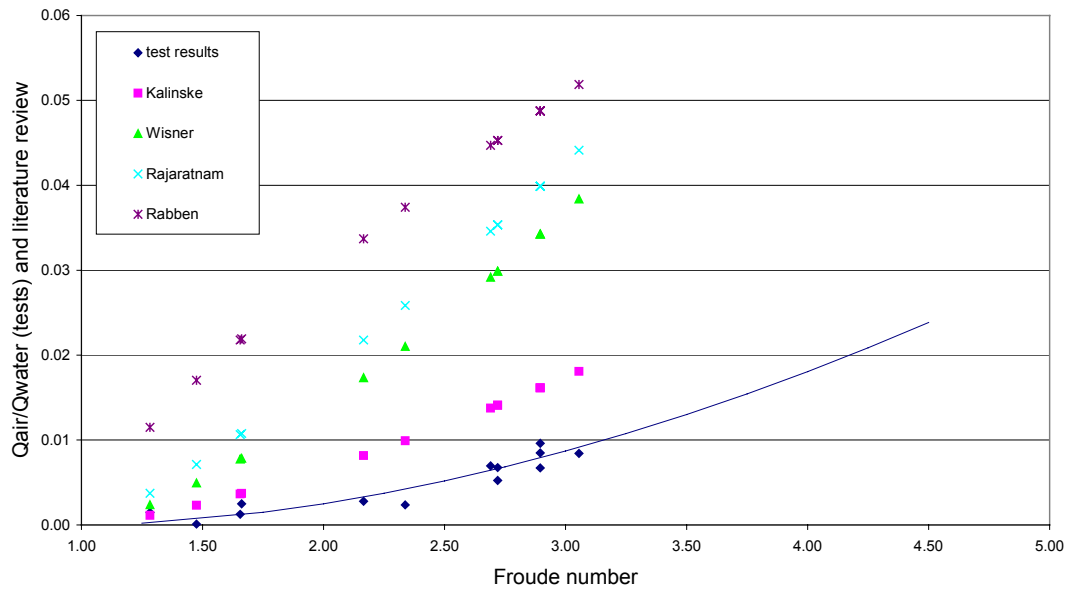


Figure 15 *Rate of air entrained at hydraulic jumps taken from Chanson and Qiao (1994) and test results*

Although a general pattern can be found in all the data presented in Figure 14, the discrepancy between results is quite marked and the present test results indicate a significantly lower rate of expulsion of air when compared with other work. In some cases, such as in work by Rabben, Rajaratnam and Wisner this difference may be attributed to the fact that the cross-section where the measurements were taken was rectangular. Kalinske's results refer to hydraulic jumps in horizontal circular pipes and are therefore closer to the conditions in the present study (which, it should be added, cover pipe slopes from 0.8 to 22.7 degrees). The downstream exit conditions are also different for many of the previous tests compared to the present study. In the present study the flow downstream of the hydraulic jump was pipe-full and there was no air at the exit. In many of the previous studies at the exit to the pipe the flow conditions were often open-channel.

Equation (17) gives a best fit to the test data:

$$Q_{\text{air}} / Q = 0.0025 * (F_r - 1)^{1.8} \quad (17)$$

7. Numerical studies

[This Chapter was adapted from C. Gahan's MRes Thesis dissertation, 2004]

A series of numerical simulations were undertaken to assess the impact of air pockets on hydraulic transients in pipelines. This Chapter, which is a summary of Gahan (2004), provides details on the background to the work, a summary of the methodology used in the assessment, and a description of the test results.

7.1 BACKGROUND

The main aim of the numerical study was to examine the potentially enhanced failure risk of pipelines subject to pressure transients as a consequence of the formation of small air pockets along the pipeline.

Air can become entrapped in pipeline systems through various operational activities with potentially destructive consequences, in terms of cost, safety, whole-life span and environmental damage. Typical problems that can result as a consequence of the presence of air, with particular relevance to water pipelines include:

- Irregular running of pumps, which can lead to long-term damage to impellers and casings.
- Pressure fluctuations due to movement and expansion/contraction of entrapped air pockets, causing vibration damage to pipes, fittings and supports.
- Increased risk of gaseous cavitation (in areas of low pressure).
- Increased risk of pipe rupture due to ‘waterhammer’ pressure surges.
- Increased head losses due to flow restrictions at air pockets.

Significant costs are incurred in an attempt to control the entry and release of air in pipelines with varying degrees of success. Control measures include: air release valves, air chambers and air vessels, however dependent upon the fluid medium, topography or location of the pipeline, it may not be possible to install such devices.

Upon consideration of the consequences of air on pipeline systems, in terms of design, construction, long-term maintenance and potential hazards, there is therefore a need for improved guidance for designers and operators on practical methods of dealing with air problems in pipelines. It is also important that current methods of analysis are modified to adequately allow for the contributory factors which can exacerbate these problems.

7.1.1 *Pressure transients*

Pressure transients in pipeline systems are caused by the interruption to fluid flow arising from operational changes, affecting the various boundary conditions which dictate behaviour. These can include starting/stopping of pumps, changes to valve settings, changes in power demand, action of reciprocating pumps and vibration of impellers or guide vanes in pumps etc.

In terms of operational performance, the effects of entrapped or entrained air on surge pressures experienced by a pipeline can be either beneficial or detrimental and will be entirely dependent on the characteristics of the pipeline concerned and the nature and cause of the transient. The existence of entrained air bubbles within the fluid, together with the presence of pockets of air complicates the analysis of the transient pressures and makes it increasingly complicated to predict the true effects on surge pressures (Wylie and Streeter, 1978).

7.1.2 *Entrapped air*

Air pockets can develop in a pipeline by bubble entrainment through the action of pump suction and by air release as the water pressure reduces. The former can result from poor suction well design and through operation cycling which permits excessive drawdown before pump switching or shutdown and the latter by the failure of an air release valve to expel the entire pocket of air.

Under low pressures the phenomenon of gas release, or cavitation, creates vapour cavities which, when swept with the flow to locations of higher pressure or subject to the high pressures of a transient pressure wave, can collapse suddenly creating further ‘impact’ pressure rise, potentially causing severe damage to the pipeline.

Many publications highlight the potential for the presence of air pockets to be further detrimental to pipelines subjected to un-suppressed pressure transients and localised cavitation such that underestimation of peak pressures might result.

Such references include:

- Jonsson (1985) showed that in certain circumstances pressures could be enhanced by the presence of air.
- Larsen and Burrows (1992), performing various simulations using the commercial package, WHPS.
- Burrows and Qiu (1995), where numerical air pocket studies were conducted using the analytical model, PTPSliv.for, developed by Qiu (1995).

In contrast to the above, the speed of travel of an induced (transient) pressure wave can be greatly reduced and its amplitude dampened. Two scenarios apply for this statement to be correct, in summary these are:

- If gas bubbles are distributed evenly throughout the liquid, the transient wave propagation speed can be greatly reduced (Wylie and Streeter, 1978).
- If the pockets are large they behave as an air ‘cushion’ and reflect and absorb the energy of the transient pressure wave (Thorley, 2004).

In addition to the effect on pressure transients, problems caused by the presence of air include:

- A reduction in pipe capacity which affects the original hydraulic analysis of a pipeline system.
- Reduced pump and turbine efficiency.
- False readings on measuring devices.
- Fluid medium property changes – including density and elasticity.
- Potential for buoyancy problems for underwater pipelines, and
- In certain pipelines, increased the risk/occurrence of erosion.

A detailed literature review on the effects of entrained and entrapped air on pressure transients in water pipelines is provided in Gahan (2004) and Lauchlan et al (2004).

7.2 COMPUTATIONAL MODEL

The computation model of Qiu (1995) was used for the simulations. It was developed for the specific purpose of establishing a numerical model to demonstrate the effect of entrapped free pockets of air upon surge pressure levels during pump shut-down and trip-out within a pipeline.

Details of the program (called PTPS) and how it was applied to the present study are given in Gahan (2004). A comprehensive review of the program can be found in Qiu (1995).

7.3 SIMULATION PROCEDURE

The purpose of the simulations was to assess through a detailed analysis the susceptibility of transient response of a pipeline to both the size and location of air pockets. It was decided that the most appropriate methodology was to choose several volumes of air pockets and follow the migration of an individual air pocket along a pipeline profile.

7.3.1 *Background*

The pipeline profile chosen for the tests was initially considered by Burrows and Qui (1996) and Burrows (2003). It is based on a real sewage pipeline in the UK. The section of the pipeline simulated consists of a sewage rising main section, which is downstream of a three-unit pumping station and is connected to a downstream gravity main (simulated by a downstream reservoir). The rising main section was constructed in 1971 from cast iron and was subject to several fractures between 1979 and 1992.

From the initial design calculations performed it was determined that surge suppression was required as cavitation was shown to be highly probable along almost the full length of the pipeline unless slow valve opening could be guaranteed (Burrows, 2003). As the likelihood of being able to ensure a slow and controlled valve opening for both pump start-up and shut-down is remote, a surge vessel was constructed just downstream of the pumps.

Although indications from the relevant parties suggested that several bursts occurred prior to 1989, as no detailed information exists these incidents could not be assessed and the two events which required further investigation work to be conducted were recorded to have happened in 1989 and 1992. Both events resulted in major incidents for the water authority and they incurred high costs both due to the required repair and from litigation by the private landowners in the immediate vicinity of the incidents.

Prior to the incident in 1989, the surge vessel was condemned by insurers and taken out of service. Coincident with this, further hydraulic assessment was made of the pipeline and it was determined that surge suppression was not required and consequently the surge vessel was not replaced. Following this decision a pipe failure occurred just downstream of the pumping station. A further failure, recorded to be beneath the highway cutting, i.e. following a local high point along the profile of the rising main, occurred in August 1992 (Burrows, 2003).

A study was conducted in order to evaluate potential causes and contributory factors for the failures by Burrows and Qiu (1996). The results of this assessment were re-evaluated more recently, by Burrows (2003).

The current study is not intended to further evaluate the failures experienced along this rising main but has been conducted to specifically consider certain air pocket effects (size and location) upon a 'real-life' case study. The results found herein are in addition to those previously obtained and it is therefore considered important to summarise the main points of the two previous post-failure assessments, as follows:

- The results of the analytical model showed that without a surge vessel the pipeline would be subject to severe pressure fluctuations, with minimum pressures resulting in cavitation. These results were obtained when no or very small pockets of air were incorporated at the local highpoint of the rising main.

- The results of the simulation showed a peak pressure at the pump exit, with no air present in the pipeline, of 67.8mwc. The simulation was repeated with several volumes of air and it was found that with a volume of air of 0.015 m³, the maximum pressures were increased to 108m at the pump exit.
- The results of the simulation showed a peak pressure under the highway, with no air present in the pipeline, of 45m. It was found that with a volume of air of 0.015 m³, the maximum pressures were increased to 70m.

*Note: Recommended working stress for grey iron, class B = 61.2m pressure head
 Pipeline nominal strength = 152m pressure head
 Test pressure for commissioning = 122m pressure head*

7.3.2 Model Description

As has been highlighted in the previous section, for the pipeline profile chosen, cavitation is likely to occur along its full length and therefore to evaluate the contributory effects of this, the profile of the pipeline has also been modelled as horizontal in order to avoid the onset of extensive cavitation. The case study using the original profile is referred to as CASE 13, while the horizontal profile case is CASE 15.

The case study has been modelled as a rising main, with a single pump drawing from a sump at its upstream end, pumping to a reservoir at its downstream end. The 'real' profile of the rising main (Figure 16) crosses over a highway cutting and has several local highpoint.

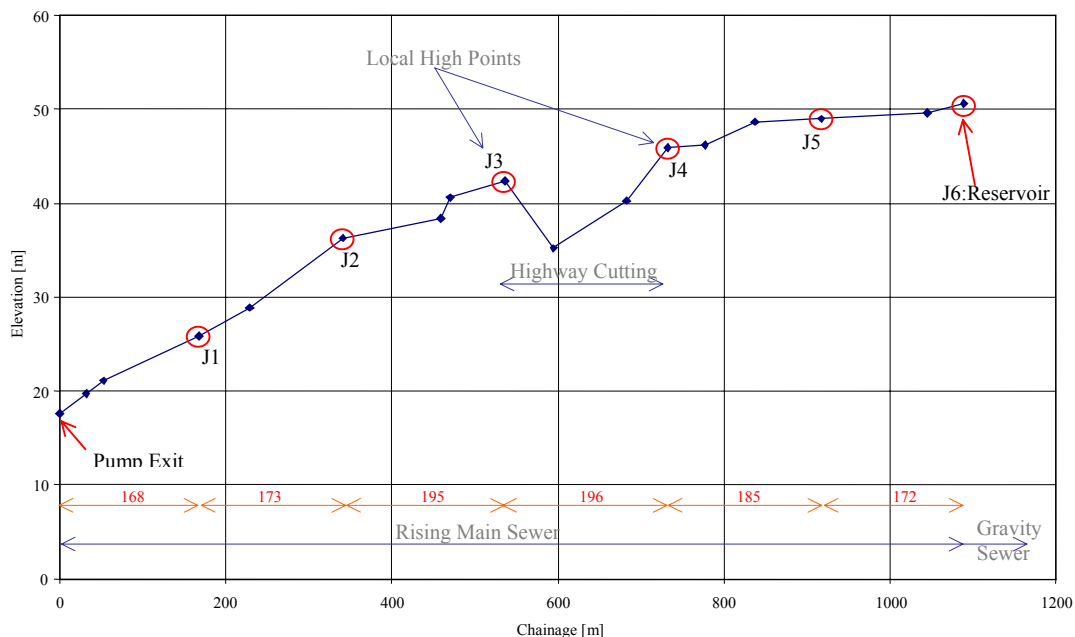


Figure 16 Pipeline profile

The data for the test profiles used are given in Table 16.

Pipe data

Pipe diameter = 0.355 m

Pipe wall roughness = 0.0015 m

Wave celerity = 1051 m/s
Head losses coefficient in pumping station in internal pipe = 10.0
Pipe diameter in internal pipe in pumping station = 0.472 m
Static lift \approx 38 m
Dynamic lift \approx several metres

Medium data

Density = 1000 kg/m³
Viscosity = 0.001005
Absolute vapour head pressure = 0.0

Pump data

Moment of inertia = 0.001 kgm²; Later altered to 0.1 kgm²
Pump rated speed = 1470.0 rpm
Pump characteristic data is given in Table 17.

Simulation data – time

Time for simulation = 40 s
Simulation time-step = 0.01 s

Simulation data – Air pockets

Polytropic exponent = 12 (describing the behaviour of the gas in the pocket)
Volumes of air – 0.001, 0.01, 0.025, 0.05, 0.1, and 1.0 m³

7.3.3 Model validation

During the initial element of the work undertaken, it was considered appropriate to validate the results in order to assess the level of accuracy and to ensure that input data had been properly interpreted and entered into the program.

Both CASE 13 and CASE 15 have been previously analysed using the commercial package WHPS, an assessment of which being published previously. The input data files for this analysis were provided at the initial stages of study. These files were re-run using the PTPS package.

A detailed description of the validation work is given in Gahan (2004). It was found that there are minor differences between the output data for WHPS and PTPS which are within acceptable tolerances. It can be concluded that the PTPS results produce slightly more conservative predictions of head within a pipeline system, however, it is considered that valid results can be obtained. It was therefore considered appropriate to continue with the use of the program for the study.

7.4 ANALYSIS OF SIMULATION RESULTS

As previously discussed, the main computational analysis element of this study was performed in order to determine the susceptibility of transient response to both size of an air pocket and its location. Therefore upon completion of case study selection, data determination and computational validation, the analysis was performed by sequentially placing air pockets along the pipeline profile for both Cases 13 and 15. Six different air pocket volumes were tested.

Details of the data input and output files used in the testing can be found in Gahan (2004).

The results are summarised under the following headings:

- Series One – Total head vs. time – For specific volumes of air.
- Series Two – Total head vs. time – Examining surges at specific junctions.
- Series Three – Total head vs. distance – For specific volumes of air.
- Series four – Total head vs. distance – For specific air pocket locations.
- Series five – Total head vs. time – For specific air pocket location.

7.4.1 *Series One – total head vs. time; for specific volumes of air*

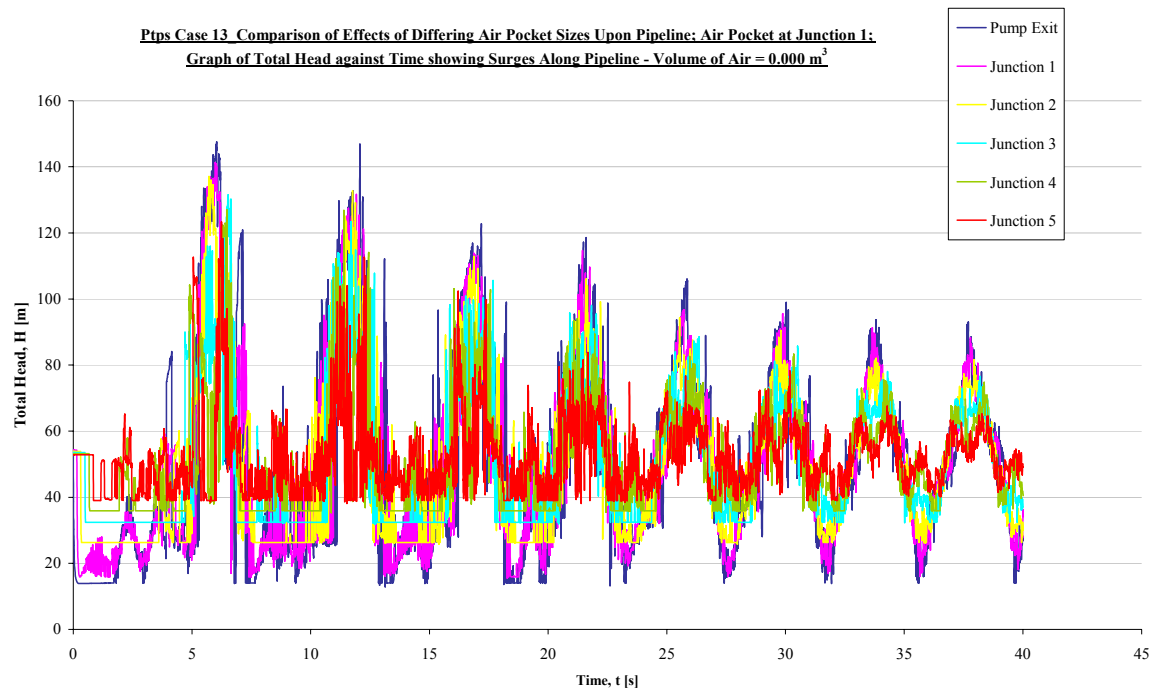
A summary of the Series One results is given in Table 18, which shows the critical locations for individual air pockets used in the simulations in terms of peak head. From the figures given in this section it can be seen that as small air pockets are introduced, variations in effect of location of air pocket become evident.

Volume of air = 0.0m³

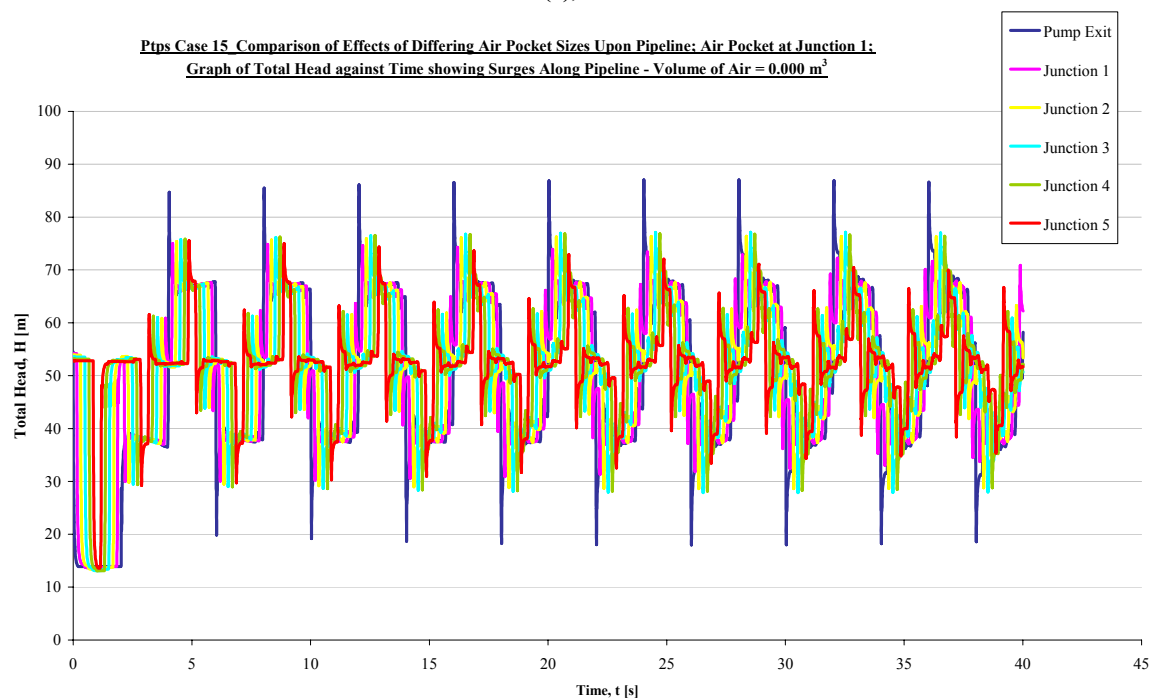
It can be seen in Figure 17 that, with no air pocket, peak pressures are higher towards the pump end of the pipeline profile, with decreasing pressures along the pipeline to a minimum peak at the reservoir end. Upon examining the table of figures from which these plots are made cavitation does not occur in the CASE 15 simulation, but occurs along the majority of the profile for CASE 13. As the maximum pressure for CASE 15 is approximately 40% lower than for CASE 13, the effect of cavitation (and profile) upon the pressures occurring within the system are apparent. All values given are in terms of total head (m).

Maximum Pressure: CASE 13 \approx 148m CASE 15 \approx 88m at Pump Exit

The following figures correspond to the most critical conditions.



(a), 'CASE 13'



(b), 'CASE 15'

Figure 17 Comparison of the Effects of Differing Air Pocket Sizes showing Total Head with Time for no air pocket

Volume of air = 0.001m^3

Plots of the maximum peak pressures that occurred at junctions along the pipeline are given in Figures 18 and 19. They show that peak pressures are higher towards the pump end of the pipeline profile, with decreasing pressures along the pipeline to a minimum peak at the reservoir end. High peaks were also achieved when the air pockets were placed at Junction 6, possibly due to reflection of the transient wave from the reservoir.

For CASE 13, the highest peak is achieved when the air pocket is placed at Junction 2 with the lowest overall peak pressure occurring when the air pocket is placed at Junction 1. For CASE 15, pressures throughout the pipeline over the 40 second simulation remain more erratic, with the effects again maximised when the air pocket is placed at the higher end of the pipeline profile – Junctions 1 and 2.

All peak values were recorded at the pump exit of the profile.

		<u>CASE 13</u>	<u>CASE 15</u>
Air at Junction 1	>	Total Head $\approx 110\text{m}$	$\approx 106\text{m}$
Air at Junction 2	>	Total Head $\approx 148\text{m}$	$\approx 104\text{m}$
Air at Junction 3	>	Total Head $\approx 138\text{m}$	$\approx 93\text{m}$
Air at Junction 4	>	Total Head $\approx 121\text{m}$	$\approx 90\text{m}$
Air at Junction 5	>	Total Head $\approx 118\text{m}$	$\approx 87\text{m}$
Air at Junction 6	>	Total Head $\approx 117\text{m}$	$\approx 88\text{m}$

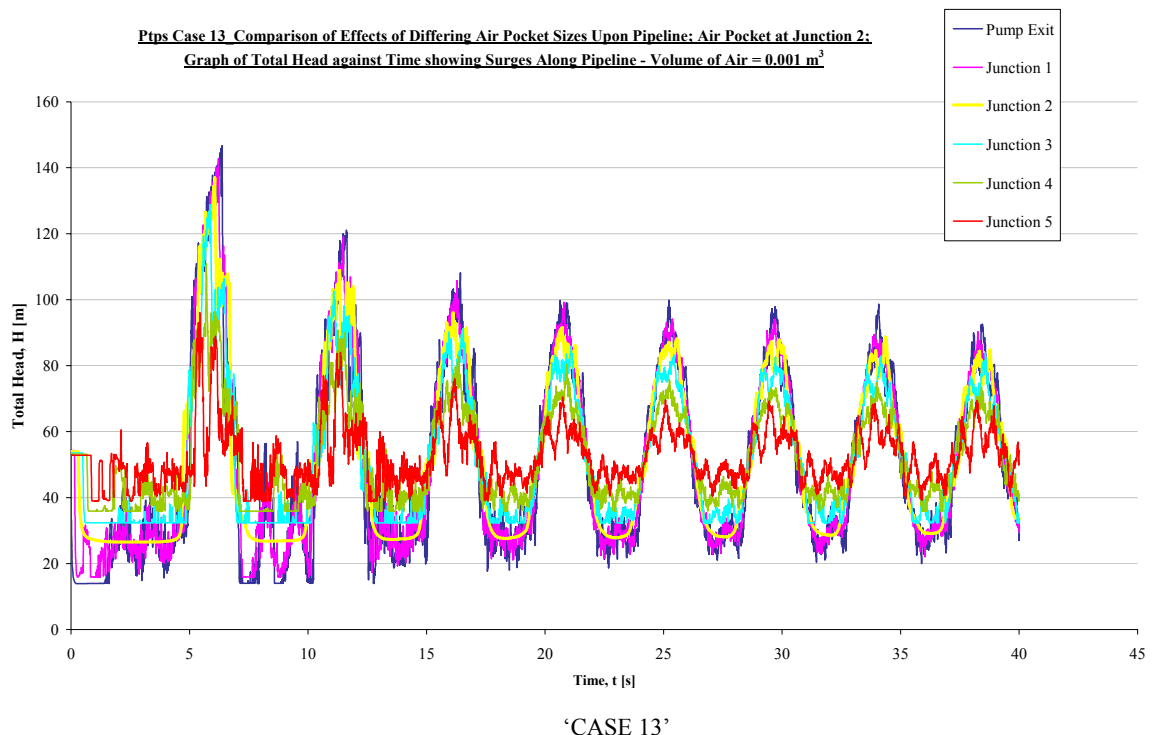


Figure 18 *Comparison of the Effects of Differing Air Pocket Sizes when placed at Junction 2 showing Total Head with Time for Volume of Air = 0.001 m^3*

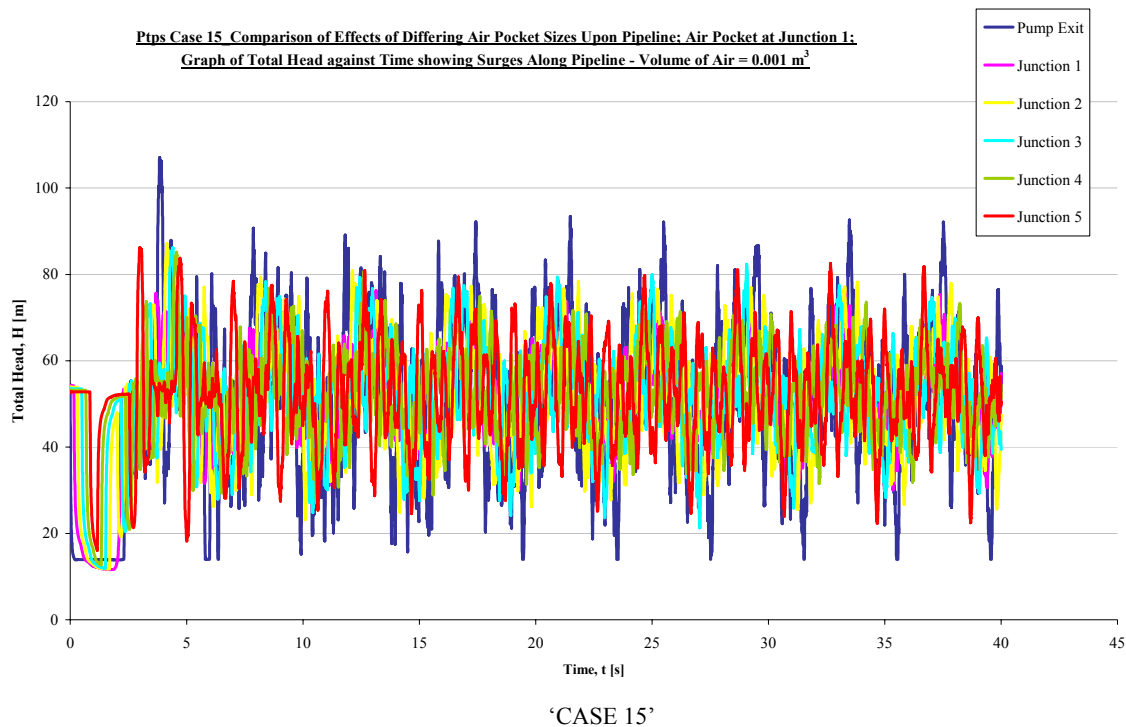


Figure 19 ***Comparison of the Effects of Differing Air Pocket Sizes when placed at Junction 1 showing Total Head with Time for Volume of Air = 0.001 m³***

Volume of air = 0.01m³

The peak pressures obtained in the simulations are shown in Figure 20. The peak pressures are higher towards the pump end of the pipeline profile, with decreasing pressures along the pipeline to a minimum peak at the reservoir end. As the air pocket size is increasing, a mass oscillation pattern is more evident, with evidence of narrow peaks and elongated troughs, typical of a pressure wave inside an isolated air cushion (Jonsson, 1985).

There is also some evidence of the air pocket acting partially as a ‘cushion’ with the frequency of oscillation decreasing and mass oscillation apparent downstream, however peaks are amplified both up and downstream, therefore the air pocket does not have any beneficial effect on the pressure regime within the pipeline.

For CASE 13, a clear peak is evident, whereas for CASE 15, the pressures remain generally high with the air placed at all locations along the pipeline profile, however the highest overall pressures occur at the pump exit.

All peak values were recorded at the pump exit of the profile.

		<u>CASE 13</u>	<u>CASE 15</u>
Air at Junction 1	>	Total Head ≈ 150m	≈ 164m
Air at Junction 2	>	Total Head ≈ 148m	≈ 145m
Air at Junction 3	>	Total Head ≈ 142m	≈ 118m
Air at Junction 4	>	Total Head ≈ 139m	≈ 88m
Air at Junction 5	>	Total Head ≈ 117m	≈ 103m
Air at Junction 6	>	Total Head ≈ 116m	≈ 88m

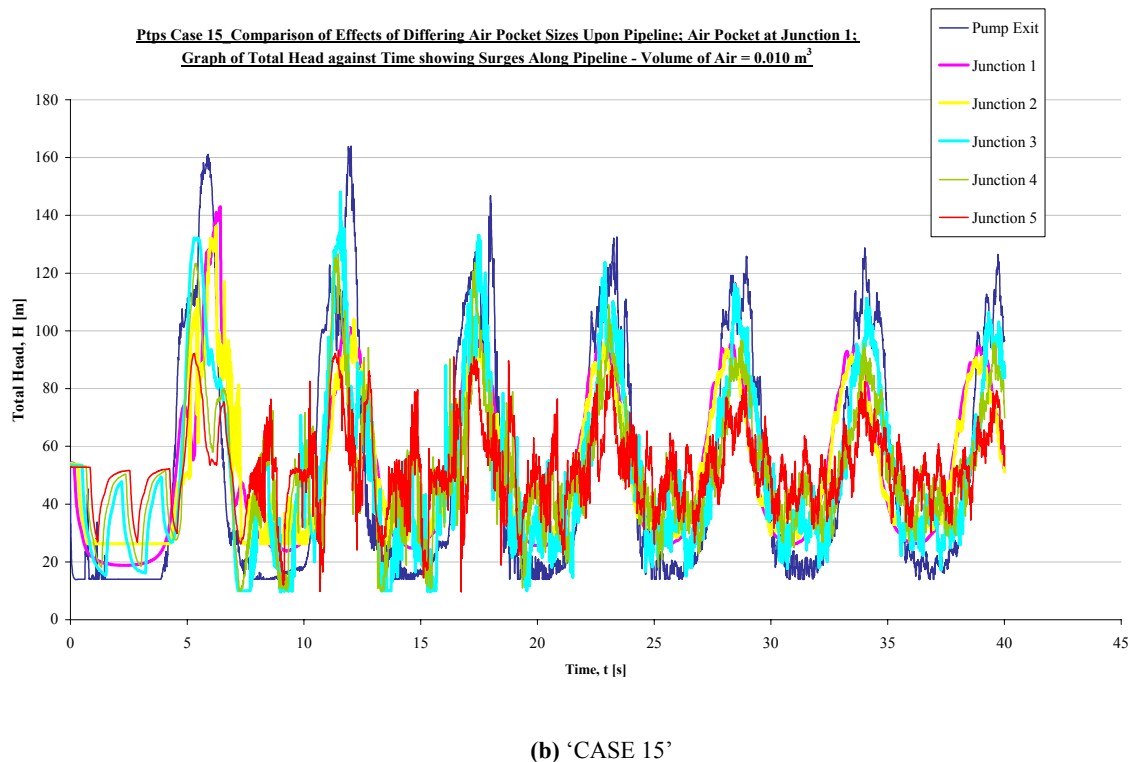
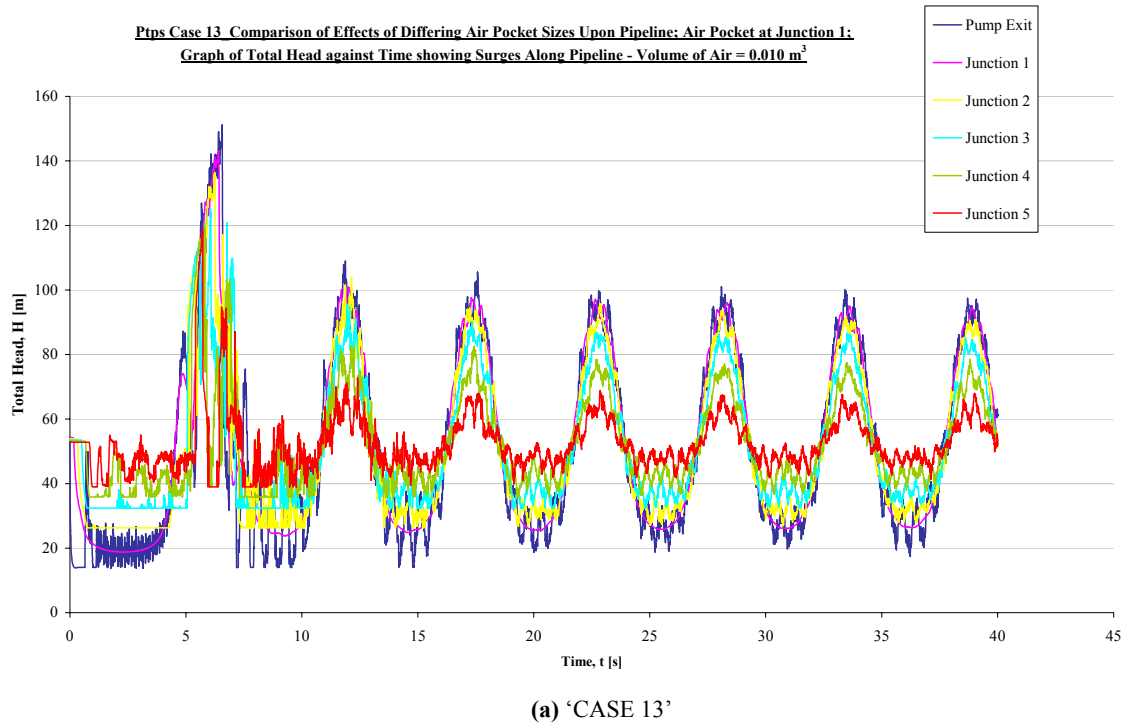


Figure 20 *Comparison of the Effects of Differing Air Pocket Sizes when placed at Junction 1 showing Total Head with Time for Volume of Air = 0.010 m^3*

Volumes of air = 0.025m³

The upper sections of the pressure head profiles (Junctions 1 to Junctions 3/4) showed similar results (Results for Junction 1 shown in Figure 21). All gave the minimum peaks at the reservoir end of the pipeline with the maximum peak pressures recorded at the pump exit. Mass oscillations are evident when considering the surge pressures at the intersection/meeting point with an air pocket which shows some evidence of absorption of wave energy – particularly evident from CASE 13 as generally higher pressures are involved.

Again the higher peaks are consistently displayed at the pump exit along the profile of the pipeline for all air pocket locations apart from when the air pocket is placed at Junction 5. When the air pocket is placed at Junction 5, the recorded pressures at Junction 5 are greater than those recorded at Junctions 3 and 4. This could possibly be due to an accumulation of the transient wave effect on pressures with this particular air pocket size

All peak values were recorded at the pump exit of the profile.

		<u>CASE 13</u>	<u>CASE 15</u>
Air at Junction 1	>	Total Head ≈ 148m	≈ 148m
Air at Junction 2	>	Total Head ≈ 146m	≈ 138m
Air at Junction 3	>	Total Head ≈ 145m	≈ 128m
Air at Junction 4	>	Total Head ≈ 142m	≈ 109m
Air at Junction 5	>	Total Head ≈ 138m	≈ 113m
Air at Junction 6	>	Total Head ≈ 116m	≈ 88m

From this it can be seen that, for CASE 13, all locations for the air pocket, except for Junction 6, result in a similar peak reading at the pump exit.

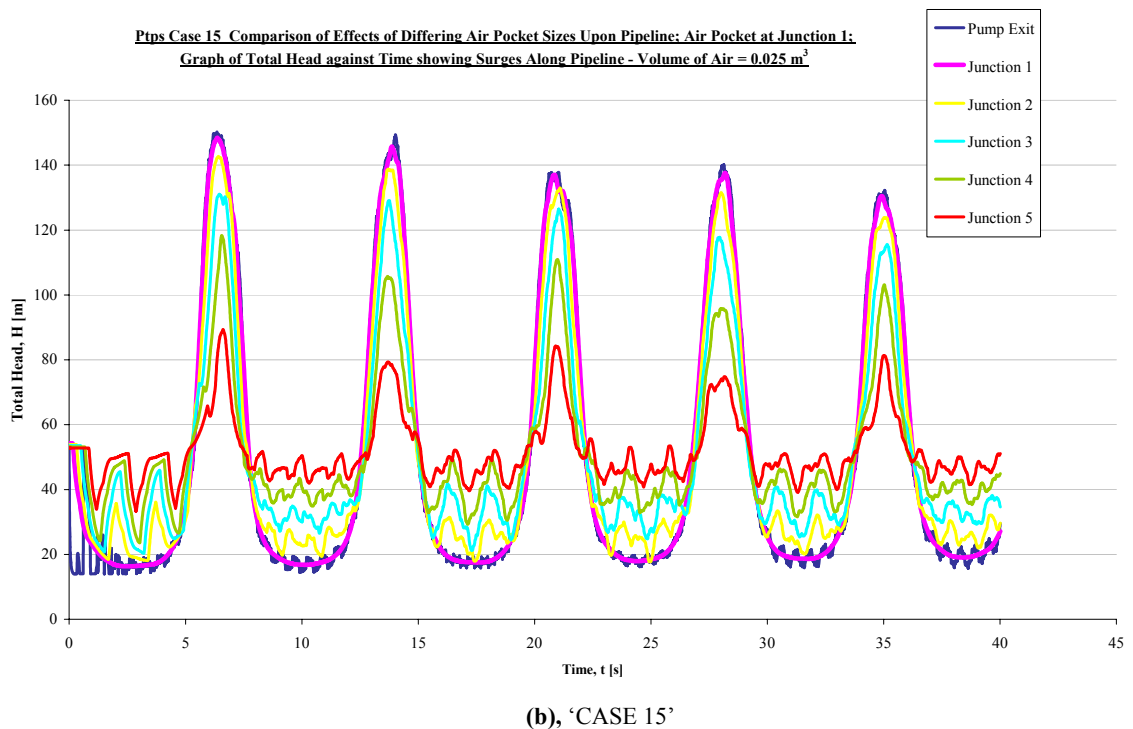
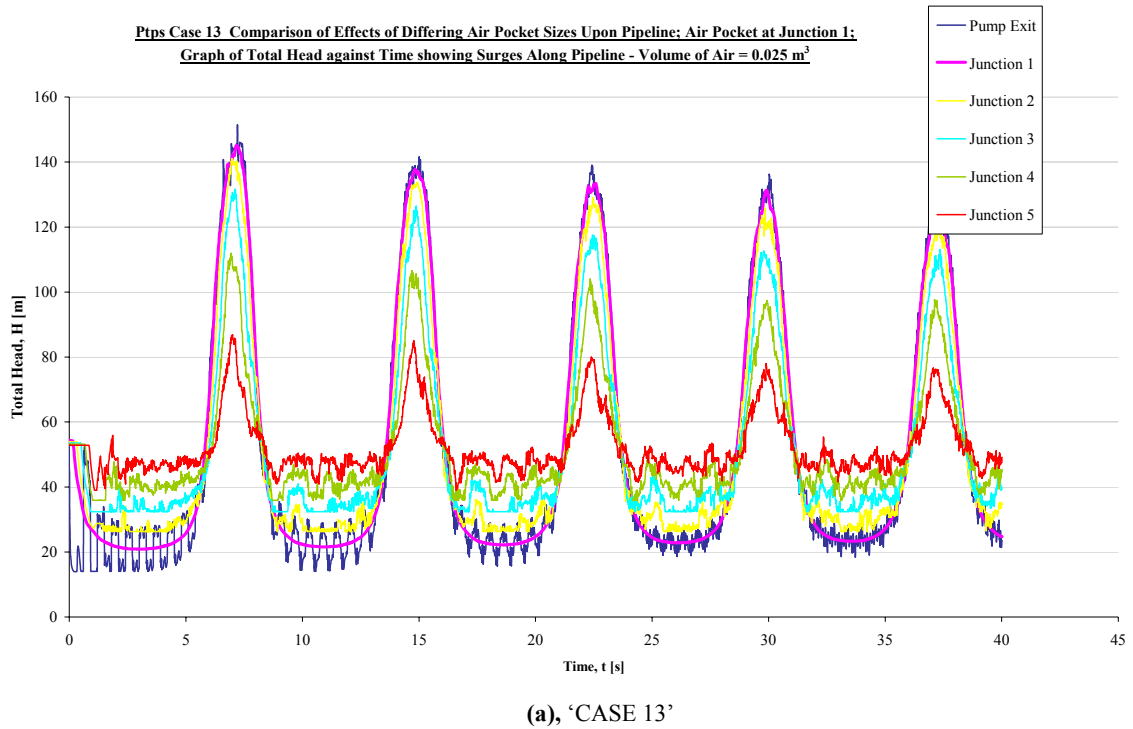


Figure 21 *Comparison of the Effects of Differing Air Pocket Sizes when placed at Junction 1 showing Total Head with Time for Volume of Air = 0.025 m³*

Volume of air = 0.05m³

The results show that for an increased size of air pocket at Junctions 1, 2, 3 and 4, longer period mass oscillations occur to a greater extent for both CASES 13 and 15,

although frequency is greater for the horizontal profile. For example, Figure 22 shows the resulting profile for Junction 1.

As with the previously discussed results, pressures are greater at the pump exit than towards the reservoir end of the pipeline profile and higher peaks are achieved throughout when the location of the air pocket is at the upstream end of the pipeline.

All peak values were recorded at the pump exit of the profile.

		<u>CASE 13</u>	<u>CASE 15</u>
Air at Junction 1	>	Total Head \approx 156m	\approx 150m
Air at Junction 2	>	Total Head \approx 141m	\approx 138m
Air at Junction 3	>	Total Head \approx 140m	\approx 133m
Air at Junction 4	>	Total Head \approx 139m	\approx 119m
Air at Junction 5	>	Total Head \approx 123m	\approx 109m
Air at Junction 6	>	Total Head \approx 117m	\approx 87m

As can be seen from the above readings, the upstream air pocket locations give the higher peak pressures at the pump exit – this effect is magnified when looking at the results from CASE 15. This is possibly due to the effect of reflection of the transient wave by the air pocket, however the size of the air pocket being such that the energy is not absorbed sufficiently to reduce peaks but contributes to an accumulation effect. The effect of the pocket further downstream is that the transient pressures have reached their peak earlier and the results of reflection are not so great.

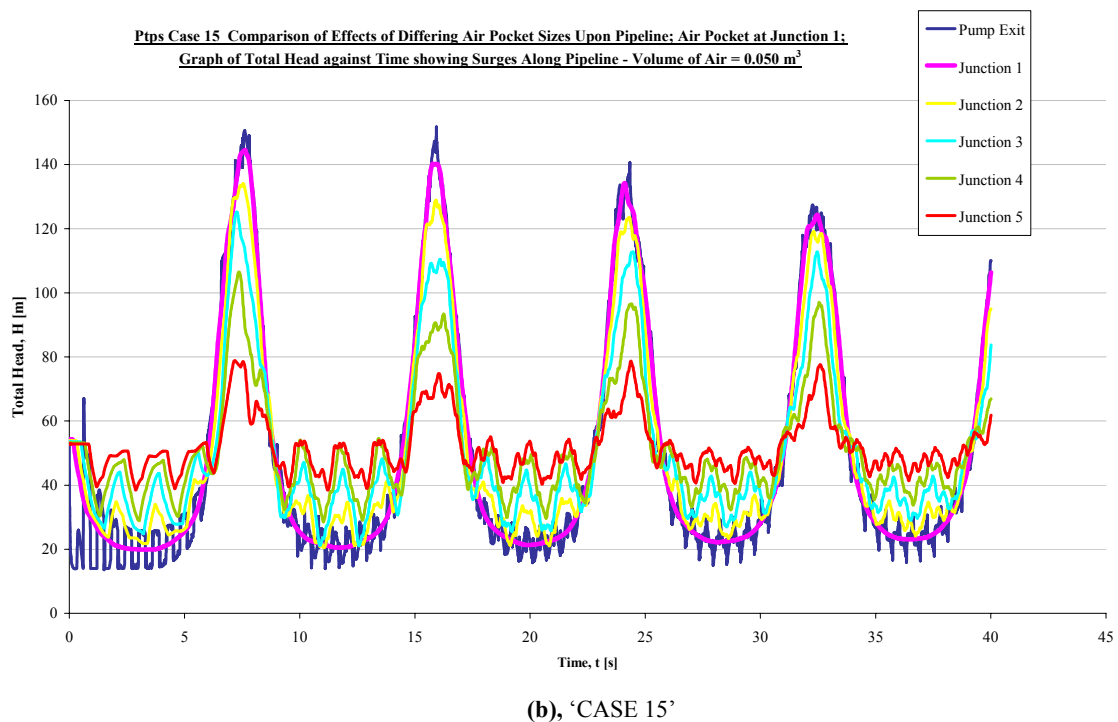
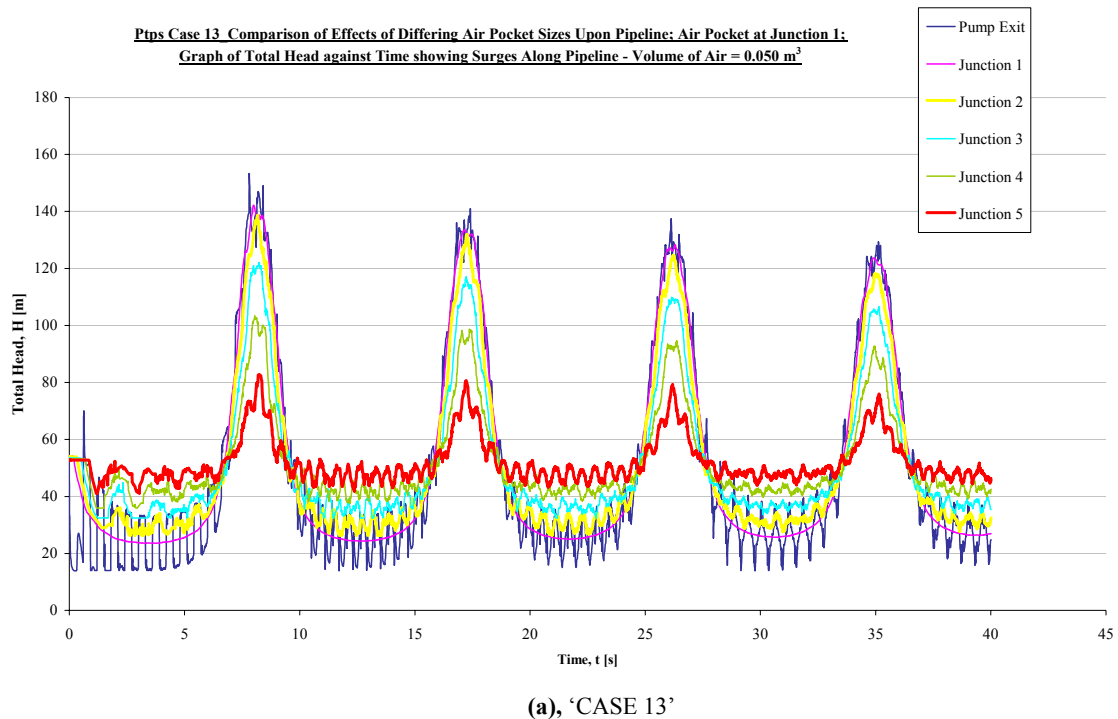


Figure 22 *Comparison of the Effects of Differing Air Pocket Sizes when placed at Junction 1 showing Total Head with Time for Volume of Air = 0.05 m³*

Volume of air = 0.1m³

For air volumes of 0.1m³ it was found that pressures are greater at the pump exit than towards the reservoir end of the pipeline profile and higher peaks are achieved

throughout when the location of the air pocket is towards the upstream end of the pipeline. Results for Junction 1 are shown in Figure 23.

Also, for CASE 13, when the air pocket is placed at Junction3 - local high point - the first peak pressures achieved are not the highest suggesting that the elevation at this point effects the way in which the transient wave ‘travels through’ the air pocket.

All peak values were recorded at the pump exit of the profile.

		<u>CASE 13</u>	<u>CASE 15</u>
Air at Junction 1	>	Total Head \approx 157m	\approx 148m
Air at Junction 2	>	Total Head \approx 132m	\approx 129m
Air at Junction 3	>	Total Head \approx 120m	\approx 118m
Air at Junction 4	>	Total Head \approx 115m	\approx 109m
Air at Junction 5	>	Total Head \approx 109m	\approx 100m
Air at Junction 6	>	Total Head \approx 114m	\approx 85m

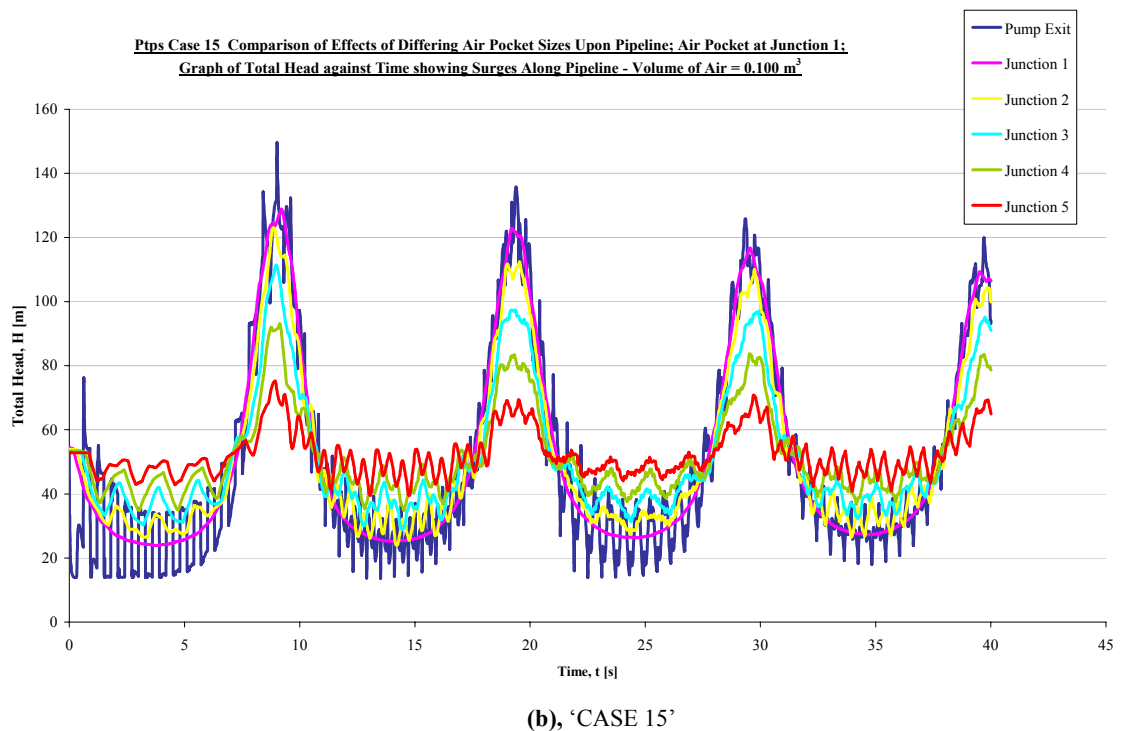
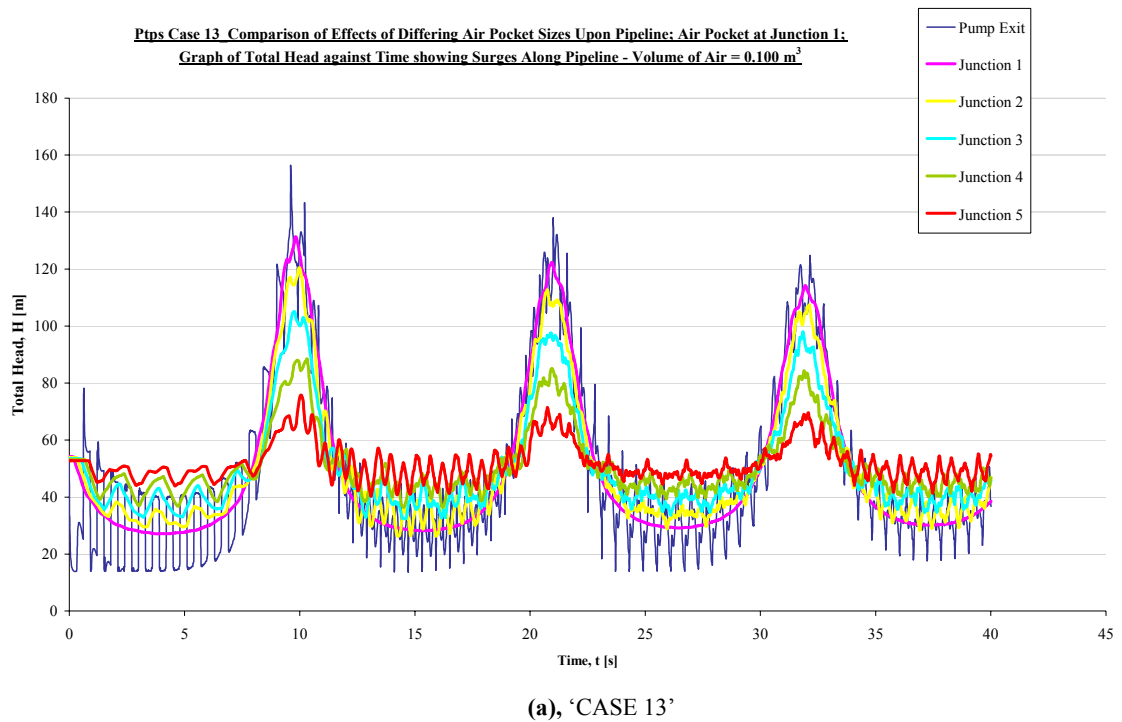


Figure 23 *Comparison of the Effects of Differing Air Pocket Sizes when placed at Junction 1 showing Total Head with Time for Volume of Air = 0.1 m^3*

Volume of air = 1.0m³

As this pocket is relatively large, the results from these simulations display the absorption of the transient pressure wave by the air pocket. This is shown from where the wave meets with a location of air pocket in the pipeline. The pocket is large enough to absorb the energy of the transient wave, resulting in a long period mass oscillation at the point of interception and downstream of this point. The reflected energy creates a higher frequency oscillation upstream of the air pocket, but of a reduced magnitude for CASE 13 when compared to the 'NO AIR' model. For CASE 15, all peaks are slightly higher than for the 'NO AIR' model. Peak results for these simulations are shown in Figures 24 and 25.

All peak values were recorded at the pump exit of the profile.

		<u>CASE 13</u>	<u>CASE 15</u>
Air at Junction 1	>	Total Head \approx 105m	\approx 107m
Air at Junction 2	>	Total Head \approx 98m	\approx 94m
Air at Junction 3	>	Total Head \approx 88m	\approx 100m
Air at Junction 4	>	Total Head \approx 89m	\approx 95m
Air at Junction 5	>	Total Head \approx 106m	\approx 96m
Air at Junction 6	>	Total Head \approx 114m	\approx 85m

From the above set of results, it can be seen that there is a shift of 'critical' air pocket location for CASE 13 to Junction 6. This may be due to a greater amount of reflection accumulating at the pump exit as the transient wave is not absorbed at any earlier point. Therefore the pressures induced by the transient surge could accumulate and be reflected by the reservoir.

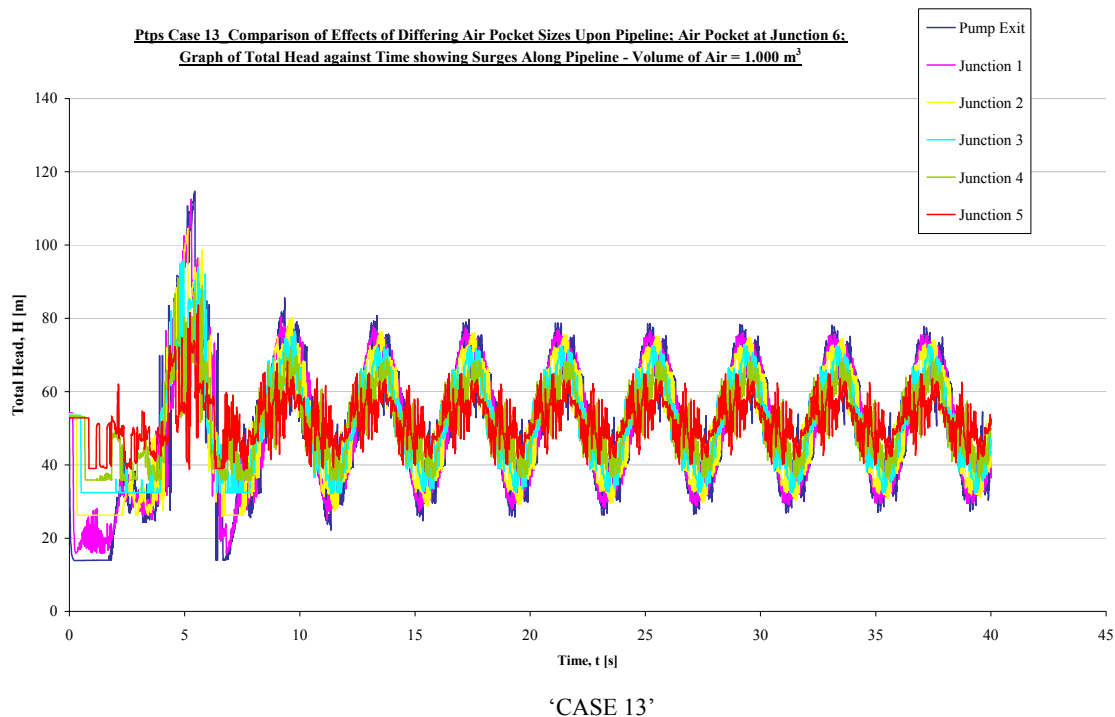


Figure 24 *Comparison of the Effects of Differing Air Pocket Sizes when placed at Junction 6 showing Total Head with Time for Volume of Air = 1.0 m³*

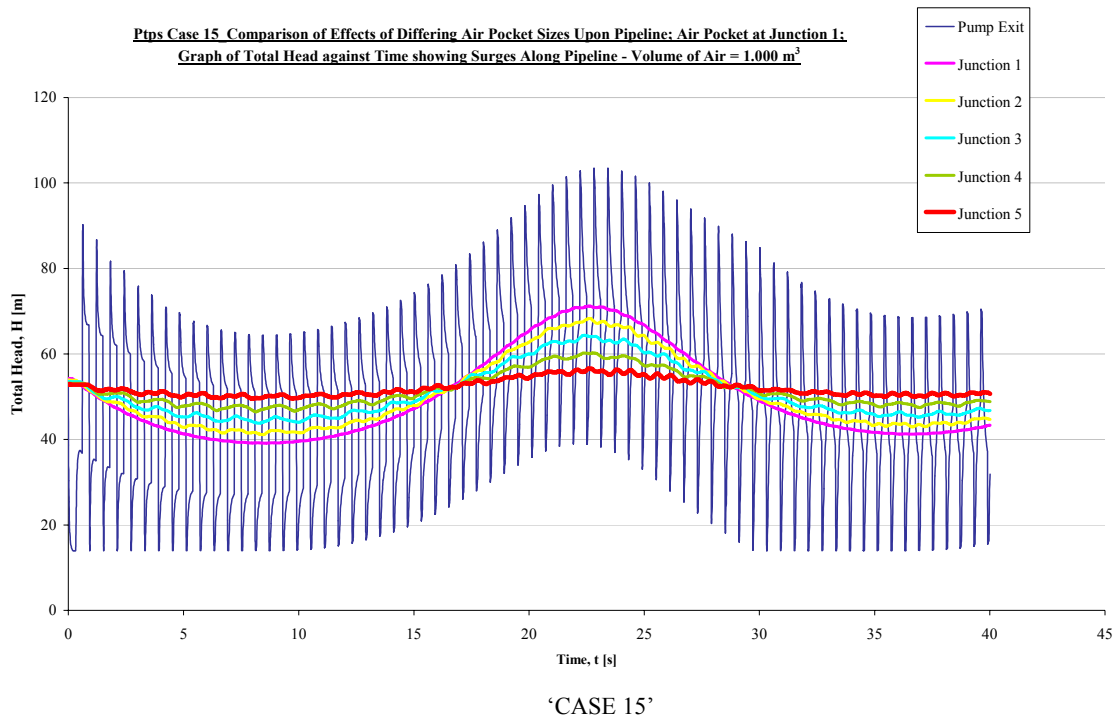


Figure 25 *Comparison of the Effects of Differing Air Pocket Sizes when placed at Junction 1 showing Total Head with Time for Volume of Air = 1.0 m³*

7.4.2 Series Two – total head vs. time; surges at specific junctions

A summary of the effects highlighted by this series of simulations is provided in Table 19.

In addition to Table 19, the following comments can also be made; A smaller air pocket has the potential to give peak pressures when placed at locations towards the upstream section of the pipeline and consequently has a greater influence on the surges at these upstream positions. The ‘NO AIR’ model produces the greater effects at downstream junctions for CASE 13.

From examining the results it is possible to suggest that a ‘band’ of smaller air pocket sizes can contribute to peak enhancement. Smaller than this size and ‘NO AIR’ would give the worst results and larger would result in absorption of the transient pressures.

7.4.3 Series Three – total head vs. distance; for specific volumes of air

From the resultant profiles shown in Figures 26 to 31 the following observations were made:

CASE 13 – Although the ‘NO AIR’ model follows closely the maximum pressures observed at the upstream section of the pipeline, the maximum values are recorded with the smaller pockets of air, 0.010 m³ to 0.050 m³ - this applies up to approximately Junction 3. From the local highpoint of the pipeline, the maximum pressures are given by the ‘NO AIR’ model.

CASE 15 – Generally the ‘NO AIR’ model gives the lowest maximum pressures – apart from 1.0 m³ over certain sections of the pipeline. Therefore it can be said that a lack of cavitation has a significant effect by lowering the pressures in the system with ‘NO AIR’, however the models which included small air pockets still reached similar peaks to CASE 13 as cavitation was present over the majority of the pipeline profile.

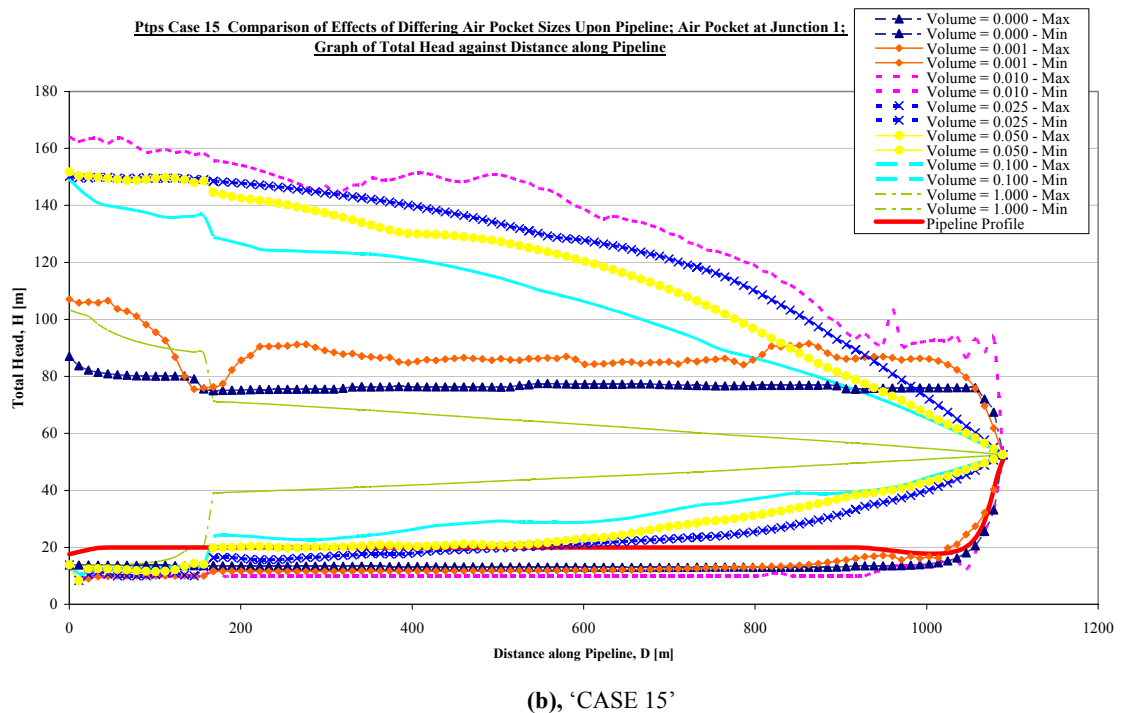
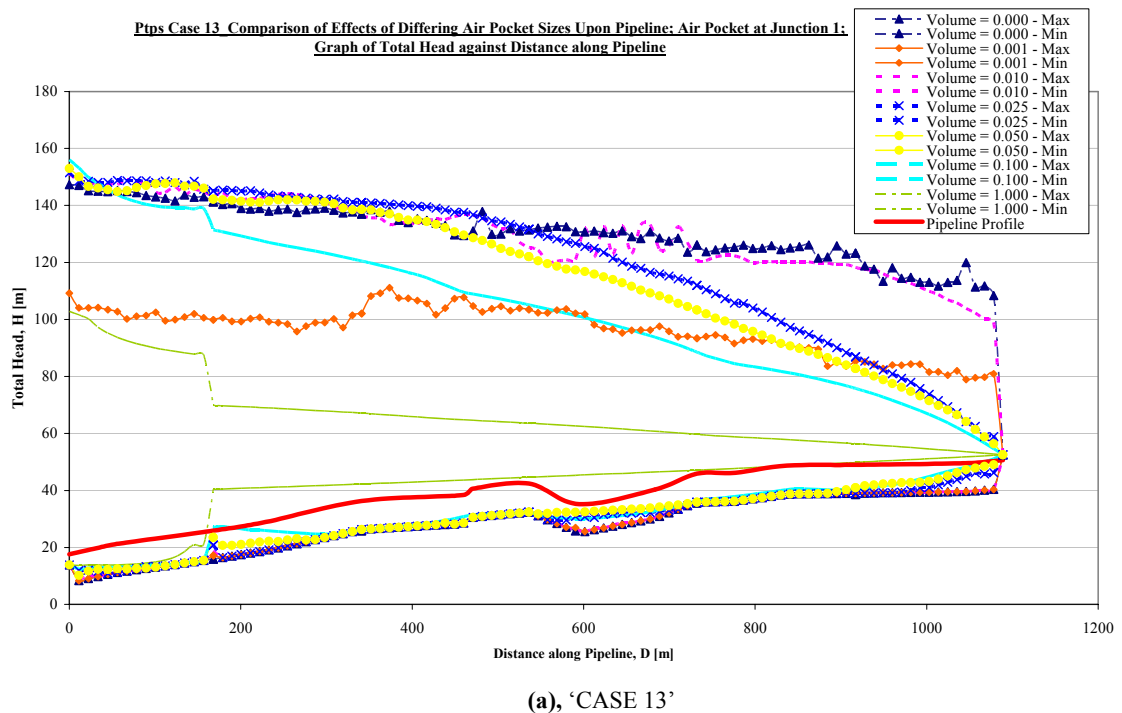
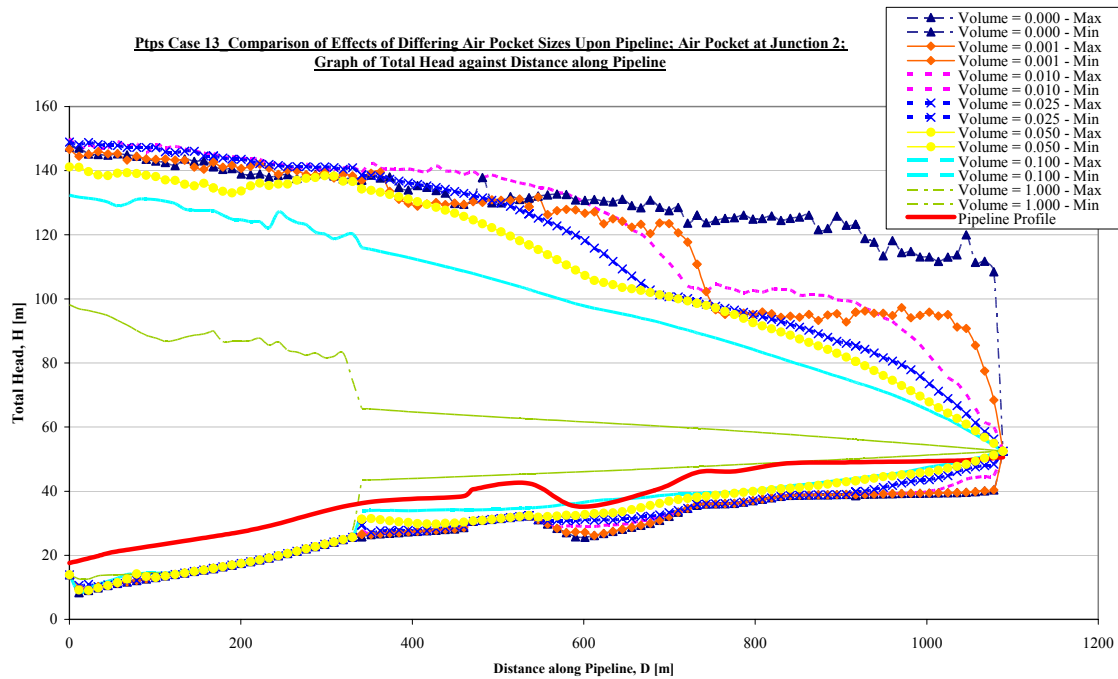
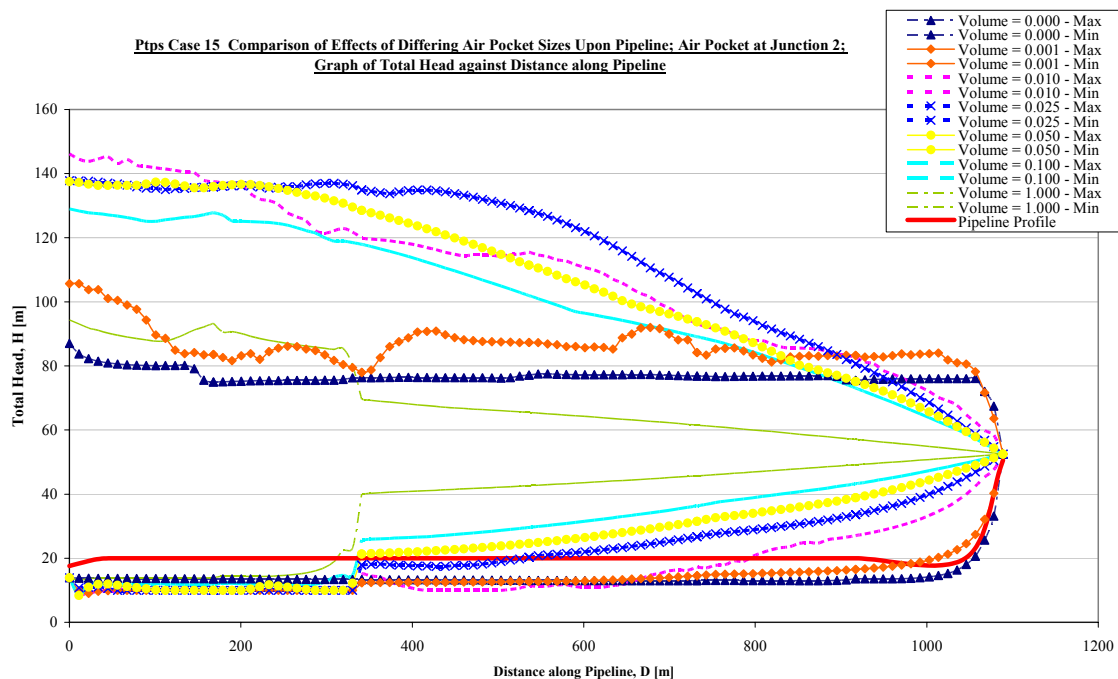


Figure 26 Comparison of the Effects of Differing Air Pocket Sizes when placed at Junction 1 showing Max/Min Head with Time



(a), 'CASE 13'



(b), 'CASE 15'

Figure 27 Comparison of the Effects of Differing Air Pocket Sizes when placed at Junction 2 showing Max/Min Head with Time

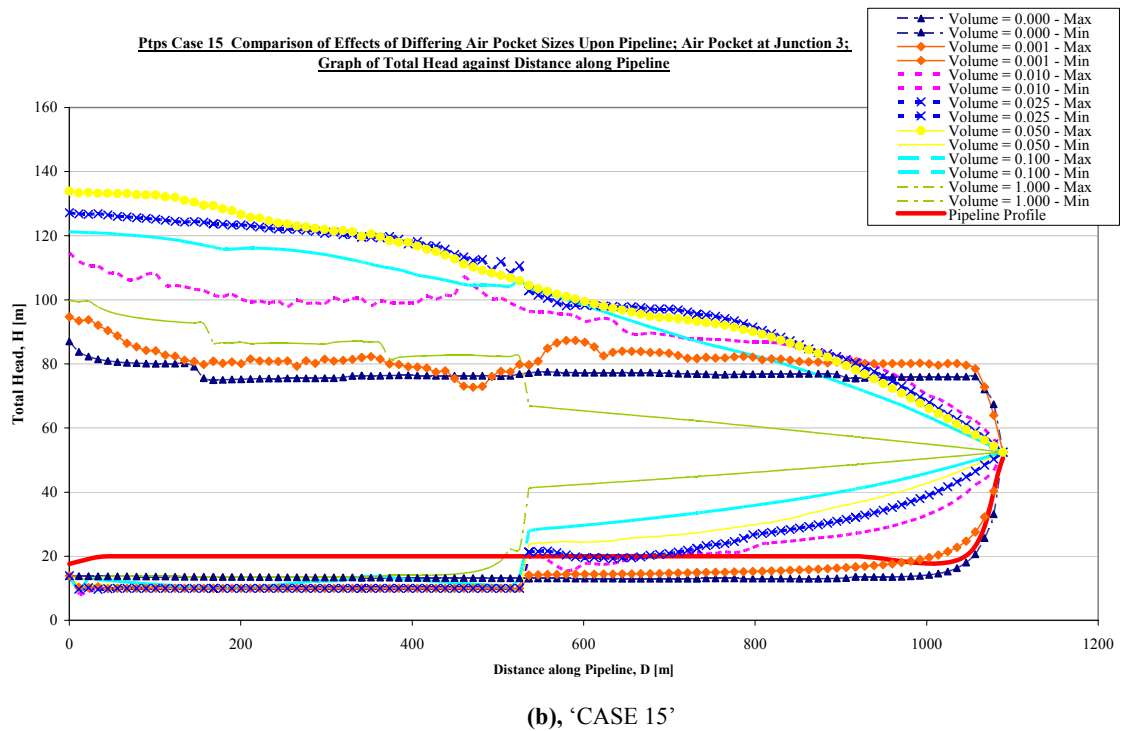
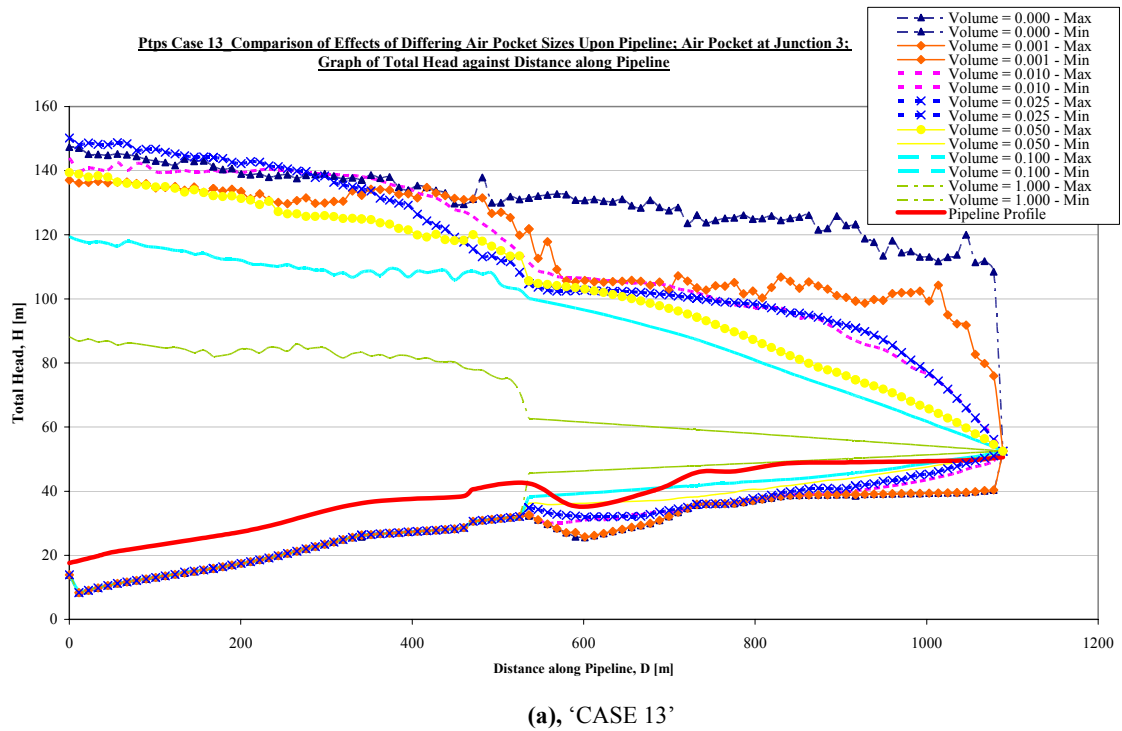
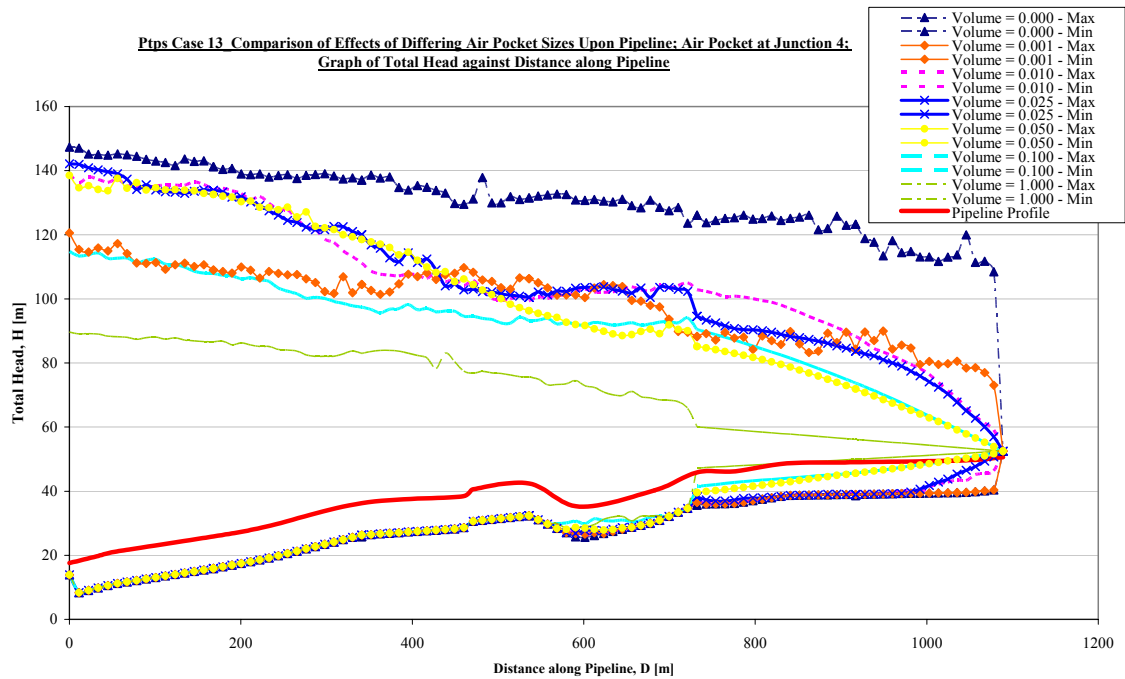
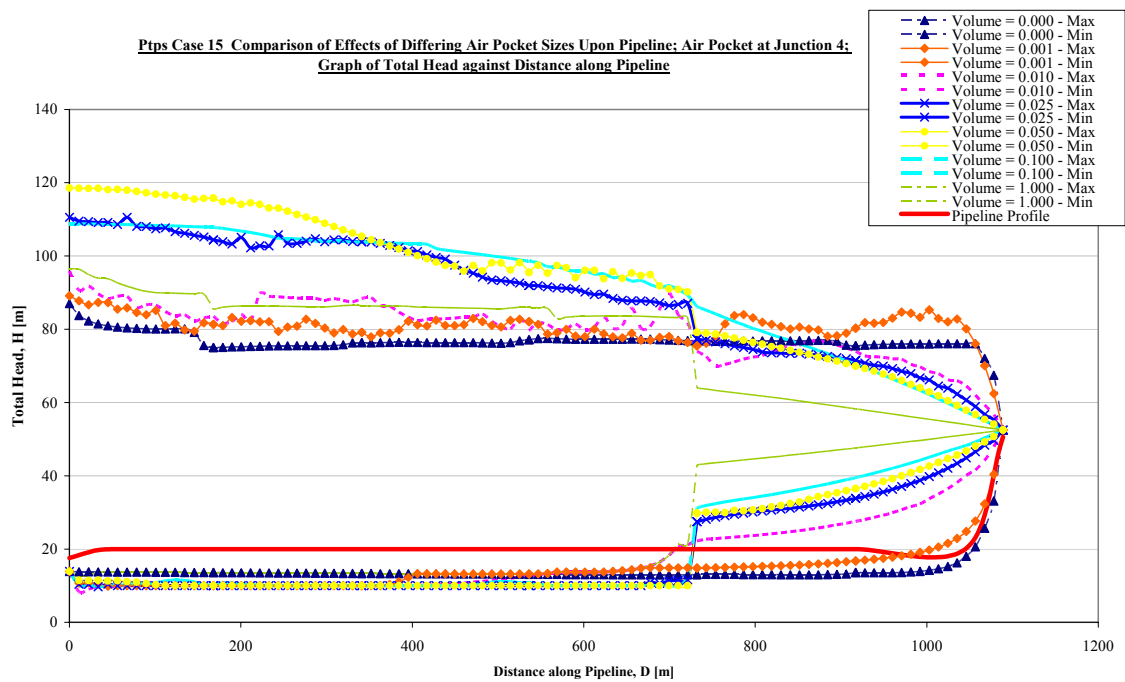


Figure 28 Comparison of the Effects of Differing Air Pocket Sizes when placed at Junction 3 showing Max/Min Head with Time

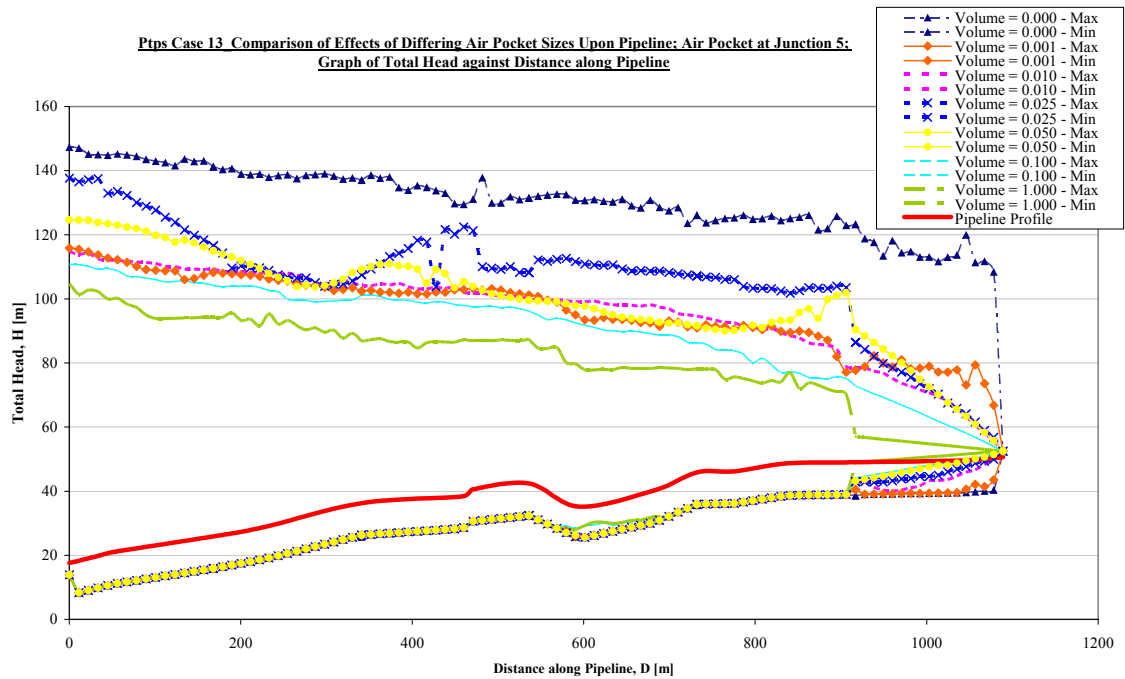


(a), 'CASE 13'

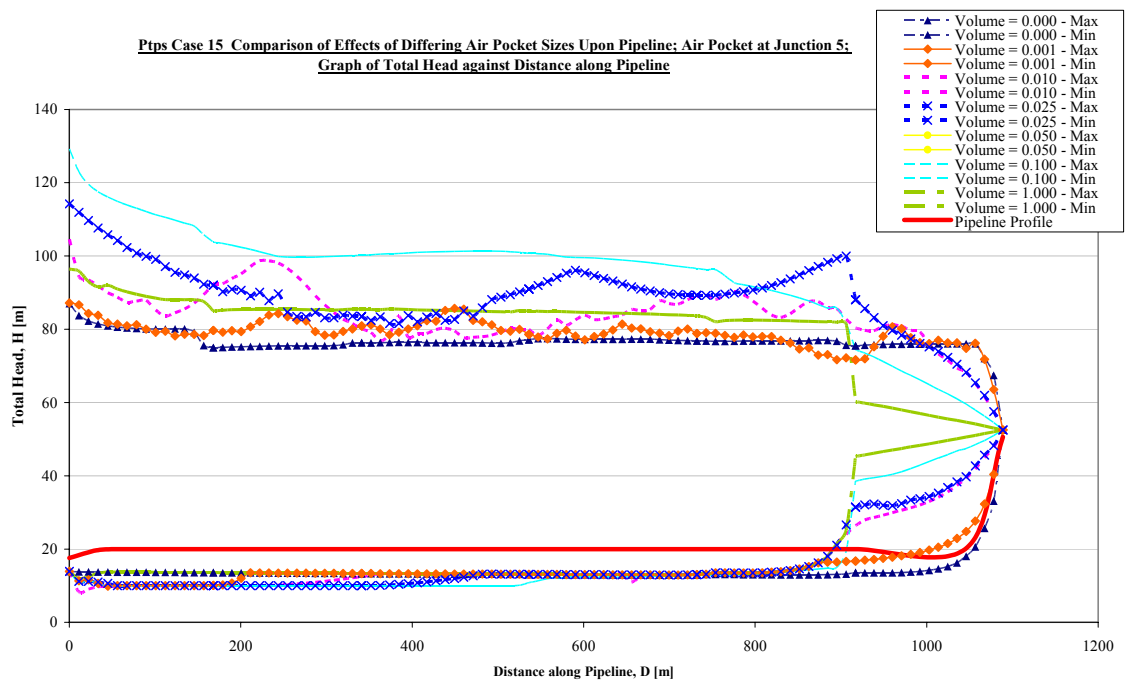


(b), 'CASE 15'

Figure 29 Comparison of the Effects of Differing Air Pocket Sizes when placed at Junction 4 showing Max/Min Head with Time

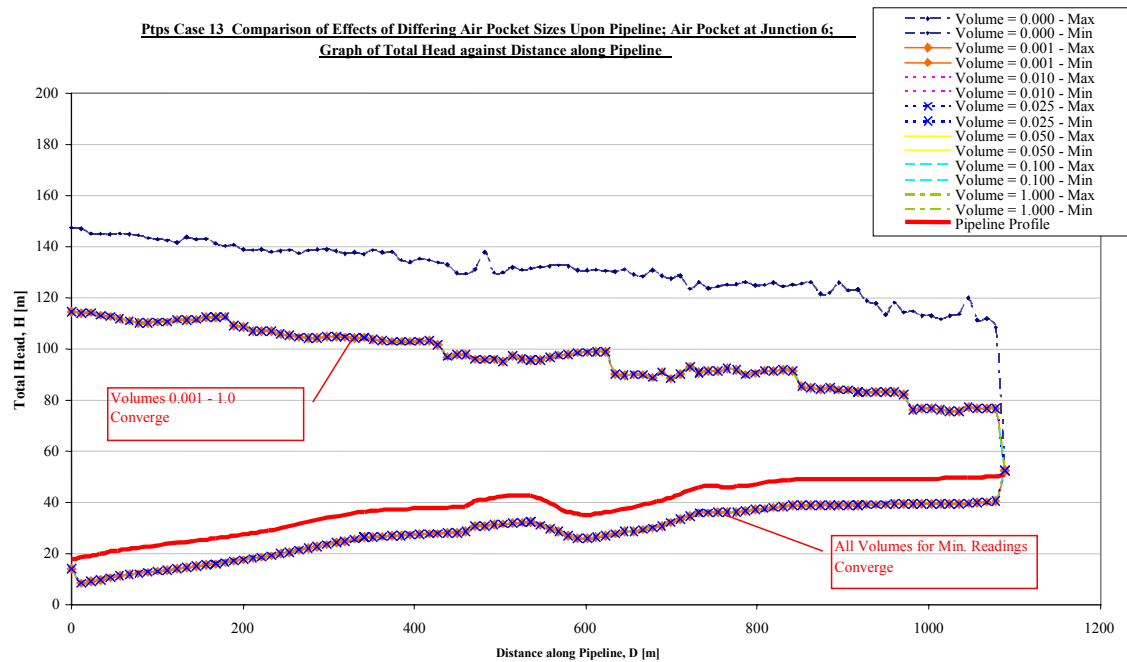


(a), 'CASE 13'

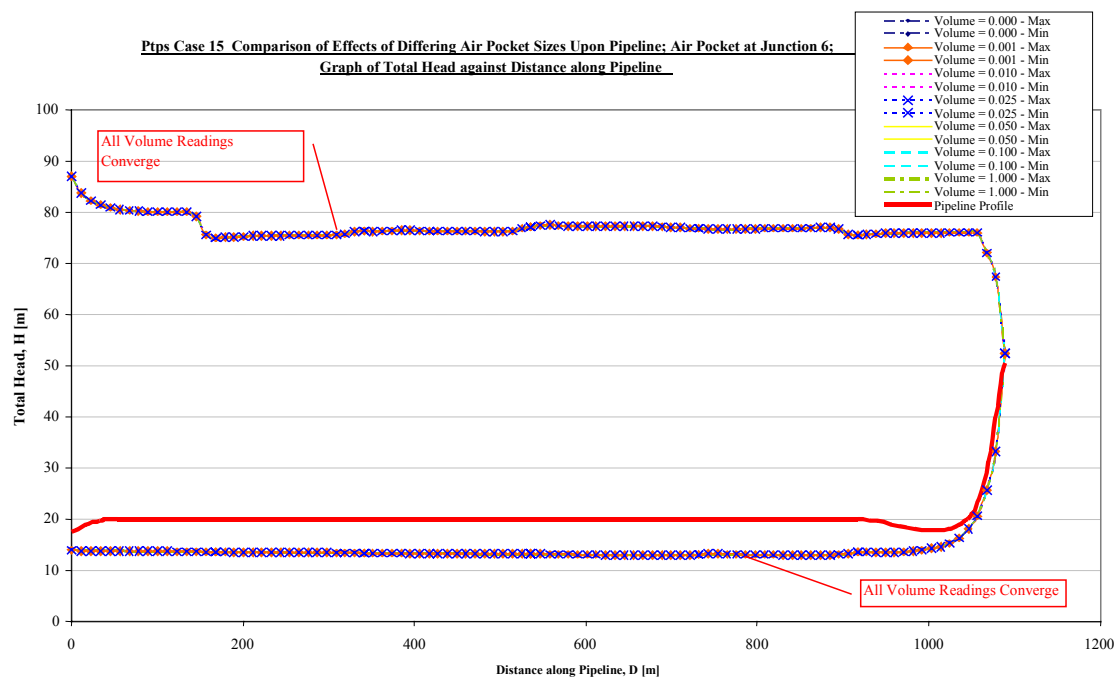


(b), 'CASE 15'

Figure 30 *Comparison of the Effects of Differing Air Pocket Sizes when placed at Junction 5 showing Max/Min Head with Time*



(a), 'CASE 13'



(b), 'CASE 15'

Figure 31 Comparison of the Effects of Differing Air Pocket Sizes when placed at Junction 6 showing Max/Min Head with Time

7.4.4 Series Four – total head vs. distance; for specific air pocket locations

Results for Series Four are shown in Figures 32 to 37.

For CASE 13: From the following series of figures it can be seen that generally the air pocket location of Junction 1 gives the worst total head in the pipeline system, with the location of Junction 6 giving the smallest maximum readings.

The above is true for volumes of air pocket, 0.01 m³ to 0.1 m³.

For the air pocket volume of 0.001 m³, worst to best location follows:

- Junction 2 giving the worst pressures; followed by Junctions 3, 4, 5 and 6, with Junction 1 giving the lowest results.

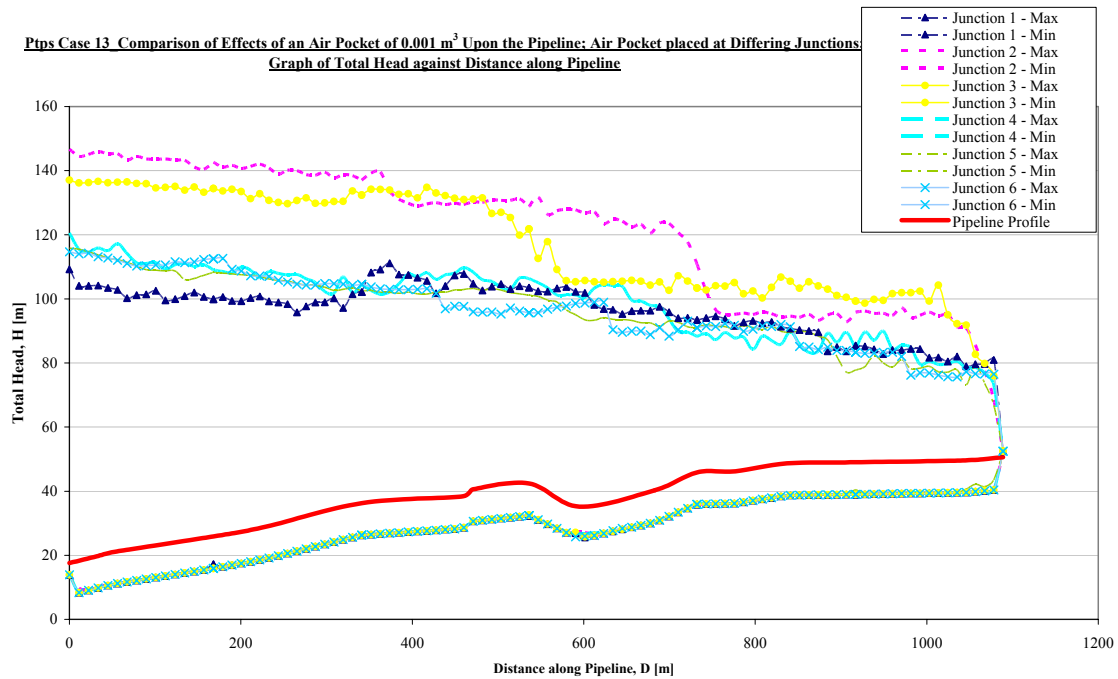
For the air pocket volume of 1.0 m³, worst to best location follows:

- Junction 6 giving the worst pressures; followed by Junctions 5, 4, 3 and 2, with Junction 1 giving the lowest results.

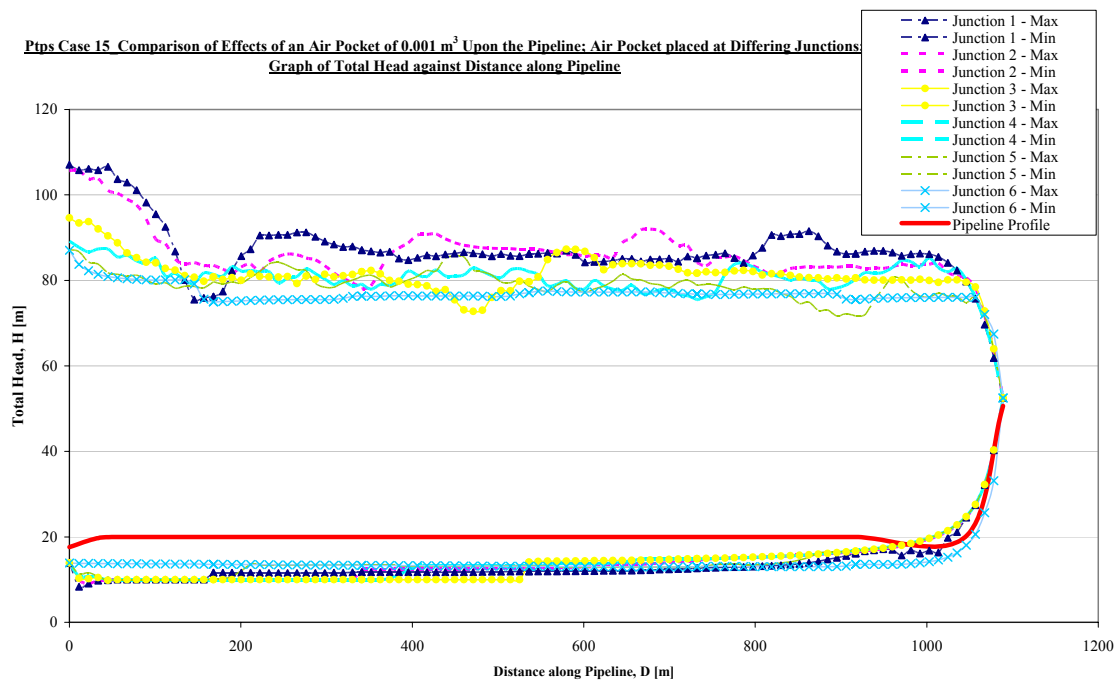
The overall worst results were given by the pocket size 0.1 m³.

This also demonstrates the effects of surge suppression, as this would normally be placed immediately after the pumps. Therefore the lowest pressures were experienced by the pipeline with a pocket of 1.0 m³ placed at Junction 1.

For CASE 15: The plots of these simulations show a similar result to CASE 13, in terms of the effect of air pocket location.

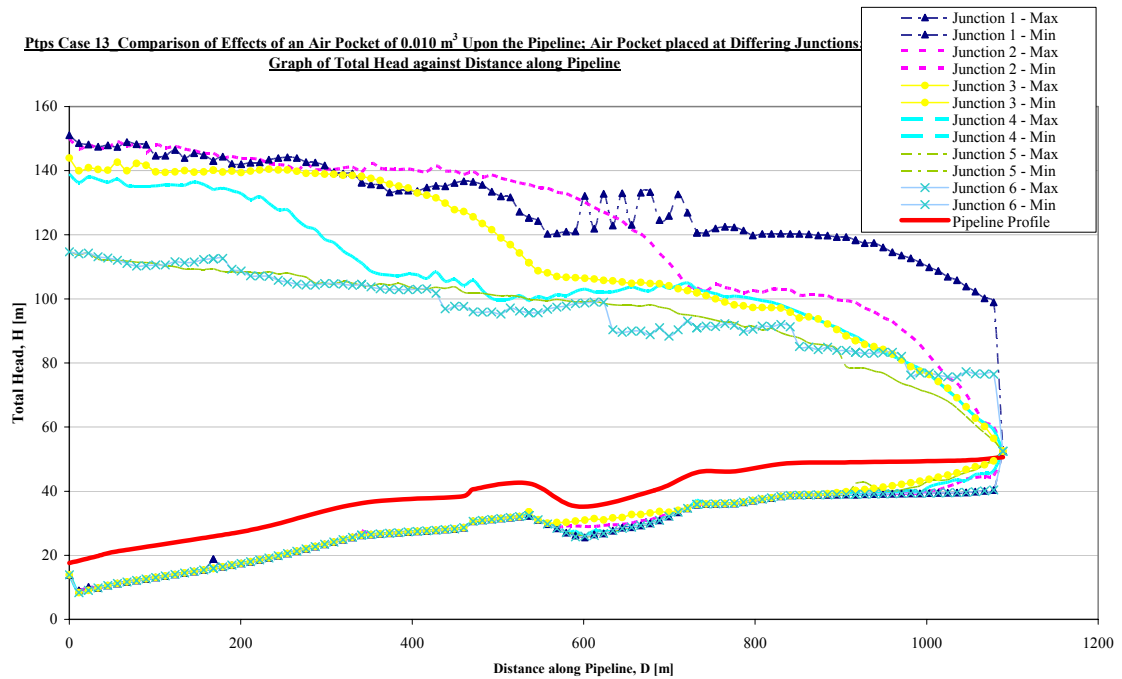


(a), 'CASE 13'

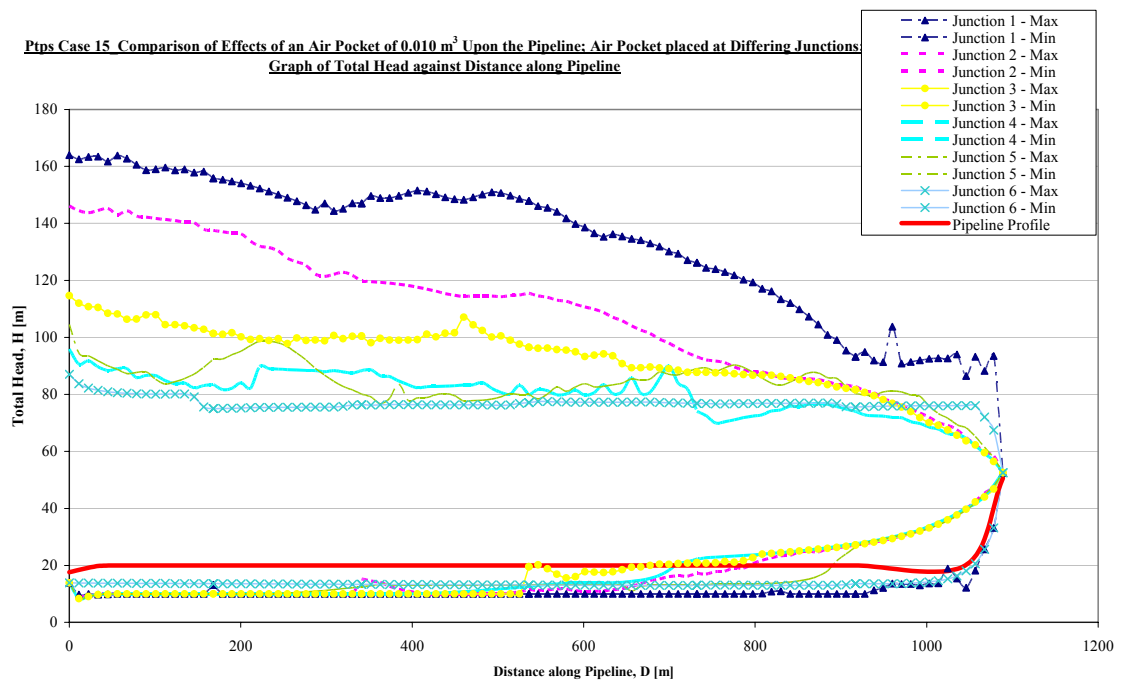


(b), 'CASE 15'

Figure 32 Comparison of the Effects of an Air Pocket of 0.001 m^3 when placed at Differing Junctions showing Max/Min Head with Time

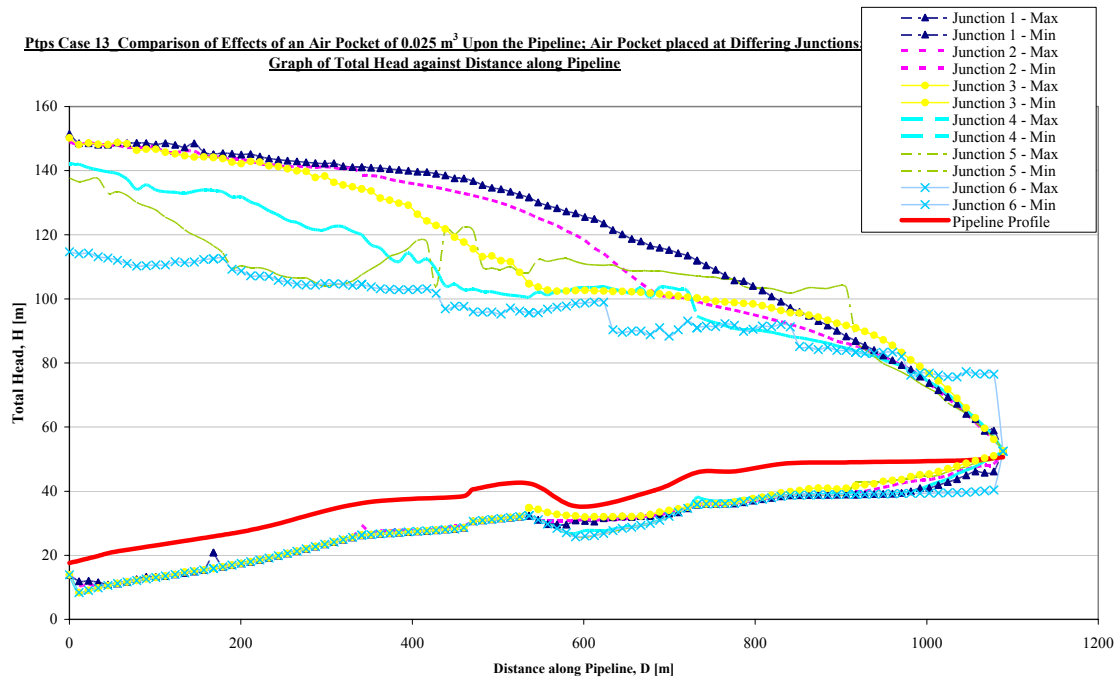


(a), 'CASE 13'

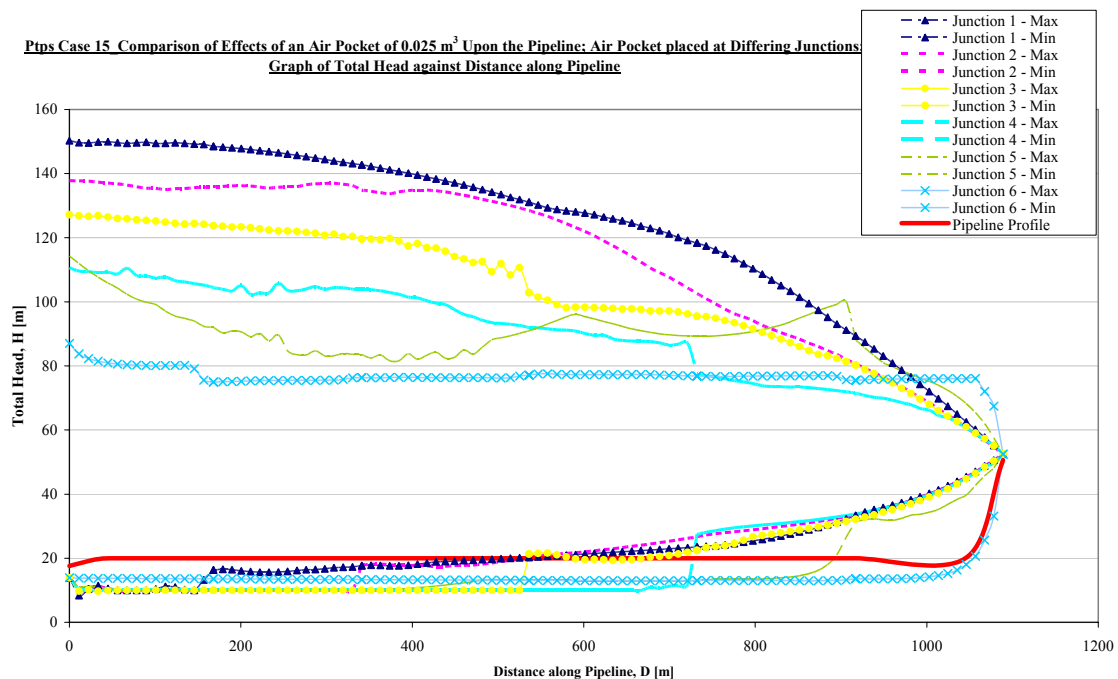


(b), 'CASE 15'

Figure 33 Comparison of the Effects of an Air Pocket of 0.01m³ when placed at Differing Junctions showing Max/Min Head with Time

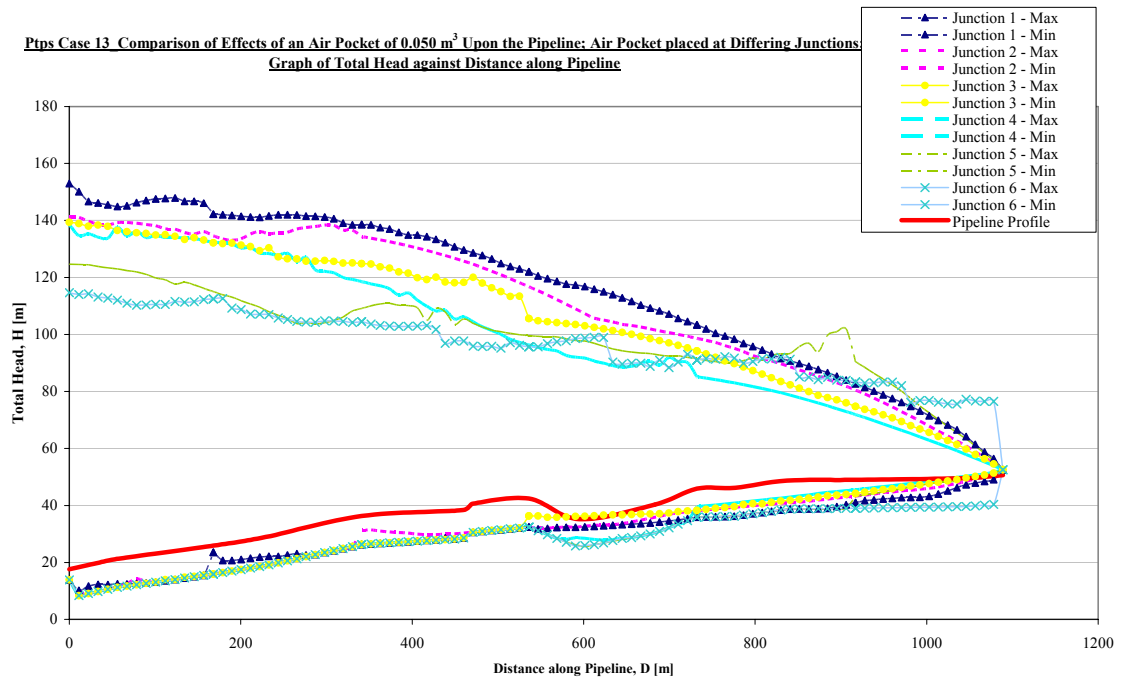


(a), 'CASE 13'

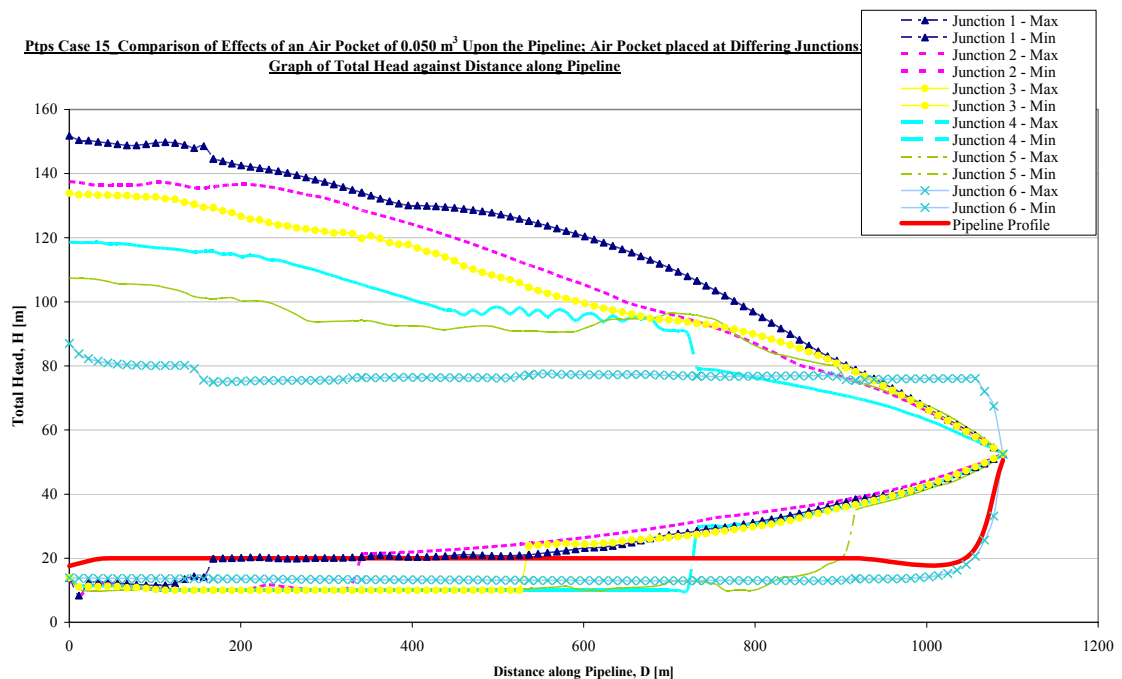


(b), 'CASE 15'

Figure 34 Comparison of the Effects of an Air Pocket of 0.025 m^3 when placed at Differing Junctions showing Max/Min Head with Time

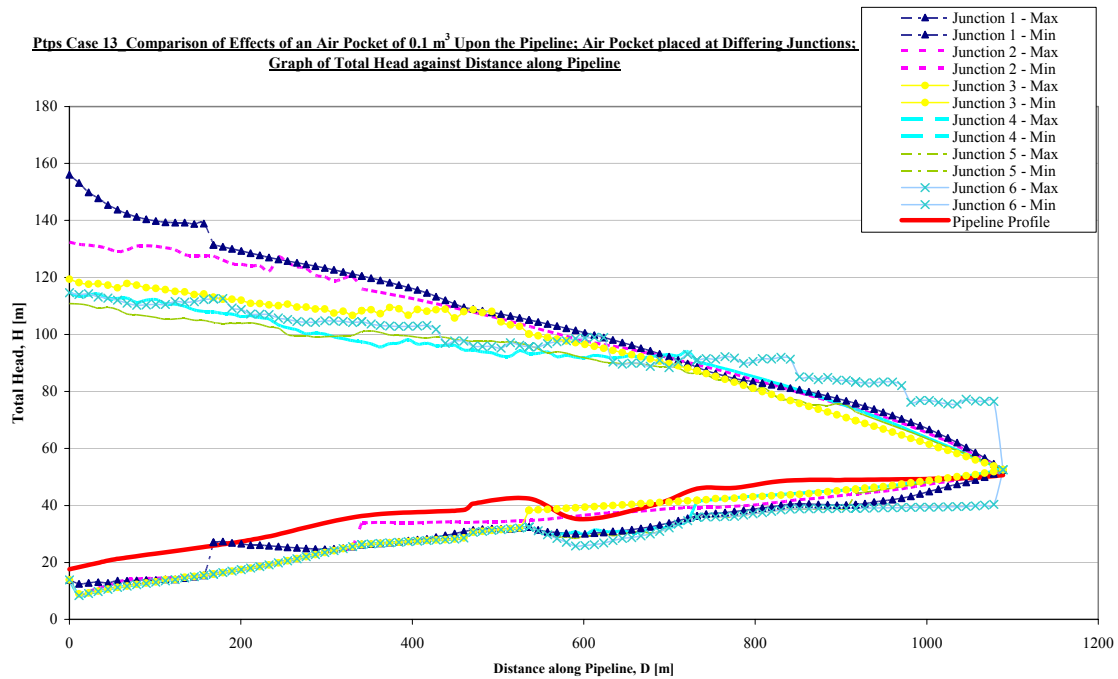


(a), 'CASE 13'

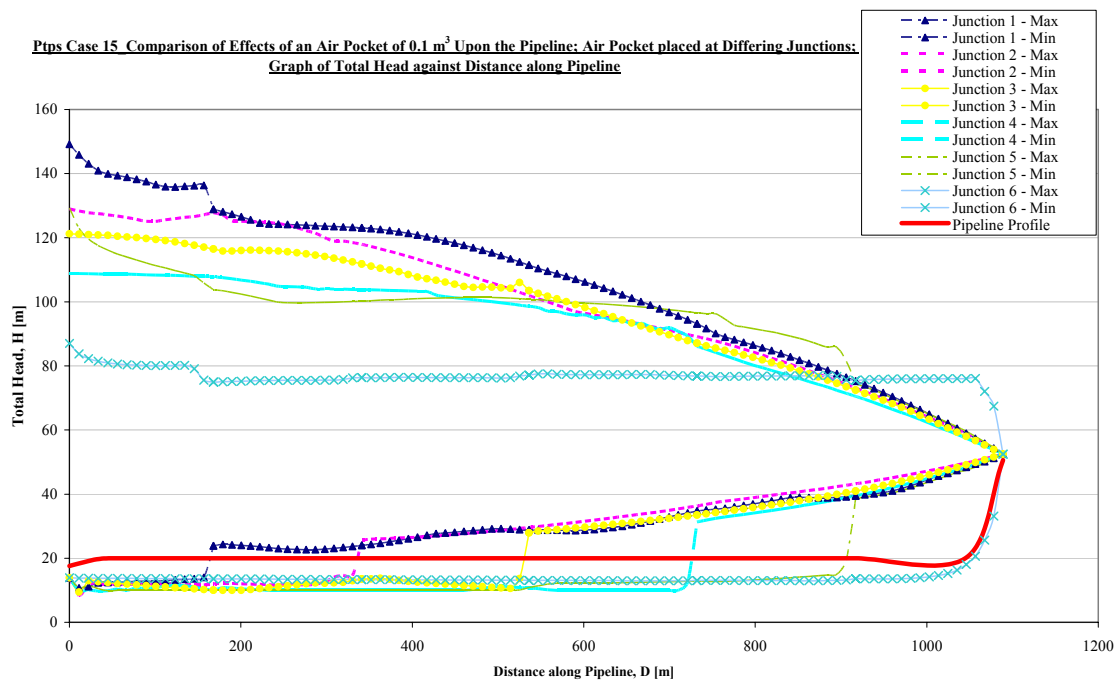


(b), 'CASE 15'

Figure 35 Comparison of the Effects of an Air Pocket of 0.05m³ when placed at Differing Junctions showing Max/Min Head with Time

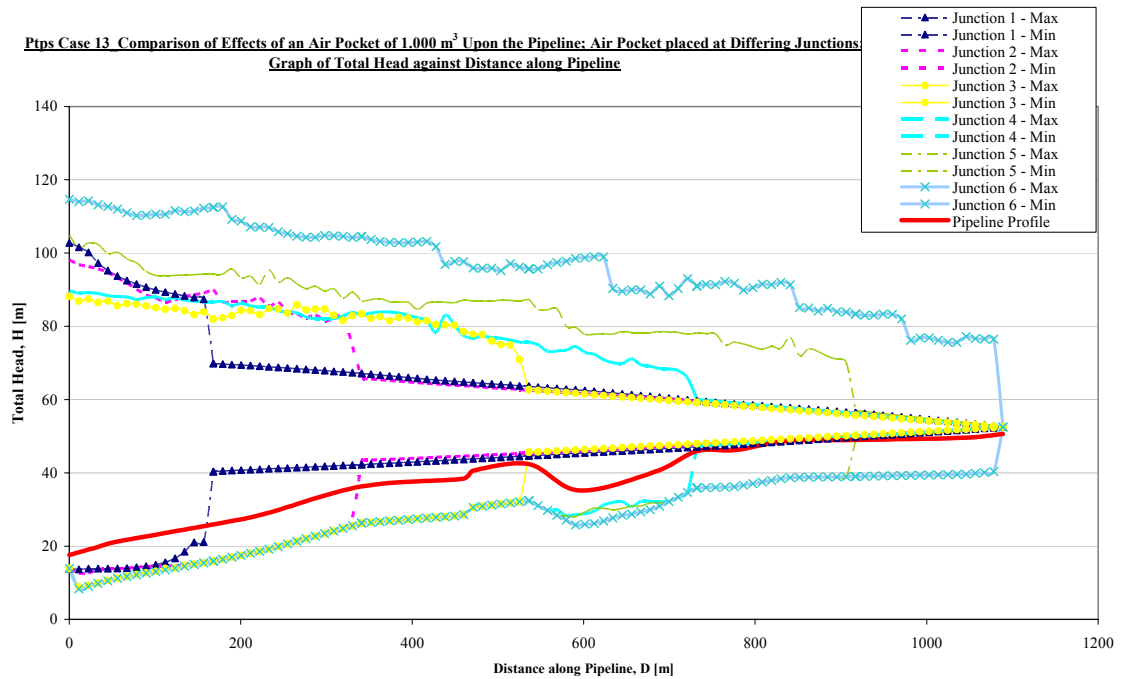


(a), 'CASE 13'

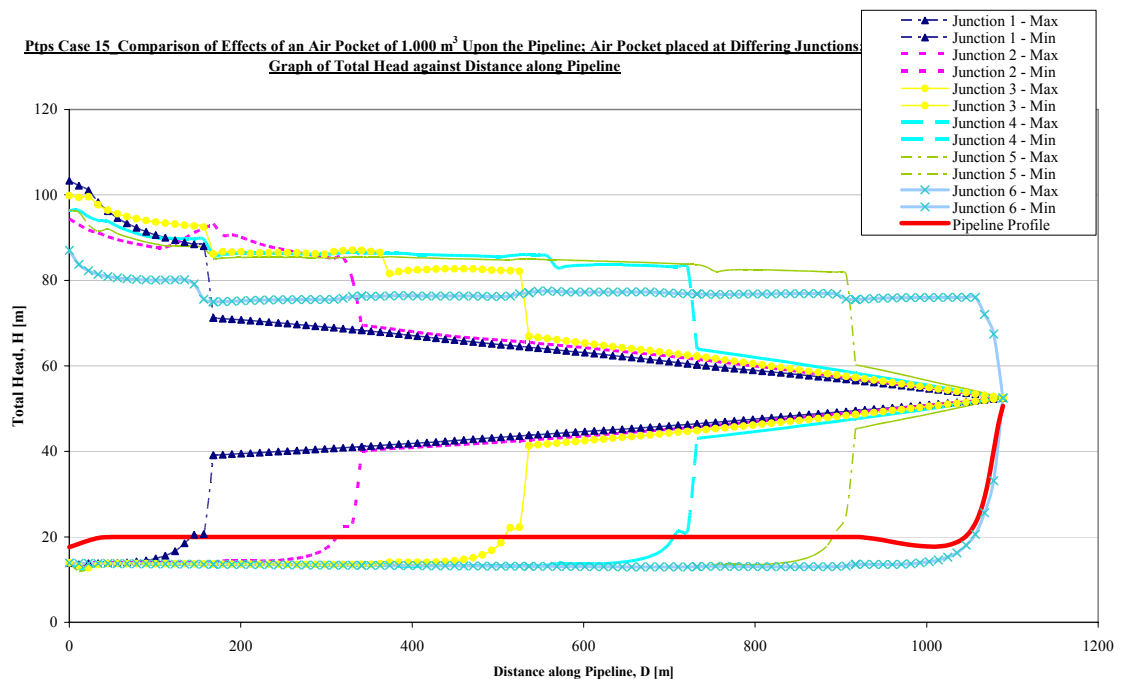


(b), 'CASE 15'

Figure 36 Comparison of Effects of an Air Pocket of 0.1 m^3 when placed at Differing Junctions showing Max/Min Head with Time



(a), 'CASE 13'



(b), 'CASE 15'

Figure 37 Comparison of the Effects of an Air Pocket of 1.0m³ when placed at Differing Junctions showing Max/Min Head with Time

7.4.5 Series Five – total head vs. time; for specific air pocket locations

A summary of the effects highlighted by this series of results is provided in Table 20.

The data in Table 20 show the Junction locations most likely to produce the worst effects through the pipeline profile for the various air pocket sizes tested as part of this study. In summary, the table shows a trend highlighted by the previously discussed results. However, it can be seen that for peak surges at Junction 5 for CASE 13, for example, that the air pocket locations vary from the more normal effect of air pockets at the upstream junctions having the worst effect, although greater pressures are achieved without the presence of any air pocket in this case.

8. *Evaluation of numerical study results*

8.1 INTRODUCTION

As a consequence of performing analyses on hydraulic systems, which by design are all dynamically different in terms of operation, pipeline configuration, location etc, it is not possible to obtain a definitive ‘answer’ in terms of critical air pocket size and critical location. However, the previous Chapter has highlighted that by comparing the effects of simulations with clearly defined differences, e.g. same air pocket size at sequential junctions, etc., it is possible to make common observations. These common observations could then serve to assist the designer to more accurately predict critical conditions for various pipeline configurations.

In order to quantify these observations, a detailed analysis – of the type conducted within this study – would be recommended as the ideal, however this would be extremely time consuming and costly. Therefore it is considered appropriate that a guideline be determined, which would relate potential peak pressure enhancements to the standard transient analysis scenario, i.e. no air present.

This Chapter summarises the main observations from the numerical simulations together with an evaluation of peak pressure enhancement factors.

8.2 OBSERVATIONS

Based on the results outlined in Chapter 7, the following observations can be made.

- The time-plots produced show characteristic pressure waves and mass oscillations which increase with period as air pocket sizes increase – air pockets acting as energy accumulators;
- The results show that the small air pockets have the ability to reflect only part of the pressure wave and the majority of the wave will pass through to be reflected by a downstream reservoir. Frequency and amplitudes have the potential for enhancement under these conditions;
- The results also show that larger air pockets can absorb the transient pressure wave, thereby resulting in a positive effect on the pressure regime within the pipeline system;
- Pressures are of a smaller magnitude further from the pumping station and conversely are larger at the upstream section of a piped system;

- Potentially destructive enhancements of pressures by the presence of air pockets have a more significant impact at the upstream/pump end of a pipeline, where pressures are already higher;
- Smaller air pockets produce higher pressures in the pipeline when present at upstream junctions;
- Larger air pockets produce higher pressures in the pipeline when present at downstream junctions;
- Results show that peak pressures can be enhanced due to small air pockets, but there is a limit to the size of pocket which can have this affect. This suggests that there is potentially a ‘critical’ air pocket size for any given pipeline configuration;
- Realistic Profile Simulation (CASE 13): Generally small air pockets have a greater effect on the peak pressures when placed at upstream junction locations;
- Realistic Profile Simulation (CASE 13): Peak pressures are reached along the upstream section of the pipeline with small air pockets present – 0.010 m³ to 0.1 m³;
- Realistic Profile Simulation (CASE 13): Peak pressures are reached along the downstream section of the pipeline with no air present;
- Realistic Profile Simulation (CASE 13): For very small pockets of air or when air is assumed to be absent, extensive cavitation occurs, depicted by pressure heads locally 10 metres (or more) below ground level;
- Horizontal Profile Simulation (CASE 15): The reduction in cavitation along the majority of the profile results in the ‘NO AIR’ model producing the lowest peak pressures;
- Horizontal Profile Simulation (CASE 15): Generally the presence of small air pockets produce peak pressures along the majority of the pipeline and also result in cavitation along part of the pipeline profile which consequently contribute to the enhancement of the pressures;
- Horizontal Profile Simulation (CASE 15): The presence of a larger pocket of air can also enhance peak pressures along sections of the pipeline profile;

The above statements are specifically related to the results presented in the previous Chapter, however their implication can be utilised by the designer in order to modify transient analysis to reflect and obtain critical conditions more rapidly, thereby reducing the amount of modelling required.

8.3 PRESSURE ENHANCEMENT FACTOR

As discussed in Section 8.1, an assessment of peak pressure enhancement to the standard transient analysis scenario has been performed.

8.3.1 Case study simulations for 'realistic' profile and horizontal profile

Realistic profile (CASE 13)

Table 21 presents calculations to determine pressure enhancement factors resulting from the location of various sizes of air pockets at sequential junctions along the pipeline profile. The results are presented graphically in Figures 38 to 43.

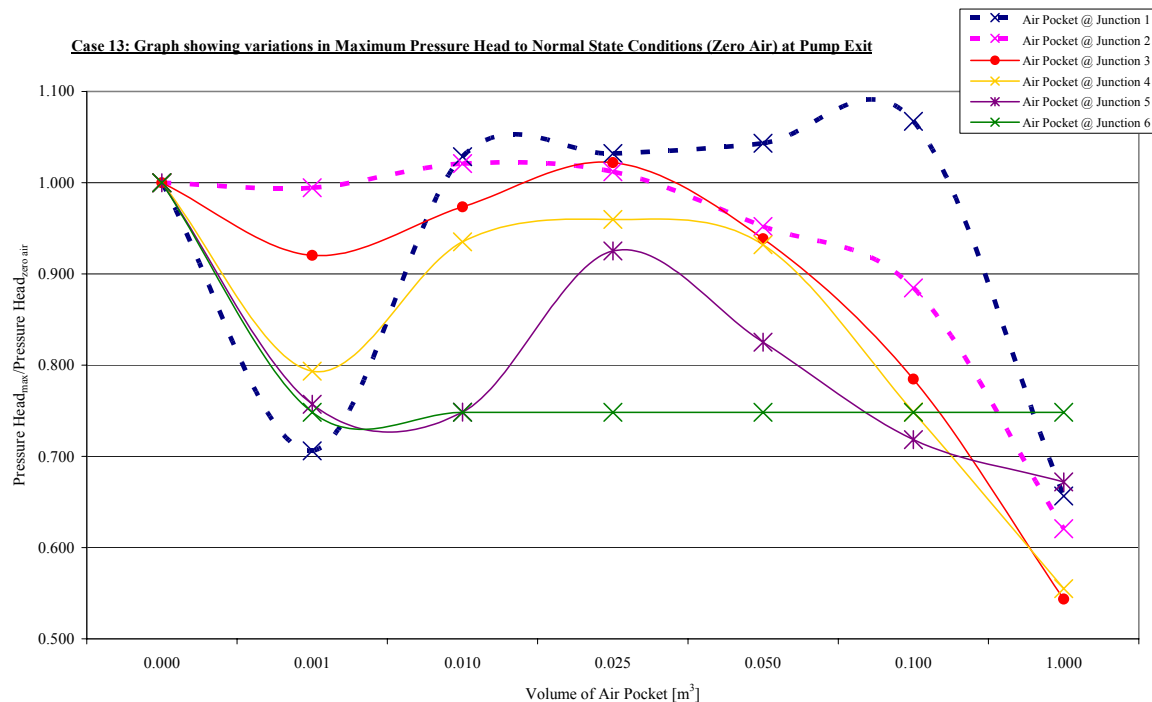


Figure 38 CASE 13 - Pressure Enhancement Factors at Pump Exit

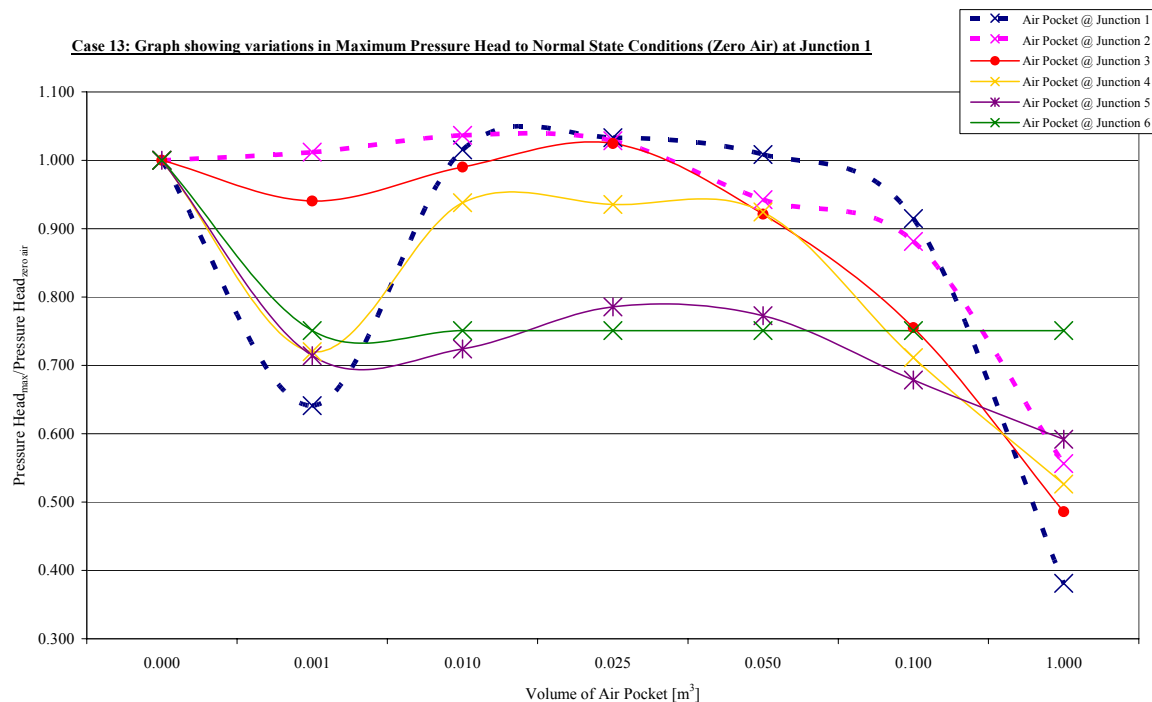


Figure 39 CASE 13 - Pressure Enhancement Factors at Junction 1

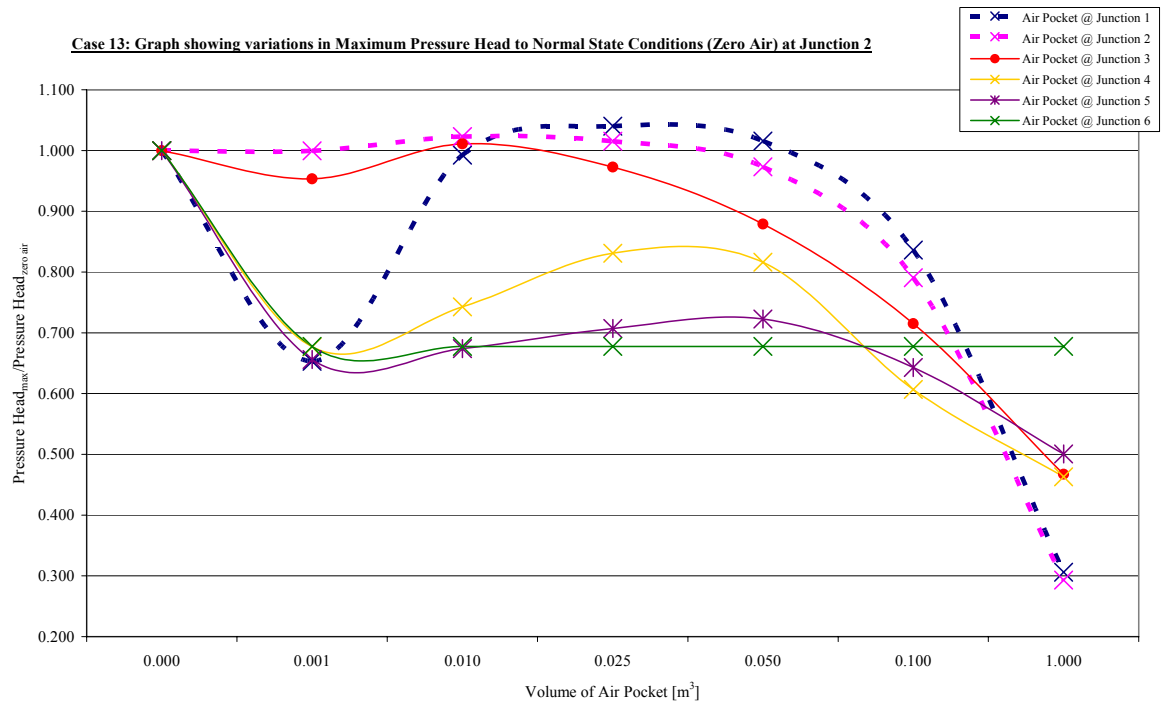


Figure 40 *CASE 13 - Pressure Enhancement Factors at Junction 2*

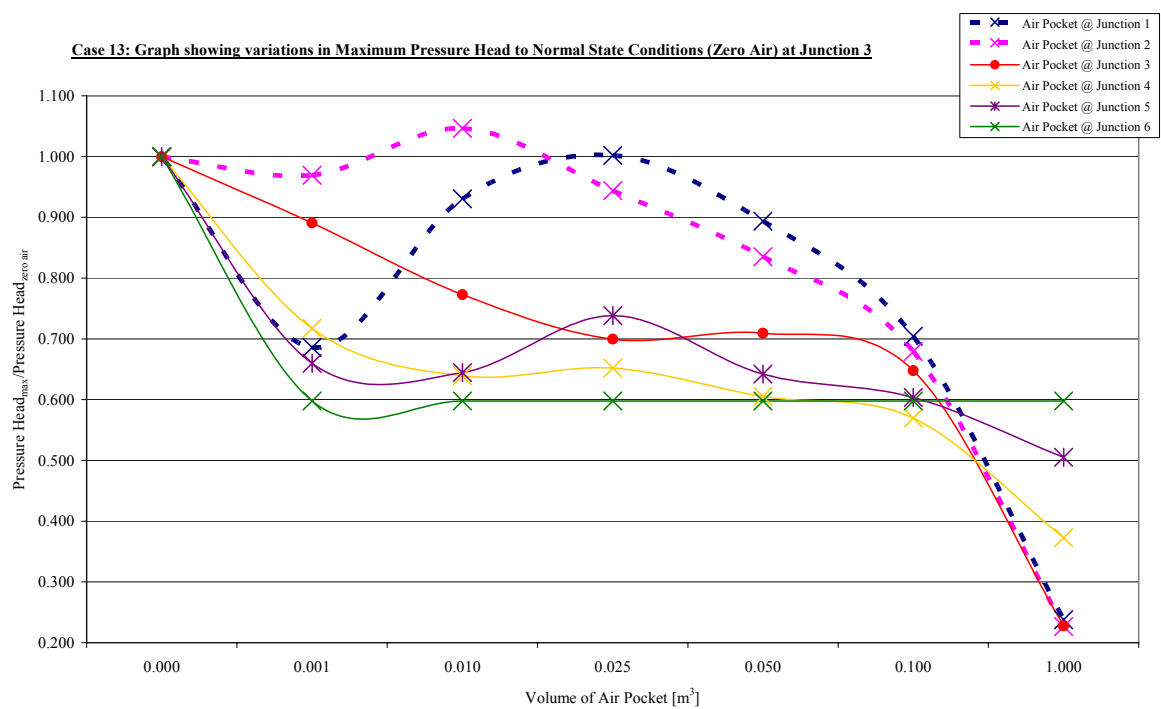


Figure 41 *CASE 13 - Pressure Enhancement Factors at Junction 3*

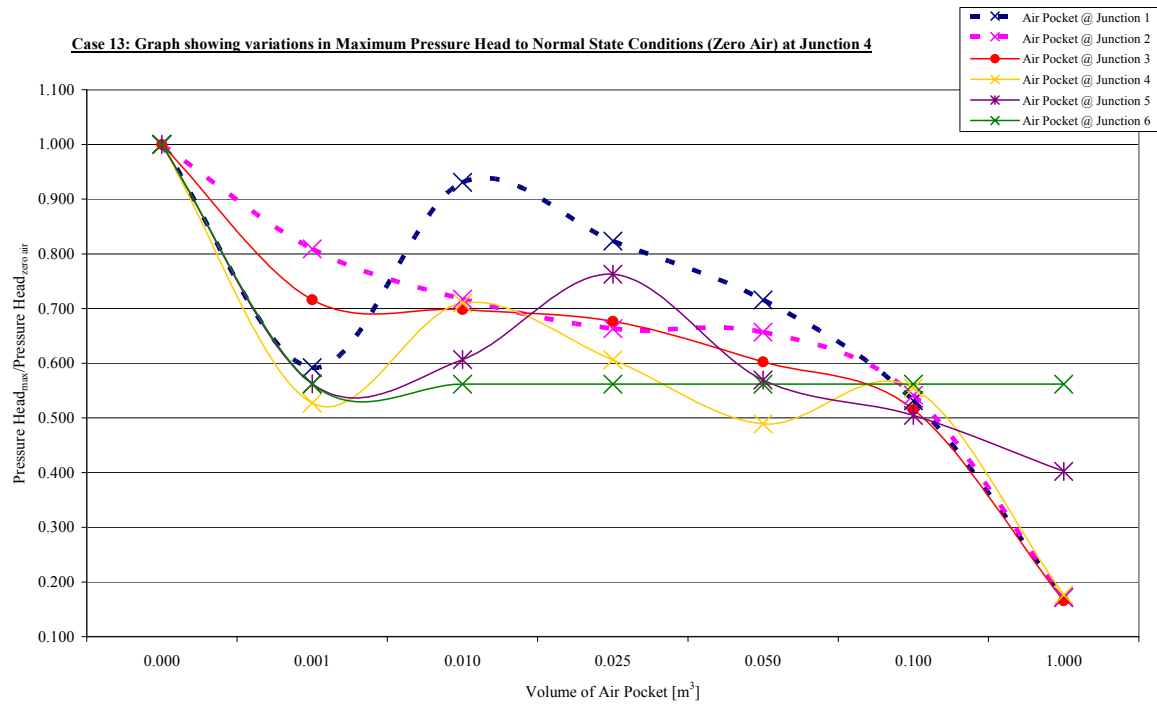


Figure 42 CASE 13 - Pressure Enhancement Factors at Junction 4

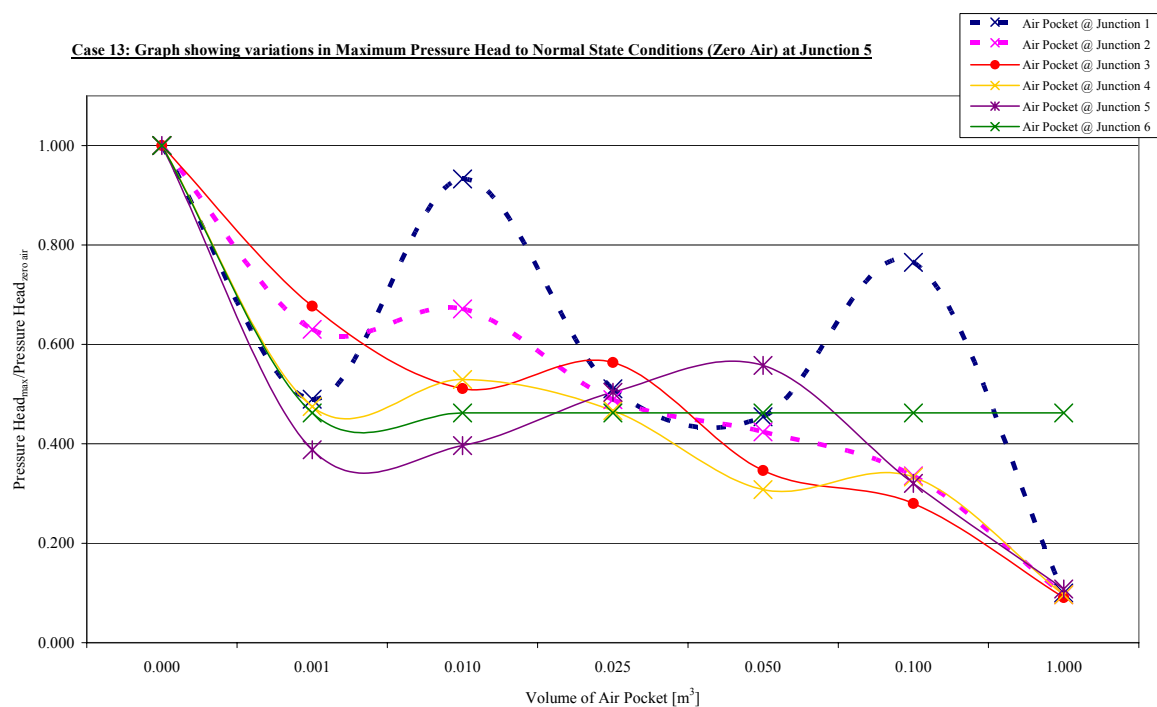


Figure 43 CASE 13 - Pressure Enhancement Factors at Junction 5

Horizontal profile (CASE 15)

Table 22 presents calculations to determine pressure enhancement factors resulting from the location of various sizes of air pockets at sequential junctions along the pipeline profile. The results are presented graphically in Figures 44 to 49.

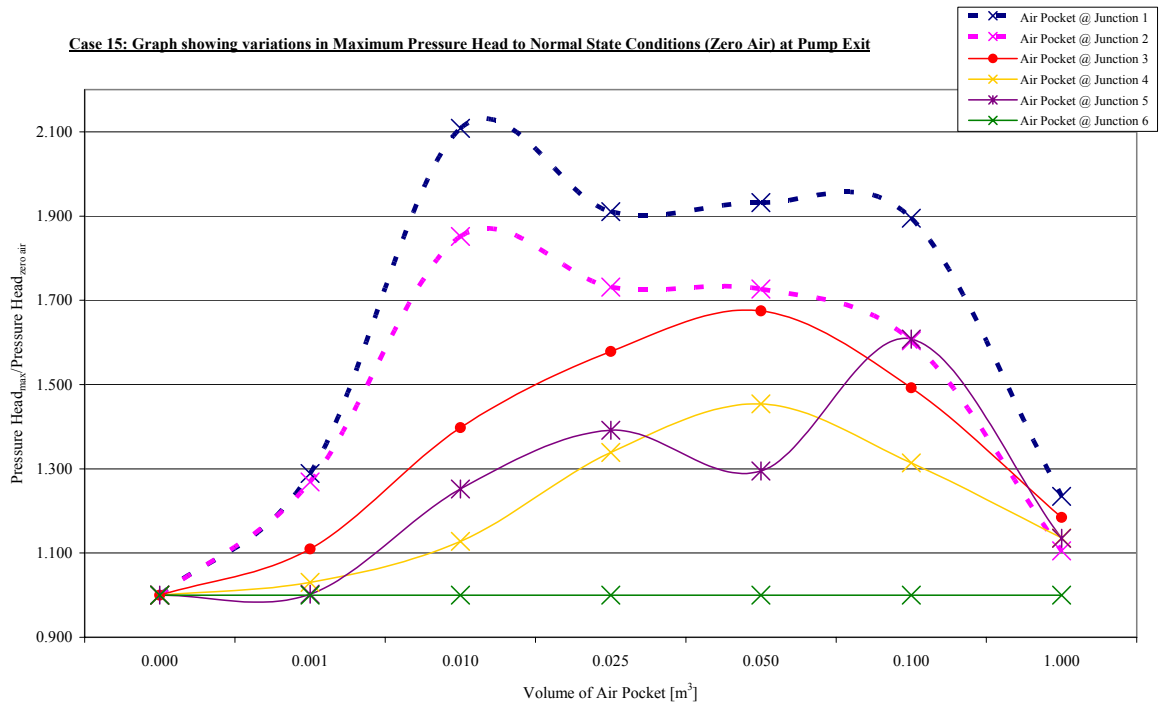


Figure 44 CASE 15 - Pressure Enhancement Factors at Pump Exit

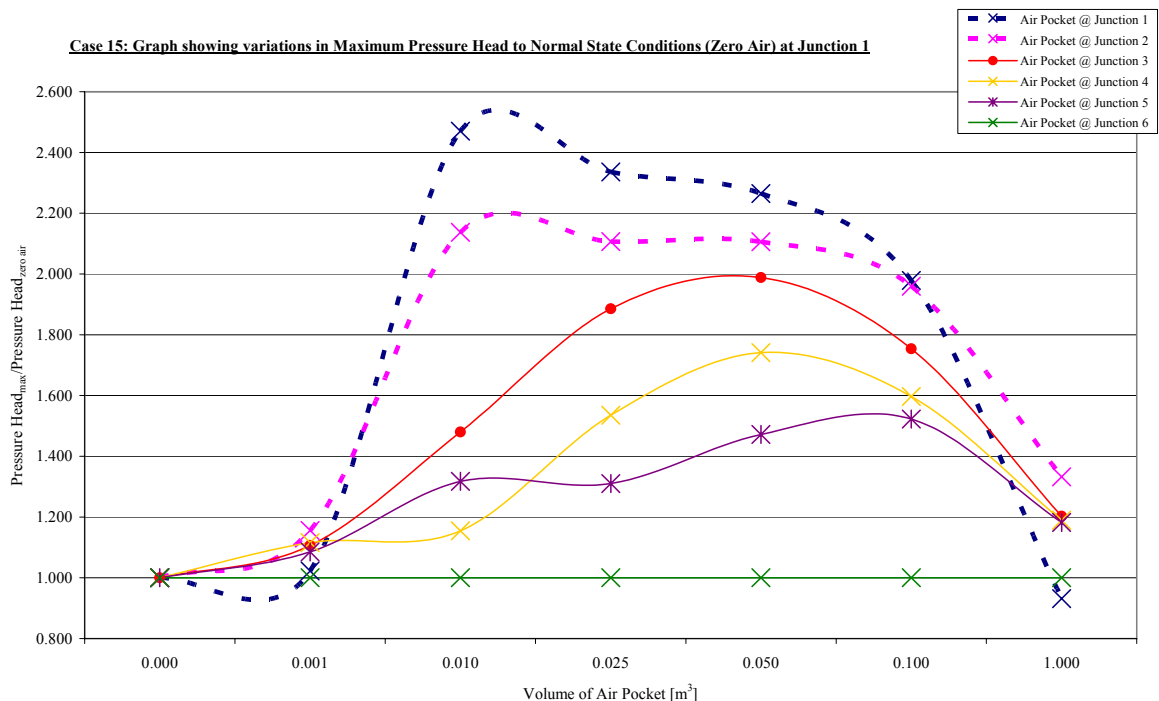


Figure 45 CASE 15 - Pressure Enhancement Factors at Junction 1

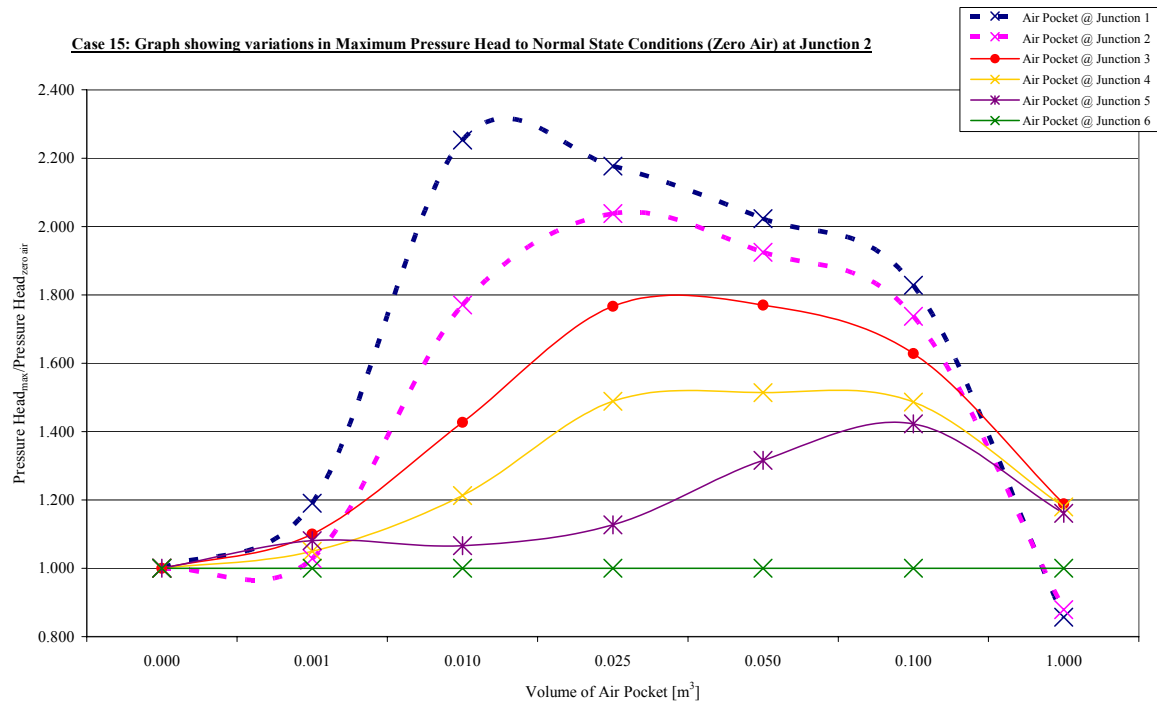


Figure 46 CASE 15 - Pressure Enhancement Factors at Junction 2

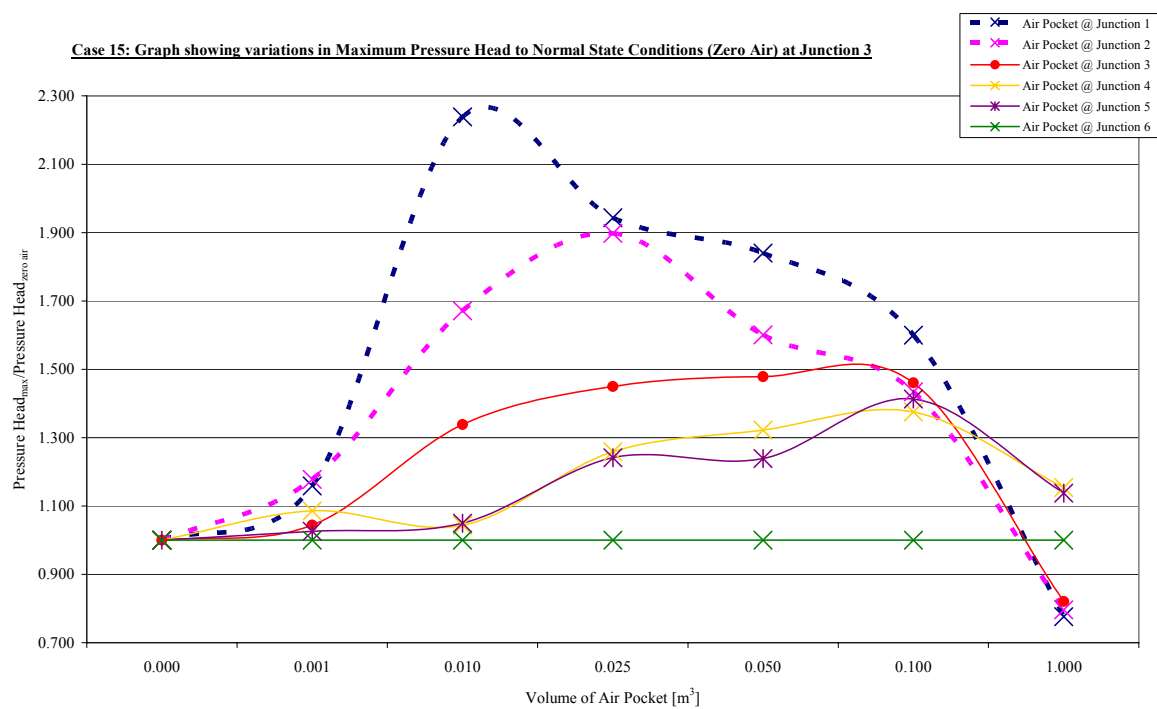


Figure 47 CASE 15 - Pressure Enhancement Factors at Junction 3

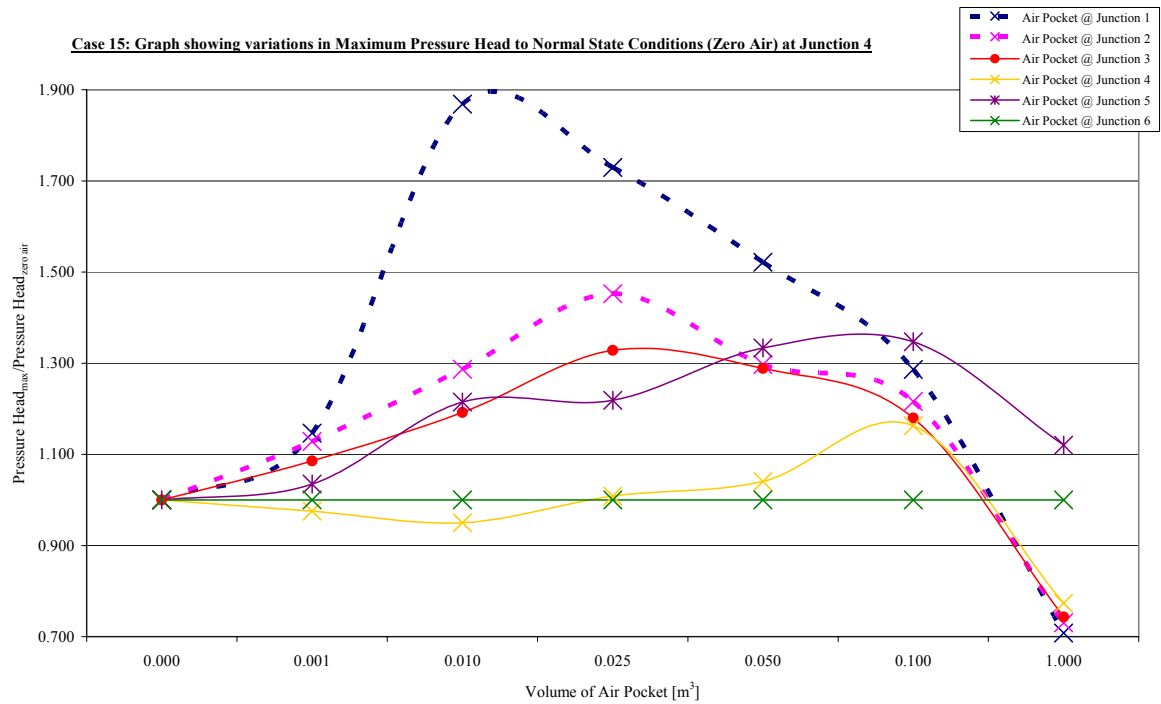


Figure 48 *CASE 15 - Pressure Enhancement Factors at Junction 4*

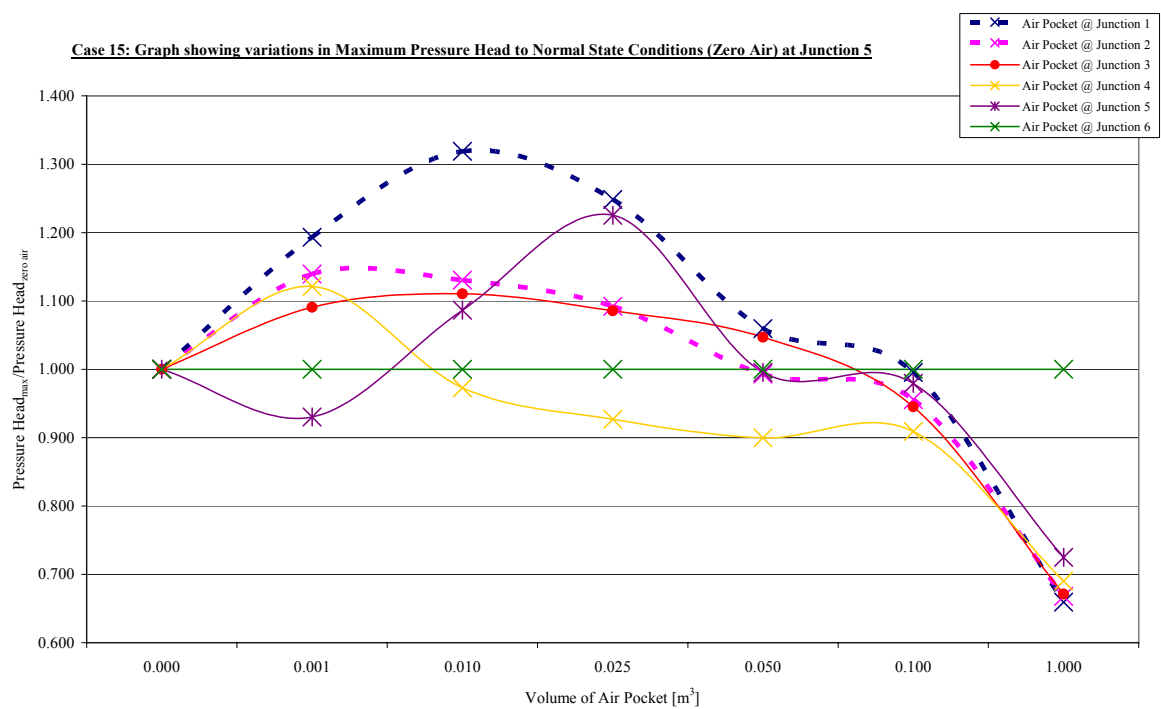


Figure 49 *CASE 15 - Pressure Enhancement Factors at Junction 5*

Additional case study simulations

(Denoted as CASE 1, CASE 2 and CASE 3)

It is important to note that whilst these results have been presented for comparative purposes, no validation has been undertaken for these case studies. Therefore, the results are assumed to be valid. The main parameters for these three case studies are:

- CASE 1
 - Total Length = 2910 m
 - Changing Diameter
 - Split into 3 Junctions
- CASE 2
 - Total Length = 1500 m
 - Diameter = 0.296 m
 - Split into 4 Junctions
- CASE 3
 - Total Length = 2924 m
 - Diameter = 0.472 m
 - Split into 7 Junctions

All three case studies have been analysed using PTPS, simulating air pockets of volumes 0.01 m^3 , 0.05 m^3 , 0.10 m^3 and 1.0 m^3 located at sequential junctions along the pipeline profiles.

CASE 1

Table 23 presents calculations to determine pressure enhancement factors resulting from the location of various sizes of air pockets at sequential junctions along the pipeline profile. The results are presented graphically in Figures 50 to 52.

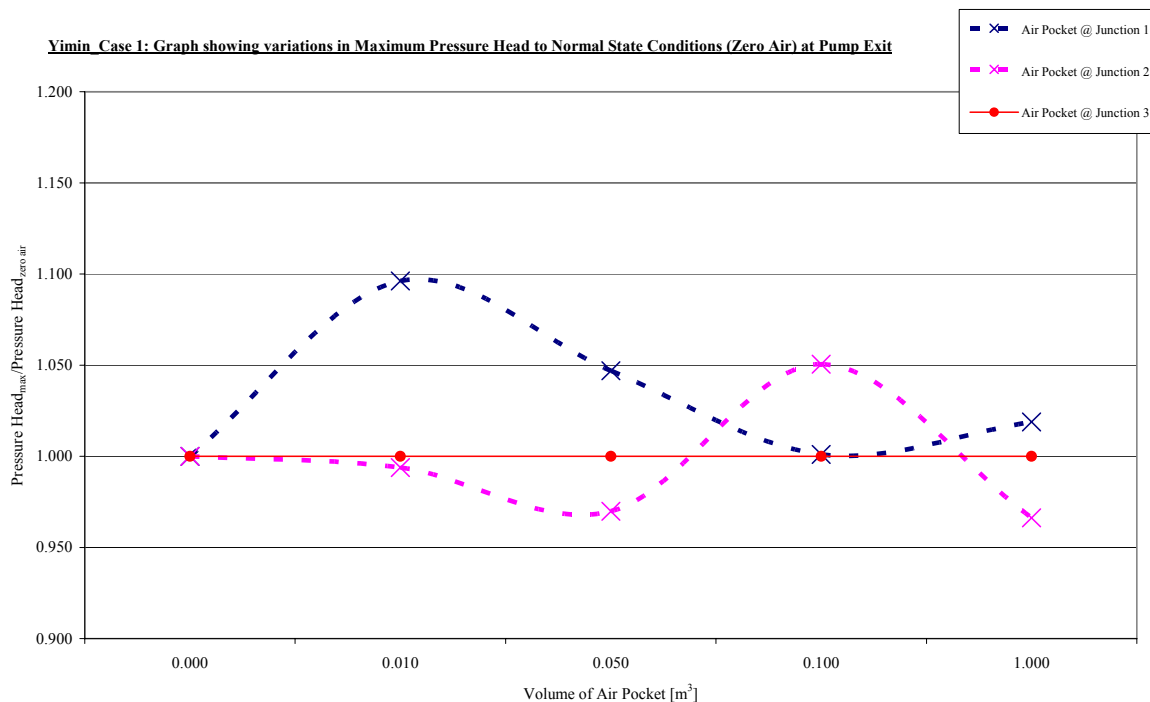


Figure 50 **CASE 1 - Pressure Enhancement Factors at Pump Exit**

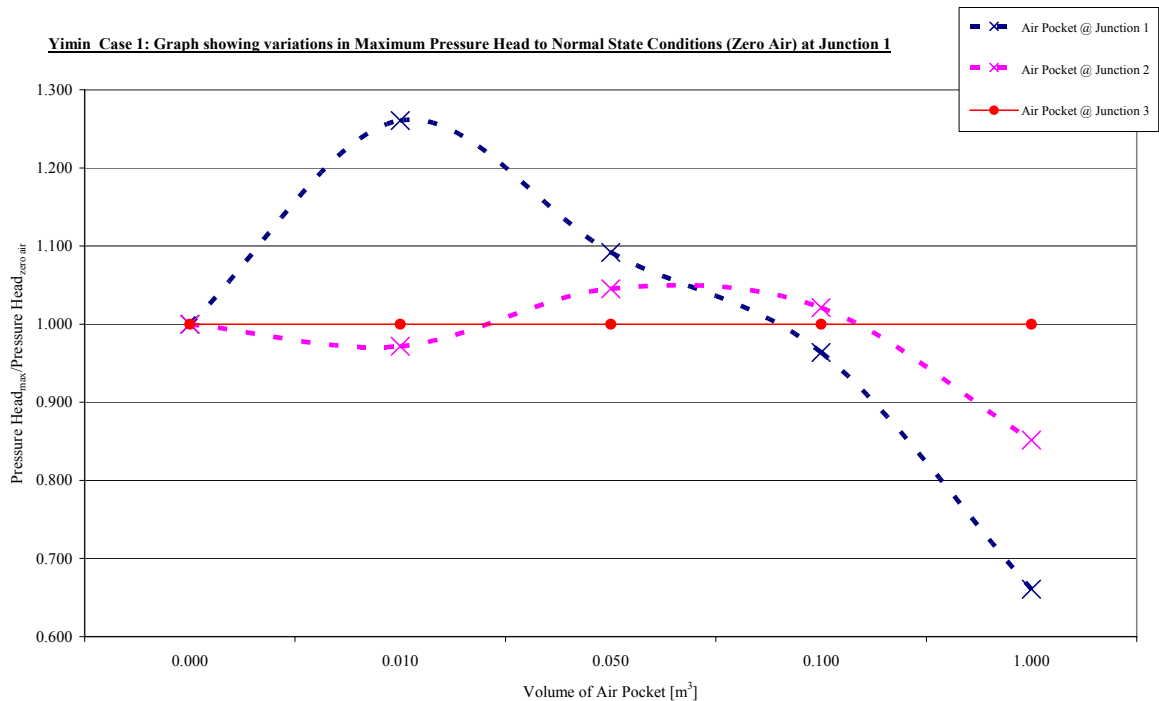


Figure 51 CASE 1 - Pressure Enhancement Factors at Junction 1

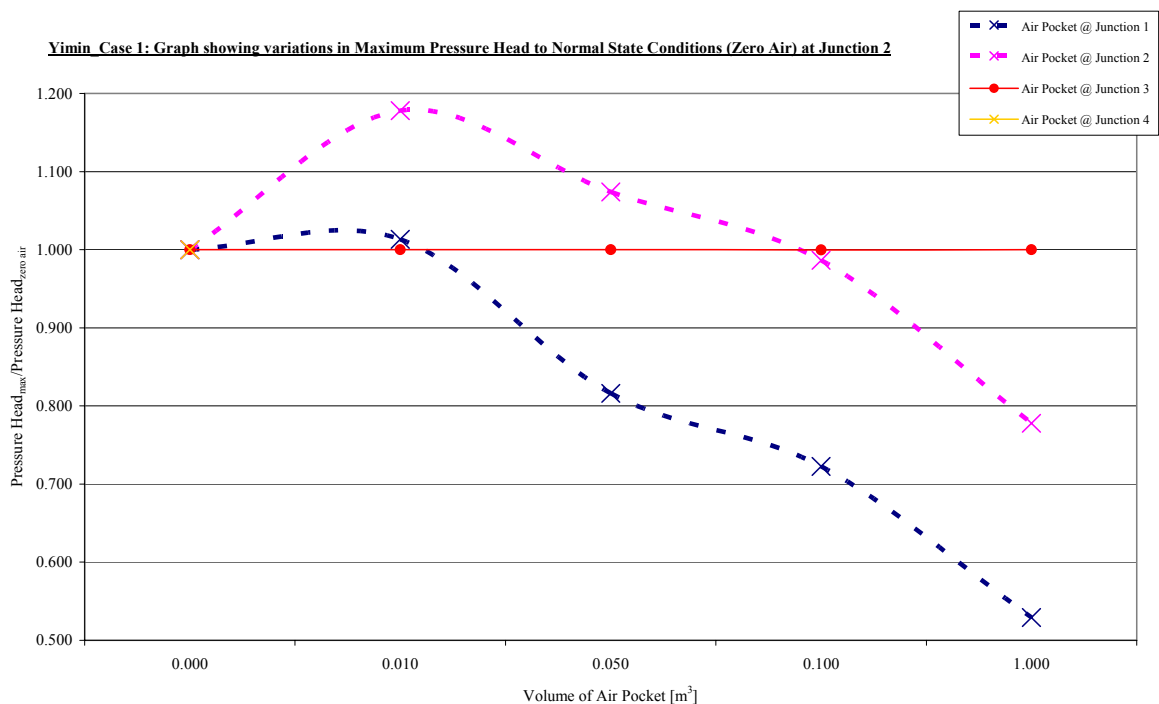


Figure 52 CASE 1 - Pressure Enhancement Factors at Junction 2

CASE 2

Table 24 presents calculations to determine pressure enhancement factors resulting from the location of various sizes of air pockets at sequential junctions along the pipeline profile. The results are presented graphically in Figures 53 to 56.

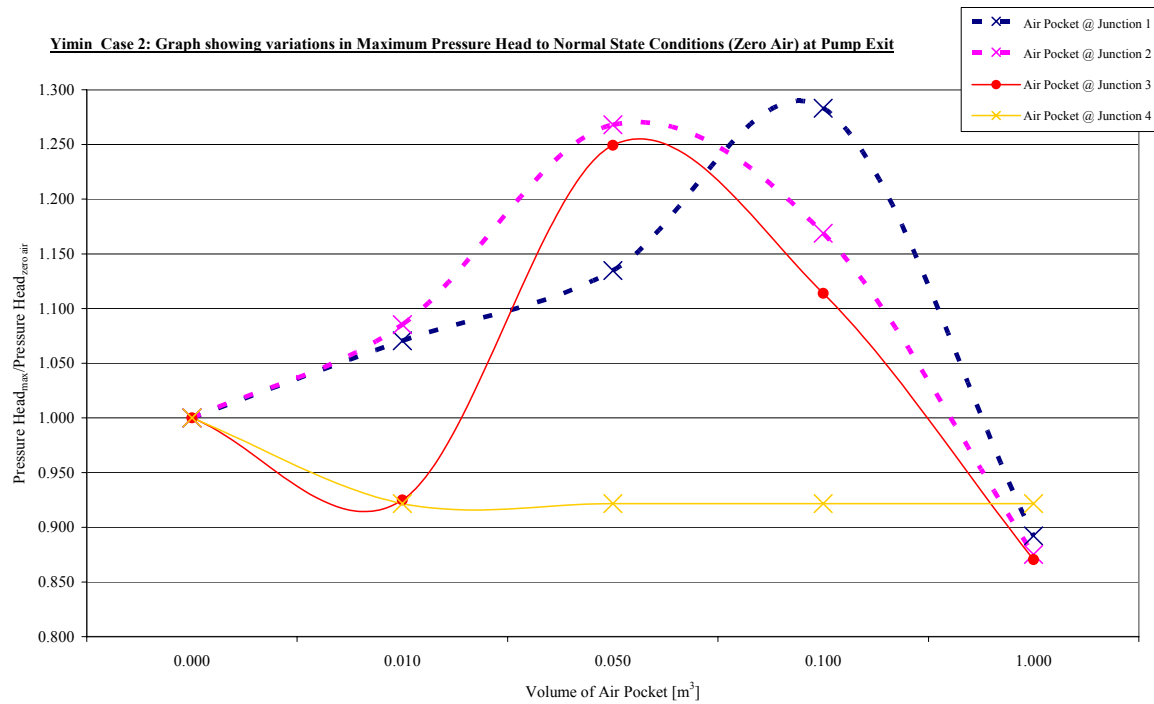


Figure 53 CASE 2 - Pressure Enhancement Factors at Pump Exit

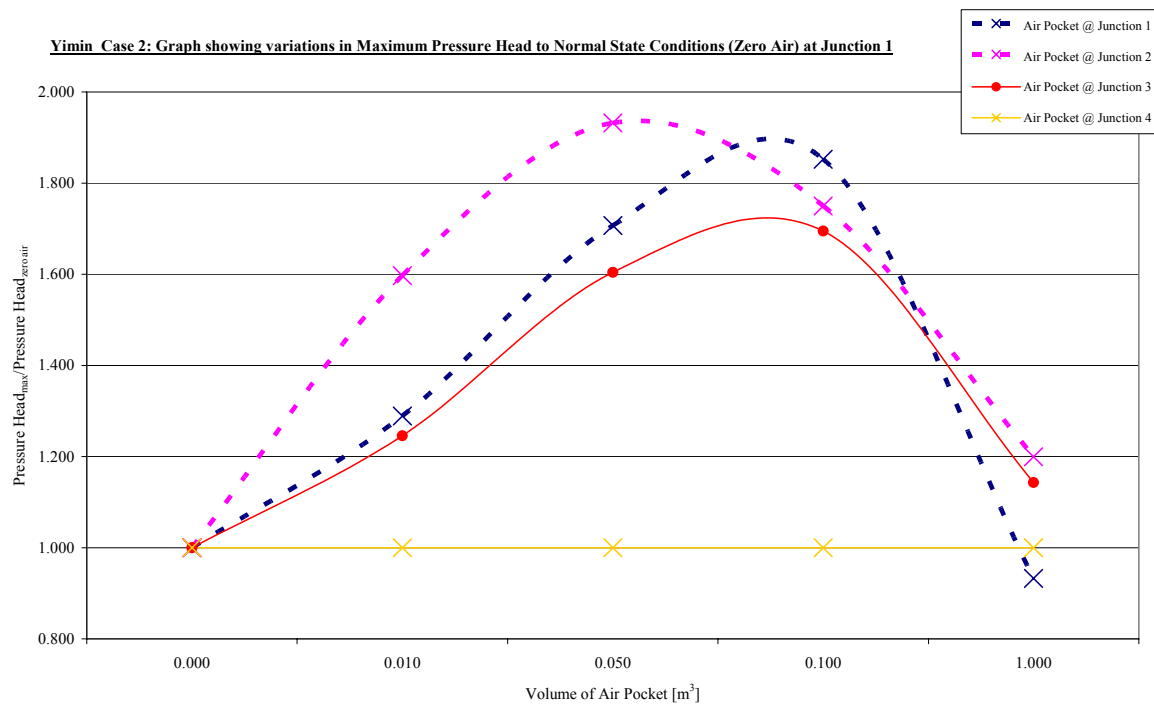


Figure 54 CASE 2 - Pressure Enhancement Factors at Junction 1

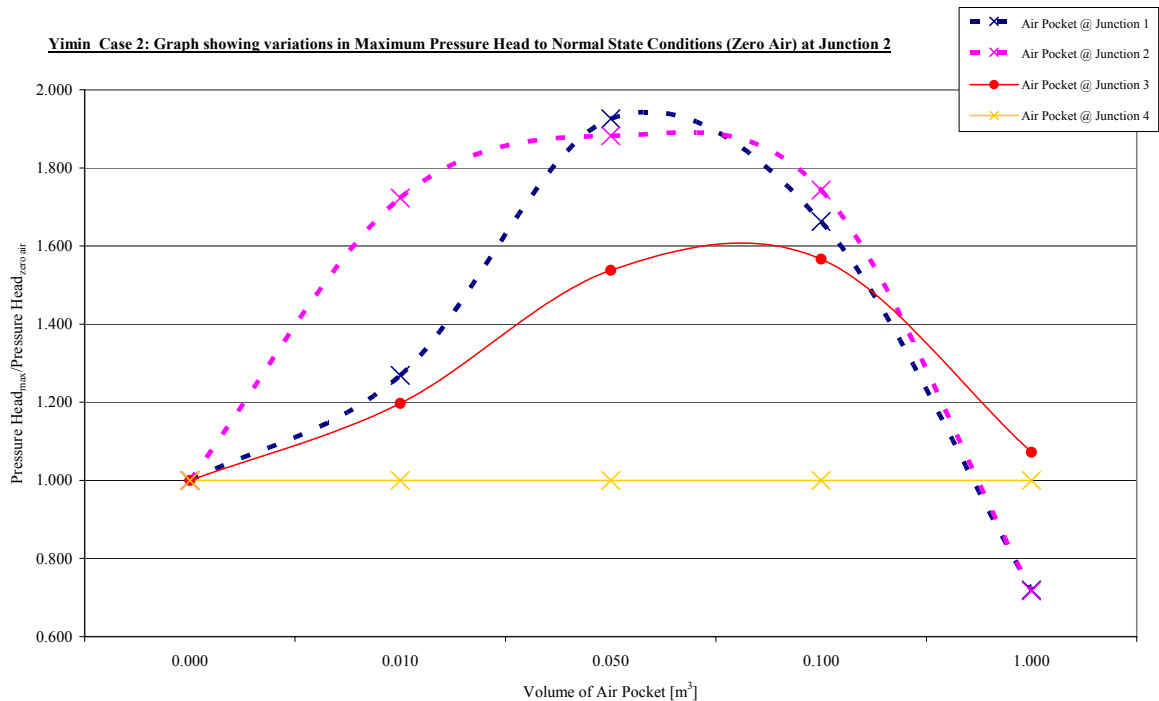


Figure 55 CASE 2 - Pressure Enhancement Factors at Junction 2

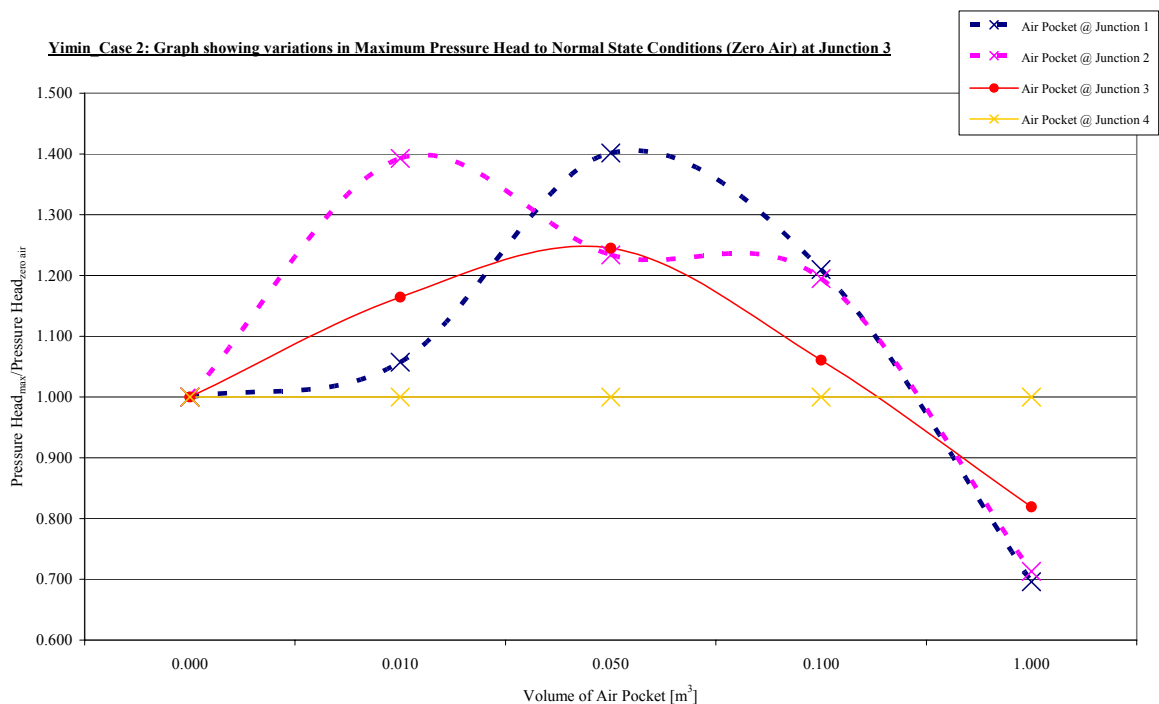


Figure 56 CASE 2 - Pressure Enhancement Factors at Junction 3

CASE 3

Table 25 presents calculations to determine pressure enhancement factors resulting from the location of various sizes of air pockets at sequential junctions along the pipeline profile. The results are presented graphically in Figures 57 to 63.

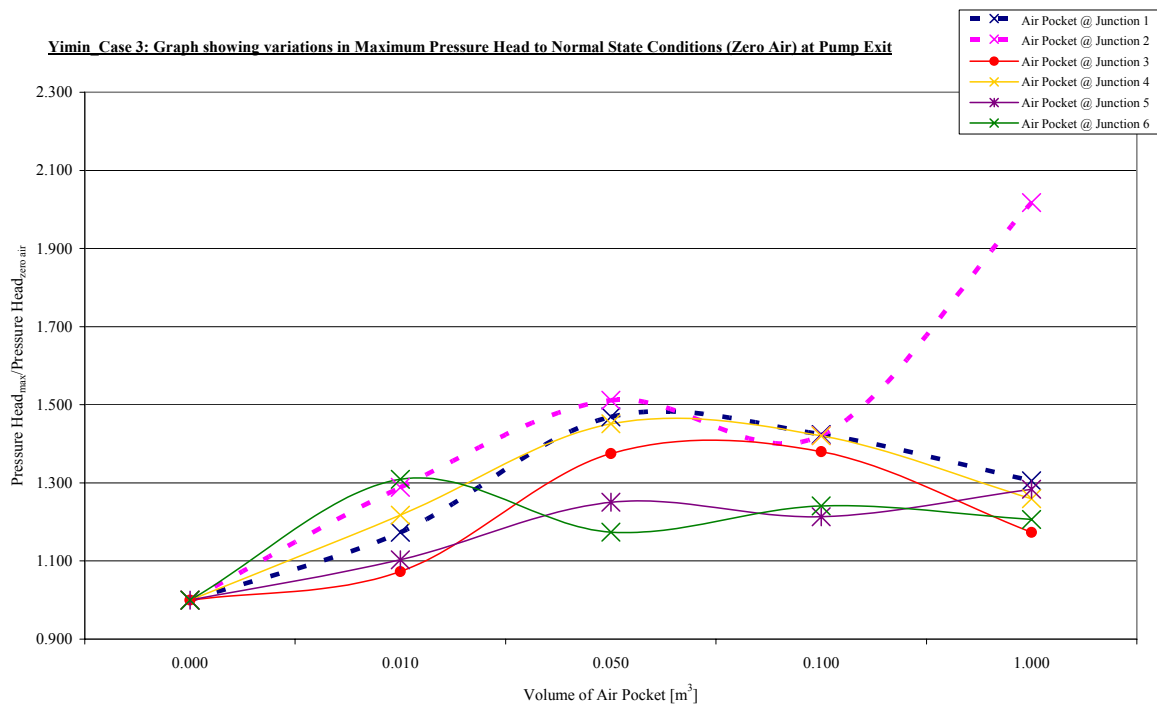


Figure 57 *CASE 3 - Pressure Enhancement Factors at Pump Exit*

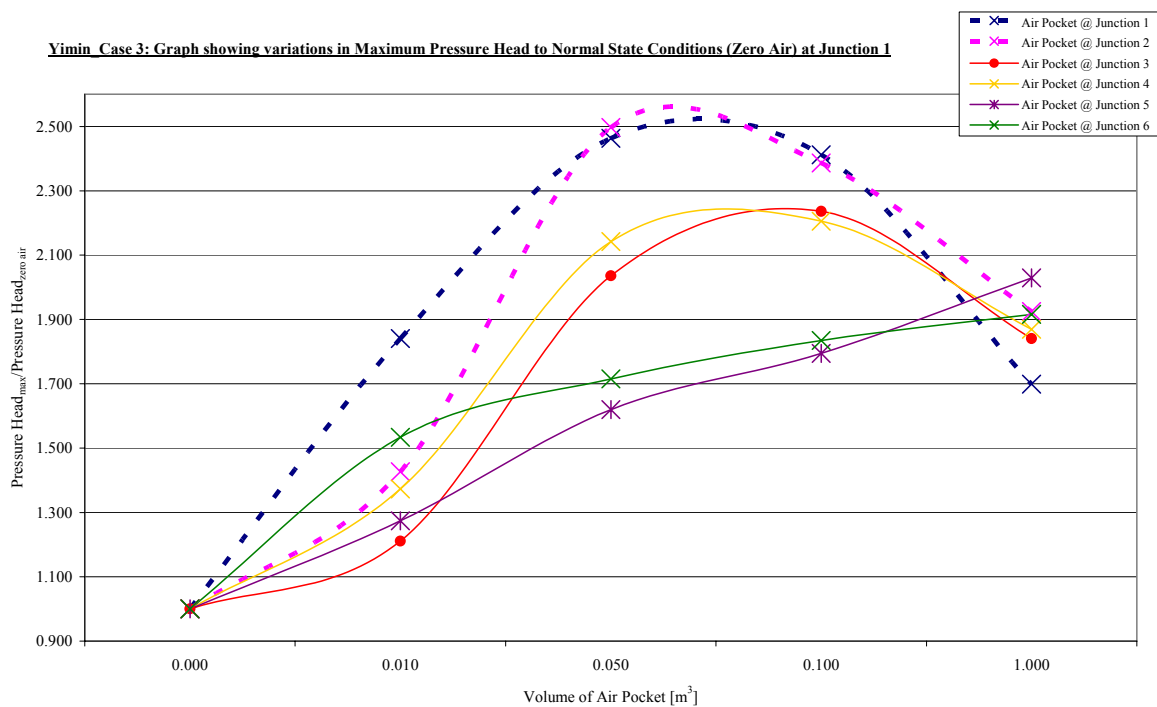


Figure 58 *CASE 3 - Pressure Enhancement Factors at Junction 1*

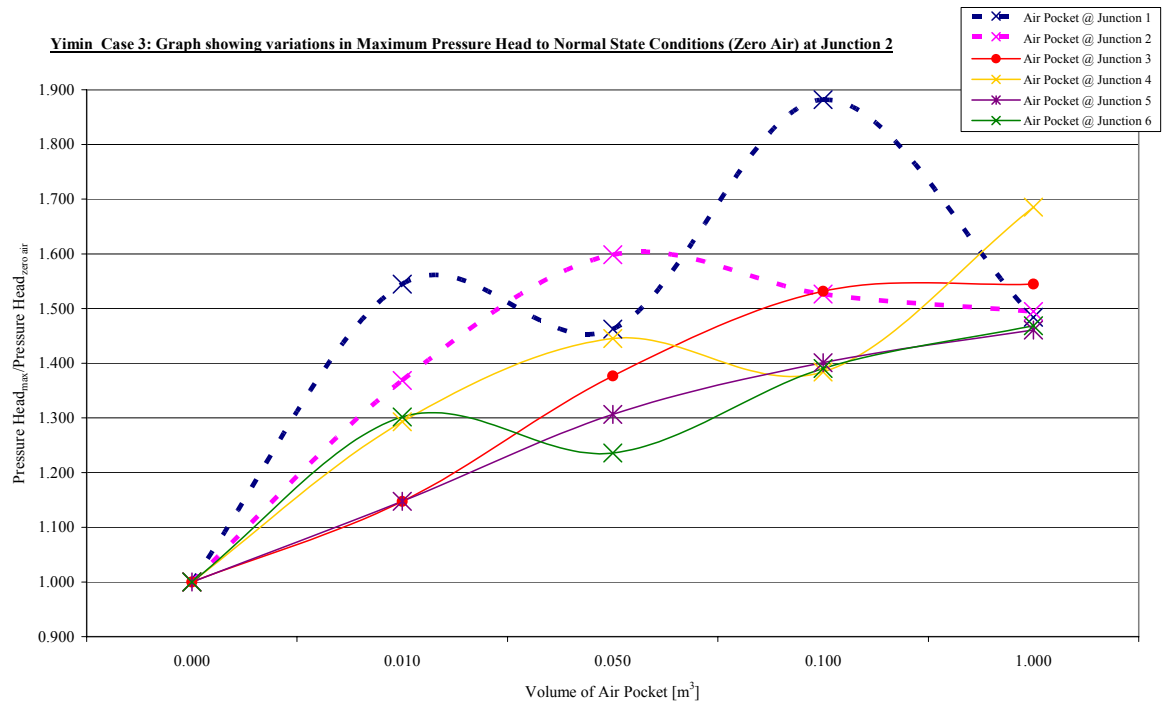


Figure 59 CASE 3 - Pressure Enhancement Factors at Junction 2

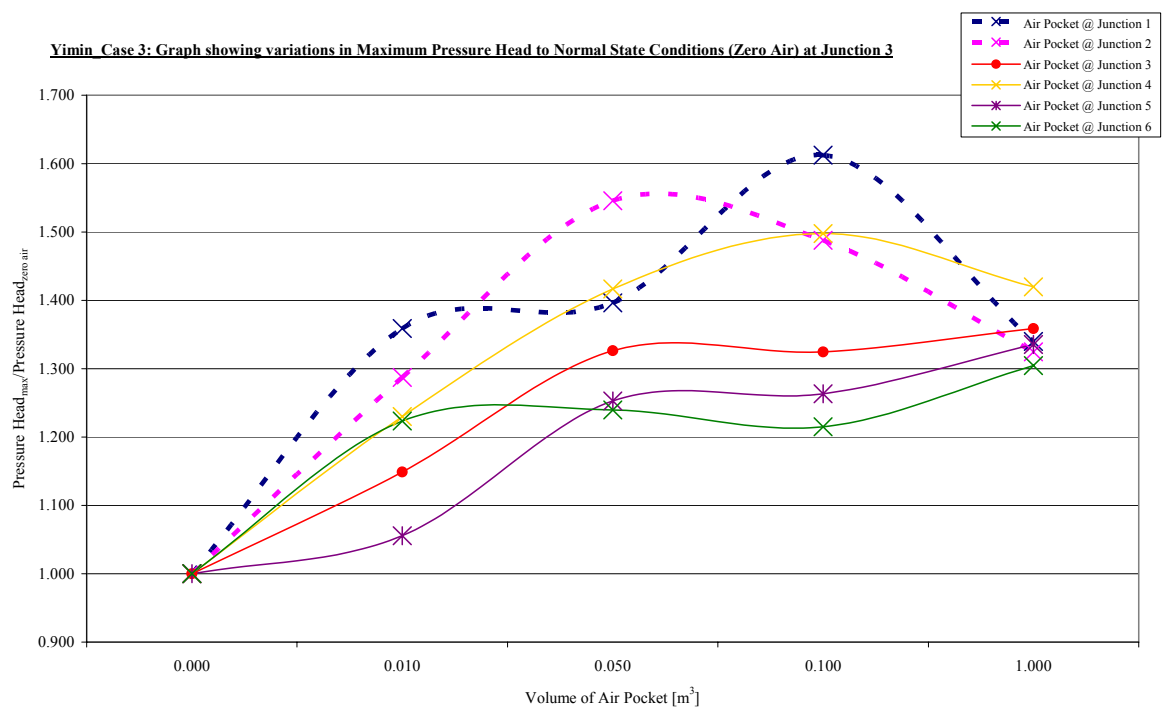


Figure 60 CASE 3 - Pressure Enhancement Factors at Junction 3

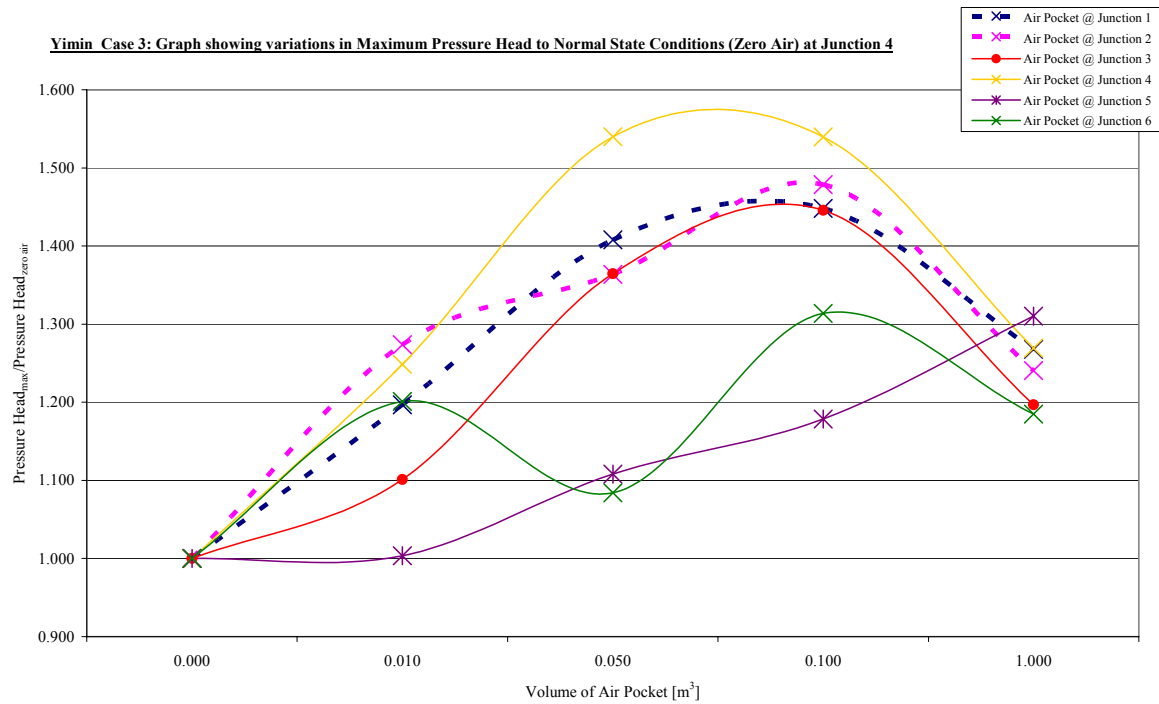


Figure 61 CASE 3 - Pressure Enhancement Factors at Junction 4

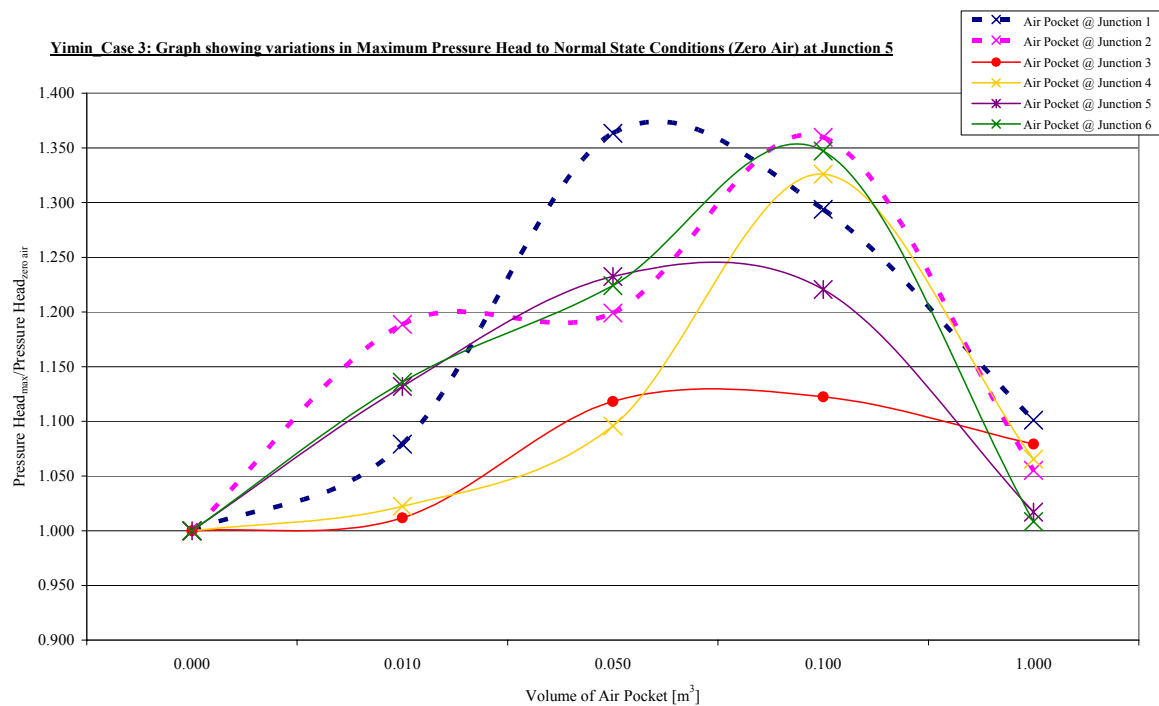


Figure 62 CASE 3 - Pressure Enhancement Factors at Junction 5

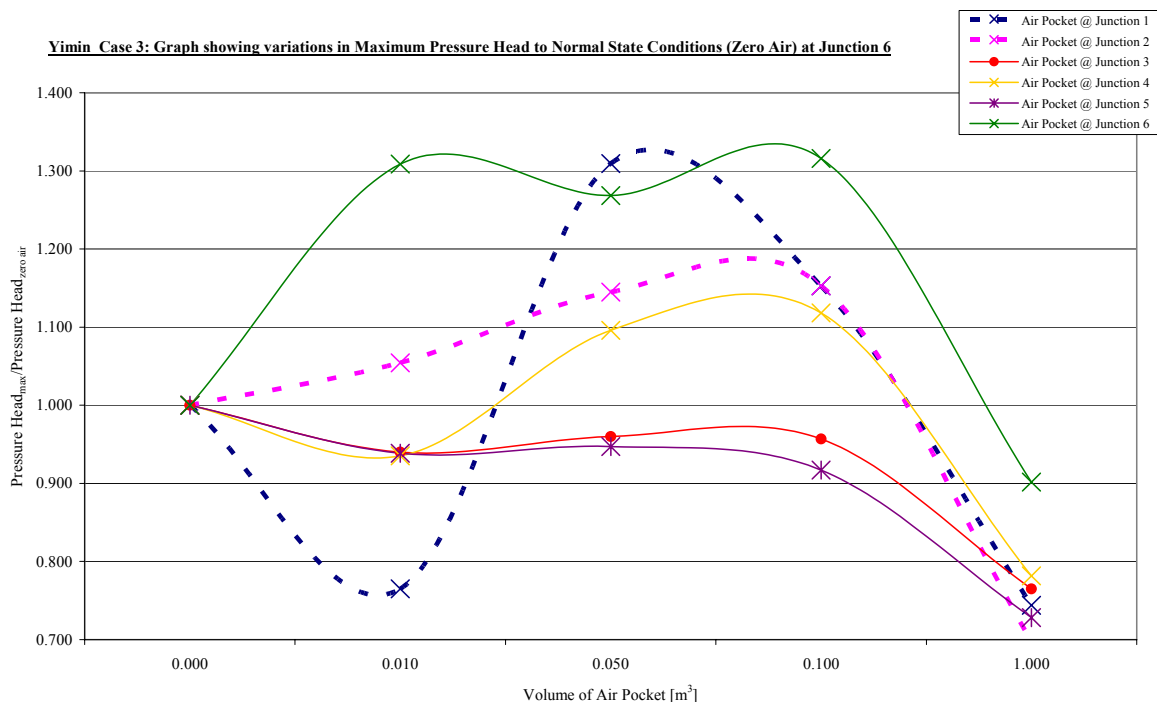


Figure 63 CASE 3 - Pressure Enhancement Factors at Junction 6

Summary

Table 26 presents a summary of findings from examining the outputs from the five case studies analysed. The approximate peak enhancement factor ranged from 1.3 to 2.6 and the pressure peak was predominantly located at Junction 1. The size of the air pocket varied from 0.05 to 0.1 m^3 and was located at either Junction 1 or 2.

8.3.2 Summary

From the results obtained, an appropriate guideline to designers wishing to take into full account the potential peak enhancements of air pockets would be to use an enhancement factor of 2.6. This would provide the cautious designer with a suitably conservative prediction of the pressures that could potentially be present in a pipeline system, under transient conditions. However, if it were found that these figures would result in a highly expensive system, or indeed in an un-buildable system, a more rigorous analysis of the system would be required where the observations and statements made in this Chapter could be utilised in order to obtain 'critical' conditions.

9. Conclusions

9.1 LABORATORY EXPERIMENTS

- A range of laboratory tests were carried out to investigate air movement in downward sloping pipes. Detailed measurements were taken in the range of 0 to 22.5 degrees (0 to 1/2.4) to fill an important gap in previous research.
- Some general conclusions were possible from the tests:

- Air moves freely upwards on upward sloping pipes under its own buoyancy with no flow. The velocities of air pockets in upwards sloping pipes are similar to the air pocket velocities observed in downward sloping pipes.
 - Air spreads widely along horizontal pipes with no flow
 - A critical velocity is required to move air pockets along horizontal and downward sloping pipes.
- An equation for estimation of critical flow velocity for air pocket movement was obtained from the experimental tests (Equation 15) which shows the dependency of the critical flow velocity on the slope and air pocket size (and implicitly on the pipe diameter too). For design purposes and given the uncertainties associated with air movement in pipes, it is reasonable to simplify the numerical terms in Equation (15), which was presented in Section 6. This equation was developed based on a range of air pocket sizes and the maximum values of critical velocity associated with each of the air pocket classes were used in its development. It can therefore be said that the equation was based on an envelope to the data. However, no safety factor was applied and for engineering applications consideration of a safety factor, S_f is advisable:

$$V/(gD)^{0.5} = S_f [0.56 (\sin S)^{0.5} + a] \quad (18)$$

where a equals:

0.45	for	$n < 0.06$
0.50	for	$0.06 \leq n < 0.12$
0.57	for	$0.12 \leq n < 0.30$
0.61	for	$0.30 \leq n < 2$

In the above equation V is the minimum flow velocity required for movement of an air pocket with size defined by the parameter $n (= 4V_{\text{air}} / (\pi D^3))$ in a downward pipe of slope S and diameter D . V_{air} is the volume of the air pocket and S_f is a safety factor (a value of 1.1 can be suggested in principle).

The applicability of the above equation is as follows:

- Downward slopes from 0 to 22.5 degrees (1/2.4). There is experimental evidence from other researchers (see Figure 10) that this relationship may be valid for slopes up to 40° (1/1.19) and that beyond this slope the critical flow velocity may start to decrease with the slope in a power law relationship.
- Air pockets with size in the range defined by $n=0.0001$ to 2 in a 150mm diameter pipe. This corresponded to air pocket volumes of 0.0005 litres to 5 litres. The asymptotic curve of Figure 10 indicates that for larger air pockets the required critical velocity for pocket movement may not increase significantly. It is thus suggested that taking $a=0.61$ for pocket sizes above 5 litres may be reasonable, until further work is done in this field.
- Tests were performed in a single pipe diameter of 0.150mm. There is evidence from previous research that scale effects due to surface tension can be neglected and therefore extending the results to larger pipe diameters is legitimate. It appears appropriate to say that Equation (18) can be used with reasonable confidence for pipe diameters of up to 1.5m. For this size, the required flow velocity for air pocket movement in a horizontal pipe as

predicted by Equation (18) for large air pockets is 2.1m/s and 2.6m/s respectively (including a safety factor of 1.1). The applicability of the recommended equation to larger pipe diameters is a matter of debate as it would need to be verified in practice.

- Although limited reliable data was collected, the test results appear to show that, for the same flow conditions, the hydraulic gradient associated with flow with an air pocket is 25 to 35% bigger than that associated with water alone.
- Tests with hydraulic jumps in downward circular pipes suggested that the rate of expulsion of air may be given by Equation (17). However, a comparison of results with those of other researchers, appear to indicate that the actual flow conditions and cross-sectional shape of the pipe are important factors that strongly influence the results.
 - The size of bubbles released by hydraulic jumps and carried downstream by the flow is typically in the range 3-5mm. The speed of movement of these bubbles varies between 0.4 and 0.7m/s; the ratio bubble vel. /flow vel. varies between 0.6 and 1.5.
 - For preliminary estimation of the length of hydraulic jumps in circular downward sloping pipes (0 to 22.7 degrees) the following relationships can be assumed.

JFL/D varies between 1.3 and 5 and OJL/D varies between 2 and 11, where D is the pipe diameter, JFL is the length of the steep face of the jump and OJL is the overall jump length.

- The tests indicated that, for the same pipe diameter, the velocity of movement of air pockets down the pipe is highly dependent on the pipe slope. The steeper the slope the smaller the ratio air pocket velocity/critical flow velocity becomes. It was found that the time required to remove an air pocket in a steeper pipe can be several times greater than in a mild slope.
- Tests carried out in upward slopes showed that even in very mild slopes (of less than 2 degrees) air pockets would move for static flow conditions, thus not requiring a threshold velocity.

9.2 NUMERICAL STUDY

- Through an extensive literature review and several analytical examples, the varying influences of air pocket size and location upon transient pressures have been simulated.
- The presence of air pockets have been shown, in certain circumstances to cause both high and low pressure fluctuations which are sufficiently large to potentially cause pipe fracture and pipeline failure. This therefore highlights a need for consideration of the transient wave interaction with entrapped air pockets during design stage.
- A larger pocket of air has the potential to act as an energy accumulator, which absorbs the transient pressures in a piped system.

- A small pocket of air has the potential to severely exacerbate maximum peak pressures.
- Results have highlighted that a small or large air pocket can be defined in terms of its effect upon pressure transients, but that there are limits upon size/volume, outside of which, these effects do not occur. This therefore suggests that a ‘critical’ spectrum of air pocket volume exists for a particular pipeline configuration and additionally, a further ‘critical’ size is relative to the actual location of the air pocket within the pipeline. (In the examples presented within this study, this spectrum of air pocket size = 0.01 m³ to 0.10 m³).
- Greater pressure enhancement occurs when small pockets of air are placed towards the upstream section of the pipeline. However, larger pockets of air can also enhance pressures when located at downstream locations, depending on pipeline configuration.
- Potentially destructive scale enhancements of pressures, due to the presence of air pockets, have a more significant impact at the upstream/pump section of a pipeline, due to the higher pressures already present along these sections.

10. References

- Bendiksen, K.H. 1984. An experimental investigation of the motion of long bubbles in inclined tubes, *Int. J. Multiphase Flow*, Vol. 10, No. 4, pp467-483
- Burrows, R. 2003. *A cautionary note on the operation of pumping mains without appropriate surge control and the potentially detrimental impact of small air pockets*, Paper submission for IAHR / IWA International Conference – PEDS-2003 – Valencia, Spain, April 22nd-25th.
- Burrows, R. and Qiu, D.Q. 1995. *Effect of air pockets on pipeline surge pressure*, Proceedings of the Institution of Civil Engineers, Journal of ‘Water, Maritime and Energy’, Volume 112, December, Paper 10859, pp. 349-361.
- Burrows, R. and Qiu, D.Q. 1996. *The effect of air pockets on pressure surge in sewage rising mains*, Hydrodynamics, (Eds.) Chwang, Lee and Leung, Balkema, ISBN 90 54 10 860 6, pp.1193-1198.
- Chanson, H. and Qiao, G.L. 1994. Air bubble entrainment and gas transfer at hydraulic jumps. Research Report No. CE149, Department of Civil Engineering, The University of Queensland, Brisbane, Australia
- Falvey, H.T. 1980. Air-water flow in hydraulic systems, Bureau of Reclamation, Engineering monograph No. 41
- Gahan, C. M. 2004. A review of the problem of air release/collection in water pipelines with in-depth study of the effects of entrapped air on pressure transients, MRes Thesis, Department of Civil Engineering, University of Liverpool, UK
- Gandenberger, W. 1957. *Über die wirtschaftliche und betriebssichere Gestaltung von Fernwasserleitungen*, R. Oldenbourg Verlag, Munich, Germany Design of overland water supply pipelines for economy and operational reliability (rough translation by W.A. Mechler, discussion of “Factors influencing flow in large conduits.”, Report of the Task Force on Flow in Large Conduits of the Committee on Hydraulic Structures, ASCE, Vol.92, No. HY4, 1966.
- James W. and Silberman E. 1958. Two-phase flow studies in horizontal pipes with special reference to bubbly mixtures, Technical Paper No. 26, Series B, St Antony Falls Hydraulics Laboratory, University of Minnesota, Minnesota
- Jonsson, L. 1985. *Maximum transient pressures in a conduit with check valve and air entrainment*, Proceeding of the International Conference on the Hydraulics of Pumping Stations, British Hydromechanics Research Association, Manchester, pp.55-76.
- Kalinske, A.A and Bliss, P.H. 1943. Removal of air from pipelines by flowing water, ASCE Vol. 13, No. 10, pp480-482
- Kent, J.C. 1952. The entrainment of air by water flowing in circular conduits with downgrade slopes. Doctoral thesis, University of California, Berkley, California

Larsen, T. and Burrows, R. 1992. *Measurements and computations of transients in pumped sewer plastic mains*, Proceedings of the BHR Group / IAHR International Conference on Pipeline Systems, Manchester, pp.117-123.

Lauchlan C.S., Escarameia M. and May R.W.P. 2004. Air in pipelines – literature review. HR Report SR649

Qiu, D.Q. 1995. *Transient Analysis and the Effect of Air Pockets in a Pipeline*, University of Liverpool, Department of Civil Engineering, M.Phil Thesis, 216 pp.

Rabben, S.L., Els, H., and Rouve, G. 1983. Investigation on flow aeration at offsets downstream of high-head control structures, Proc. 20th IAHR Congress, Moscow, USSR, Vol. 4, pp354-360

Rajaratnam, N. 1967. Hydraulic Jumps, Advances in Hydrosience, Ed. V.T. Chow, Academic Press, New York, USA, vol. 4, pp197-280

Thorley, A.R.D. 2004. *Fluid transients in pipeline systems – 2nd Edition*, D and L George, UK.

Viana, F., Pardo, R., Yanez, R., Trallero, J.L., Joseph, D.D. 2003. Universal Correlation for the rise velocity of long gas bubbles in round pipes, Journal of Fluid Mechanics, vol. 494, pp379-398

Wisner, P.E., Mohsen, F.N. and Kouwen, N. 1975. Removal of air from water lines by hydraulic means. ASCE, Journal of the Hydraulics Division, Vol. 101, HY2, pp243-257

Wylie, E.B. and Streeter, V.L. 1978. *Fluid Transients*, McGraw-Hill International Book Company, New York, 384 pp.

Zukoski, E.E. 1966. Influence of viscosity, surface tension and inclination on motion of long bubbles in closed tubes, J. of Fluid Mechanics, 25(4), pp 821-837.

Tables

Table 1 Test data for 0 degree downward slope (horizontal); critical flow velocity

Slope = 0 degrees (horizontal)

Test conditions:			beginning of tests	end of tests
atm pressure (mb)			1003	1002.5
temp (water) (C)			18	18.6
temp (air) (C)			20.8	21.05
test	Q (m ³ /s)	critical flow velocity (m/s)	air volume injected using cylinder (mm ³)	estimated air volume (mm ³)
A1				
A1.1	0.0077	0.44	57256	
A1.2	0.0079	0.45	82702	
A1.3	0.0074	0.42	136777	
A7				
A7.1	0.0049	0.28		9640
A7.2	0.0065	0.37		46801
A7.3	0.0074	0.42		28220
A7.4	0.0074	0.42		52994
A7.5	0.0074	0.42		40607
A7.6	0.0074	0.42		52994
A7.7	0.0095	0.54		96349
A7.8	0.0095	0.54		92633
A7.9	0.0095	0.54		83962
A7.10	0.0095	0.54		121123
A7.11	0.0095	0.54		145897
A7.12	0.0095	0.54		121123
A7.13	0.0083	0.47		114929
A7.14	0.0083	0.47		102542
A7.15	0.0083	0.47		114929
A7.16	0.0108	0.61		121123
A7.17	0.0108	0.61		158284
A7.18	0.0108	0.61		164477
A7.19	0.0108	0.61		158284
A7.20	0.0108	0.61		183058

Table 2 Test data for 0.8 degree downward slope (1 in 72); critical flow velocity
slope 0.8 degrees (1 in 72)

Test conditions:		beginning of tests	end of tests	
atm pressure (mb)		1008	1008	
temp (water) (C)		18.35	18.8	
temp (air) (C)		20	21.8	
test	Q (m ³ /s)	critical flow velocity (m/s)	air volume injected using cylinder (mm ³)	estimated air volume (mm ³)
A8				
A8.1	0.0051	0.29		524
A8.2	0.0051	0.29		5924
A8.3	0.0051	0.29		4685
A8.4	0.0074	0.42		17072
A8.5	0.0074	0.42		12117
A8.7	0.0092	0.52		34414
A8.8	0.0092	0.52		15833
A8.9	0.0092	0.52		59188
A8.10	0.0092	0.52		43085
A8.11	0.0113	0.64		303187
A8.12	0.0113	0.64		205018
A8.13	0.0113	0.64		71139
A8.14	0.0113	0.64		253866
A8.16	0.0131	0.74		168413
A8.17	0.0131	0.74		401277
A8.18	0.0131	0.74		637622
A8.19	0.0131	0.74		332444
A8.20	0.0131	0.74		222931

Table 3 Test data for 2.5 degree downward slope (1 in 23); critical flow velocity
slope 2.5 degrees (1 in 23)

Test conditions:			beginning of tests	end of tests
atm pressure (mb)			1013	1013
temp (water) (C)			15.9	16.5
temp (air) (C)			17.1	17.2
test	Q (m ³ /s)	critical flow velocity (m/s)	air volume injected using cylinder (mm ³)	estimated air volume (mm ³)
A6				
A6.2	0.0063	0.36	12723	
A6.4	0.0085	0.48		44532
A6.8	0.0081	0.46		44532
A6.9	0.0083	0.47	25447	
A6.11	0.0103	0.58		51274
A6.12	0.0107	0.61		28711
A6.13	0.0149	0.84		268526
A6.14	0.0146	0.83		240260
A6.15	0.0146	0.83		4995715
A6.16	0.0137	0.78		268526
Test conditions:			beginning of tests	end of tests
atm pressure (mb)			1015	1015
temp (water) (C)			16.35	17
temp (air) (C)			19.1	19.55
test	Q (m ³ /s)	critical flow velocity (m/s)	air volume injected using cylinder (mm ³)	estimated air volume (mm ³)
A6R				
A6R.1	0.0049	0.28		10770
A6R.2	0.0062	0.35		17197
A6R.3	0.0076	0.43		27662
A6R.4	0.0091	0.51		43360
A6R.5	0.0080	0.45		32895
A6R.6	0.0094	0.53		64290
A6R.7	0.0111	0.63		133011
A6R.8	0.0094	0.53		59057
A6R.9	0.0118	0.67		111382
A6R.10	0.0100	0.57		59057
A6R.11	0.0155	0.88		699319

Table 4 Test data for 3.4 degree downward slope; critical flow velocity

Slope 3.4 degrees (1 in 17)

Test conditions:	beginning of tests	end of tests
atm pressure (mb)	1019	1018
temp (water) (C)	15	15.85
temp (air) (C)	19.15	20

test	Q (m ³ /s)	critical flow velocity (m/s)	air volume injected using cylinder (mm ³)	estimated air volume (mm ³)
A5				
A5.1	0.0076	0.43		11536
A5.2	0.0056	0.32	6362	
A5.3	0.0070	0.39		8652
A5.4	0.0092	0.52	12723	
A5.5	0.0086	0.49		27721
A5.7	0.0107	0.61	25447	
A5.8	0.0116	0.66	69979	
A5.9	0.0123	0.70		197861
A5.10	0.0129	0.73		310809
A5.11	0.0129	0.73		177348
A5.12	0.0133	0.76		240260
A5.13	0.0135	0.76		240260
A5.14	0.0143	0.81		334769
A5.15	0.0147	0.83		673419
A5.16	0.0154	0.87		1326464
A5.17	0.0165	0.93		3583192

Test conditions:	beginning of tests	end of tests
atm pressure (mb)	1012	1011.5
temp (water) (C)	20.4	21
temp (air) (C)	16.3	16.9

test	Q (m ³ /s)	critical flow velocity (m/s)	air volume injected using cylinder (mm ³)	estimated air volume (mm ³)
A5R				
A5R.1	0.0089	0.51	25447	
A5R.2	0.0092	0.52	31809	
A5R.3	0.0104	0.59		54576
A5R.4	0.0105	0.60		63941
A5R.5	0.0105	0.59	38170	
A5R.6	0.0107	0.60		54576
A5R.7	0.0106	0.60	57256	
A5R.8	0.0109	0.62	76341	
A5R.9	0.0106	0.60		63941
A5R.10	0.0110	0.62		73306
A5R.11	0.0125	0.71	89064	

Table 5 Test data for 6 degree downward slope (1 in 9.5); critical flow velocity

Slope 6 degrees (1 in 9.5)

Test conditions:		beginning of tests	end of tests	
atm pressure (mb)		1004.5	1004.5	
temp (water) (C)		15.4	16.4	
temp (air) (C)		14.8	16	
test	Q (m ³ /s)	critical flow velocity (m/s)	air volume injected using cylinder (mm ³)	estimated air volume (mm ³)
A4				
A4.1	0.0093	0.53	25447	
A4.2	0.0093	0.53	38170	
A4.3	0.0098	0.56		36562
A4.4	0.0141	0.80		36562
A4.5	0.0084	0.47		14836
A4.6	0.0087	0.49	19085	
A4.7	0.0130	0.74		123466
A4.8	0.0093	0.53		14836
A4.9	0.0106	0.60	69979	
A4.10	0.0110	0.62		101740
A4.11	0.0100	0.57	31809	
A4.12	0.0078	0.44	6362	
A4.13	0.0087	0.49	25447	
A4.14	0.0108	0.61		36562
A4.16	0.0121	0.69		166918
A4.17	0.0120	0.68		123466

Test conditions:		beginning of tests	end of tests	
atm pressure (mb)		1004	1004.5	
temp (water) (C)		14.35	15.2	
temp (air) (C)		16.9	16.8	
test	Q (m ³ /s)	critical flow velocity (m/s)	air volume injected using cylinder (mm ³)	estimated air volume (mm ³)
A4R				
A4R.1	0.0140	0.80		203908
A4R.2	0.0151	0.86		221654
A4R.3	0.0151	0.86		221654
A4R.4	0.0151	0.86		221654
A4R.5	0.0161	0.91		257146
A4R.6	0.0161	0.91		257146
A4R.7	0.0161	0.91		328130
A4R.8	0.0169	0.96		345876
A4R.9	0.0169	0.96		257146
A4R.10	0.0169	0.96		363622
A4R.11	0.0178	1.01		381368
A4R.12	0.0178	1.01		452352
A4R.13	0.0178	1.01		612066
A4R.14	0.0153	0.87		221654

Table 5 Test data for 6 degree downward slope (1 in 9.5); critical flow velocity (continued)

test	Q (m ³ /s)	critical flow velocity (m/s)	air volume injected using cylinder (mm ³)	estimated air volume (mm ³)
A4R.15	0.0153	0.87		257146
A4R.16	0.0153	0.87		274892
A4R.17	0.0144	0.82		186162
A4R.18	0.0144	0.82		203908
A4R.20	0.0144	0.82		221654

Test conditions:	beginning of tests	end of tests
atm pressure (mb)	1022	1021.5
temp (water) (C)	14.4	15.2
temp (air) (C)	18.2	18.5

test	Q (m ³ /s)	critical flow velocity (m/s)	air volume injected using cylinder (mm ³)	estimated air volume (mm ³)
A4RR				
A4RR.1	0.0096	0.54		65171
A4RR.2	0.0096	0.54		47425
A4RR.3	0.0120	0.68		91790
A4RR.4	0.0125	0.71		136155
A4RR.5	0.0135	0.76		207139
A4RR.6	0.0142	0.80		216012
A4RR.7	0.0150	0.85		260377
A4RR.8	0.0124	0.70		136155
A4RR.9	0.0108	0.61		56298

Table 6 Test data for 11.5 degree downward slope (1 in 5); critical flow velocity

Slope 11.5 degrees (1 in 5)

Test conditions:		beginning of tests		end of tests
atm pressure (mb)		1026		1026
temp (water) (C)		15.9		15.9
temp (air) (C)		21.6		21.6
test	Q (m ³ /s)	critical flow velocity (m/s)	air volume injected using cylinder (mm ³)	estimated air volume (mm ³)
A3R				
A3R.A	0.0100	0.56	6362	
A3R.B	0.0123	0.70		76343
A3R.C	0.0126	0.71	120873	
A3R.D	0.0139	0.79		148443
A3R.E	0.0086	0.49		3766
A3R.F	0.0128	0.73	108149	
A3R.G	0.0120	0.68		76343
A3R.H	0.0126	0.71	69979	
A3R.I	0.0127	0.72		76343
A3R.J	0.0120	0.68		40293
Test conditions:		beginning of tests		end of tests
atm pressure (mb)		998.5		998.5
temp (water) (C)		20.15		20.9
temp (air) (C)		18.1		18.1
test	Q (m ³ /s)	critical flow velocity (m/s)	air volume injected using cylinder (mm ³)	estimated air volume (mm ³)
A13				
A13.5	0.0100	0.57		20329
A13.9	0.0111	0.63		50115
A13.10	0.0111	0.63		31210
A13.11	0.0111	0.63		43850
A13.12	0.0124	0.70		53247
A13.13	0.0124	0.70		62171
A13.14	0.0124	0.70		56379
A13.15	0.0124	0.70		97221
A13.16	0.0124	0.70		110843
A13.17	0.0137	0.78		69486
A13.18	0.0137	0.78		97221
A13.22	0.0146	0.82		144373
A13.23	0.0146	0.82		88894
A13.24	0.0146	0.82		144373
A13.25	0.0155	0.88		312390
A13.26	0.0155	0.88		156927
A13.27	0.0155	0.88		205677
A13.28	0.0155	0.88		246672
A13.31	0.0167	0.95		387795
A13.32	0.0167	0.95		492114

Table 6 **Test data for 11.5 degree downward slope (1 in 5); critical flow velocity (continued)**

test	Q (m ³ /s)	critical flow velocity (m/s)	air volume injected using cylinder (mm ³)	estimated air volume (mm ³)
A13.33	0.0167	0.95		644196
A13.34	0.0167	0.95		543915
A13.35	0.0185	1.05		2697148
A13.36	0.0185	1.05		2246180
A13.37	0.0185	1.05		3330477
A13.38	0.0185	1.05		4278438

Table 7 Test data for 16.5 degree downward slope (1 in 3.4); critical flow velocity

Slope 16.5 degrees (1 in 3.4)

Test conditions:	beginning of tests	end of tests
atm pressure (mb)	999	999
temp (water) (C)	18.1	18.4
temp (air) (C)	19.45	21.2

test	Q (m ³ /s)	critical flow velocity (m/s)	air volume injected using cylinder (mm ³)	estimated air volume (mm ³)
A12				
A12.2	0.0128	0.72		15111
A12.3	0.0115	0.65		15111
A12.6	0.0130	0.74		67728
A12.8	0.0132	0.75		37195
A12.9	0.0132	0.75		18133
A12.10	0.0132	0.75		18133
A12.11	0.0145	0.82		67728
A12.12	0.0145	0.82		50115
A12.13	0.0145	0.82		33440
A12.14	0.0186	1.05		310809
A12.16	0.0159	0.90		121927
A12.18	0.0159	0.90		155462
A12.19	0.0183	1.04		709305
A12.20	0.0183	1.04		709305
A12.21	0.0183	1.04		466055
A12.22	0.0183	1.04		662018

Table 8 Test data for 22.5 degree downward slope (1 in 2.4); critical flow velocity

Slope 22.5 degrees (1 in 2.4)

Test conditions:		beginning of tests	end of tests	
atm pressure (mb)		1003	1002.5	
temp (water) (C)		18	18.6	
temp (air) (C)		20.8	21.05	
test	Q (m ³ /s)	critical flow velocity (m/s)	air volume injected using cylinder (mm ³)	estimated air volume (mm ³)
A11				
A11.1	0.0128	0.72		26568
A11.2	0.0134	0.76		43886
A11.3	0.0156	0.88		88674
A11.4	0.0156	0.88		88674
A11.5	0.0159	0.90		76195
A11.6	0.0184	1.04		229053
A11.7	0.0159	0.90		99758
A11.8	0.0158	0.90		99758
A11.9	0.0209	1.18		362610
A11.10	0.0179	1.02		193814
A11.11	0.0209	1.18		490816
A11.12	0.0179	1.02		155462
A11.13	0.0210	1.19		609456
A11.14	0.0181	1.02		280074
A11.15	0.0210	1.19		537756
A11.16	0.0181	1.02		211433
A11.17	0.0211	1.19		236986

Table 9 Test data on air pocket velocity for downward slopes

test	Q (m ³ /s)	critical flow velocity (m/s)	air pocket velocity (m/s)	air pocket velocity / critical flow velocity
slope 0 degrees (horizontal)				
A7.1	0.0050	0.28	0.05	0.19
A7.2	0.0065	0.37	0.03	0.07
A7.3	0.0074	0.42	0.09	0.23
A7.4	0.0074	0.42	0.03	0.07
A7.5	0.0074	0.42	0.18	0.42
A7.6	0.0074	0.42	0.15	0.36
A7.9	0.0095	0.54	0.23	0.43
A7.10	0.0095	0.54	0.17	0.31
A7.11	0.0095	0.54	0.27	0.50
A7.12	0.0095	0.54	0.31	0.58
A7.14	0.0083	0.47	0.23	0.49
A7.15	0.0083	0.47	0.23	0.49
A7.18	0.0108	0.61	0.56	0.93
A7.19	0.0108	0.61	0.58	0.96
A7.20	0.0108	0.61	0.52	0.85
				<i>average=0.46</i>
slope 2.5 degrees (1 in 23)				
A6.2	0.0063	0.36	0.04	0.11
A6.4	0.0085	0.48	0.08	0.17
A6.8	0.0082	0.46	0.05	0.10
A6.9	0.0083	0.47	0.05	0.11
A6.11	0.0103	0.58	0.12	0.20
A6.12	0.0107	0.61	0.12	0.20
A6.13	0.0149	0.84	0.15	0.18
A6.14	0.0146	0.83	0.18	0.21
A6.16	0.0138	0.78	0.09	0.11
A6R.1	0.0049	0.28	0.02	0.06
A6R.2	0.0062	0.35	0.03	0.09
A6R.3	0.0076	0.43	0.03	0.08
A6R.4	0.0091	0.51	0.06	0.12
A6R.5	0.0080	0.45	0.05	0.10
A6R.6	0.0094	0.53	0.06	0.12
A6R.8	0.0095	0.53	0.07	0.12
				<i>average=0.13</i>

Table 9 Test data on air pocket velocity for downward slopes (continued)

test	Q (m ³ /s)	critical flow velocity (m/s)	air pocket velocity (m/s)	air pocket velocity / critical flow velocity
slope 6 degrees (1 in 9.5)				
A4R.1	0.0141	0.80	0.05	0.06
A4R.2	0.0151	0.86	0.04	0.05
A4R.3	0.0151	0.86	0.07	0.08
A4R.4	0.0151	0.86	0.05	0.06
A4R.5	0.0161	0.91	0.07	0.07
A4R.6	0.0161	0.91	0.07	0.08
A4R.7	0.0161	0.91	0.05	0.06
A4R.8	0.0169	0.96	0.07	0.08
A4R.9	0.0169	0.96	0.11	0.12
A4R.10	0.0169	0.96	0.07	0.08
A4R.11	0.0178	1.01	0.12	0.12
A4R.12	0.0178	1.01	0.09	0.09
A4R.13	0.0178	1.01	0.09	0.09
A4R.14	0.0153	0.87	0.06	0.07
A4R.15	0.0153	0.87	0.04	0.05
A4R.16	0.0153	0.87	0.03	0.04
A4R.17	0.0144	0.82	0.05	0.06
A4R.18	0.0144	0.82	0.04	0.05
A4R.20	0.0144	0.82	0.02	0.03

average=0.07

Table 10 Test data for 2.5 degree downward slope (1 in 23); hydraulic gradients with and without air pocket

Test conditions:		beginning of tests	end of tests	
atm pressure (mb)		1013	1013	
temp (water) (C)		15.9	16.5	
temp (air) (C)		17.1	17.2	
Test	Q (m ³ /s)	hydraulic gradient with air pocket (i air)	hydraulic gradient without air pocket (i)	% difference, (i air - i) / i
A6				
A6.2	0.0063	0.0035	0.0028	0.2667
A6.4	0.0085	0.0017	0.0024	-0.3077
A6.8	0.0082	0.0037	0.0031	0.1765
A6.9	0.0083	0.0036	0.0031	0.1471
A6.10		0.0033	0.0031	0.0588
A6.12		0.0050	0.0030	0.6875
A6.13	0.0107	0.0078	0.0059	0.3125
A6.14	0.0146	0.0061	0.0048	0.2692
A6.16	0.0138	0.0083	0.0059	0.4063

Table 11 Test data for 3.4 degree downward slope (1 in 17); hydraulic gradients with and without air pocket

Test conditions:		beginning of tests	end of tests	
atm pressure (mb)		1019	1018	
temp (water) (C)		15	15.85	
temp (air) (C)		19.15	20	
Test	Q (m ³ /s)	hydraulic gradient with air pocket (i air)	hydraulic gradient without air pocket (i)	% difference, (i air - i) / i
A5				
A5.1	0.0076	0.0019	0.0013	0.4167
A5.2	0.0056	0.0013	0.0009	0.4000
A5.3	0.007	0.0010	0.0006	0.7500
A5.4	0.0092	0.0033	0.0022	0.5000
A5.5	0.0086	0.0020	0.0015	0.3750
A5.7	0.0107	0.0031	0.0025	0.2222
A5.8	0.0116	0.0047	0.0041	0.1591
A5.9	0.0124	0.0039	0.0022	0.7500
A5.10	0.0129	0.0036	0.0030	0.2188
A5.11	0.0129	0.0031	0.0029	0.0794
A5.13	0.0135	0.0036	0.0037	-0.0250
A5.14	0.0143	0.0042	0.0037	0.1250
A5.15	0.0147	0.0069	0.0041	0.7045
A5.16	0.0154	0.0089	0.0044	1.0000
A5.17	0.0165	0.0111	0.0056	1.0000

Table 12 Hydraulic jump lengths

Test	Slope (degrees)	Q (m ³ /s)	Length of jump			
			Front jump length, FJL (m)	Overall jump length, OJL (m)	FJL/D	OJL/D
HJ8	0.8					
HJR8.1		0.0089	NM	1.7		11.3
HJR8.2		0.0131	NM	0.5		3.3
HJ6	2.5					
HJ6.2		0.0121	NM	0.3		2.0
HJ6.3		0.0100	NM	0.4		2.7
HJ4	6					
HJ4.1		0.0041	NM	0.5		3.3
HJ4.2		0.0134	0.26	0.75	1.7	5.0
HJ4.3		0.0111	0.25	1.2	1.7	8.0
HJ4.4		0.0146	0.2	1.7	1.3	11.3
HJ4.5		0.0062	0.3	1	2.0	6.7
HJ3	11.5	0.0076	0.7	1.25	4.7	8.3

Note: NM - not measured

Table 13 Hydraulic jump tests; tests on exhaustion of air cavity

slope 0.8 degrees

Test conditions:	beginning of tests	end of tests
atm pressure (mb)	1008	1008
temp (water) (C)	17.85	18.35
temp (air) (C)	19.2	20

Test	time (s)	Q (m ³ /s)	flow velocity (m/s)	air pocket volume (m ³)
HJR8.1	0	0.0089	0.5053	0.0333
	300			0.0281
	600			0.0276
	1200			0.0272
	2280			0.0264
HJR8.2	0	0.0131	0.7419	0.0180
	120			0.0153
	240			0.0077
	300			0.0046
	540			0.0000

slope 2.5 degrees

Test conditions:	beginning of tests	end of tests
atm pressure (mb)	1013.5	1013
temp (water) (C)	16.3	17.2
temp (air) (C)	18.8	19.9

Test	time (s)	Q (m ³ /s)	flow velocity (m/s)	air pocket volume (m ³)
HJ6.2	0	0.0121	0.6853	0.1297
	270			0.0448
	510			0.0300
	660			0.0194
	750			0.0000
HJ6.3	0	0.0100	0.5653	0.0451
	915			0.0288
	1800			0.0194
	1980			0.0175
	2250			0.0156
	2490			0.0131
	2850			0.0117

Table 13 Hydraulic jump tests; tests on exhaustion of air cavity (continued)

slope 3.4 degrees

Test conditions:	beginning of tests	end of tests
atm pressure (mb)	1011.5	1011.5
temp (water) (C)	16.9	17.6
temp (air) (C)	21	21.1

Test	time (s)	Q (m ³ /s)	flow velocity (m/s)	air pocket volume (m ³)
HJ5.1	0	0.0142	0.8007	0.0101
	60			0.0049
	120			0.0033
	270			0.0005
	315			0.0000
HJ5.2	0	0.0142	0.8007	0.0442
	500			0.0283
	780			0.0117
	900			0.0087
	1020			0.0065
	1140			0.0052
	1260			0.0027
	1380			0.0005
	1443			0.0000

slope 11.7 degrees

Test conditions:	beginning of tests	end of tests
atm pressure (mb)	998.5	998.5
temp (water) (C)	20.15	20.9
temp (air) (C)	18.1	18.1

Test	time (s)	Q (m ³ /s)	flow velocity (m/s)	air pocket volume (m ³)
HJ13.2	0	0.0181	1.0243	0.0114
	117			0.0000
HJ13.3	0	0.0181	1.0243	0.0162
	129			0.0000

slope 16.5 degrees

Test conditions:	beginning of tests	end of tests
atm pressure (mb)	999	999
temp (water) (C)	18.4	18.6
temp (air) (C)	21.2	21.4

Test	time (s)	Q (m ³ /s)	flow velocity (m/s)	air pocket volume (m ³)
HJ12.1	0	0.0184	1.0384	0.0114
	20			0.0053
	32			0.0033
	75			0.0006

Table 13 Hydraulic jump tests; tests on exhaustion of air cavity (continued)

Test	time (s)	Q (m ³ /s)	flow velocity (m/s)	air pocket volume (m ³)
HJ12.3	89	0.0198	1.1176	0.0000
	0			0.0159
	120			0.0000
HJ12.4	0	0.0198	1.1176	0.0097
	20			0.0044
	51			0.0000
HJ12.5	0	0.0198	1.1176	0.0209
	20			0.0142
	125			0.0000

slope 22.7 degrees

Test conditions:	beginning of tests	end of tests
atm pressure (mb)	1002.5	1002.5
temp (water) (C)	18.6	18.6
temp (air) (C)	19.2	20

Test	time (s)	Q (m ³ /s)	flow velocity (m/s)	air pocket volume (m ³)
HJ12.1	0	0.0211	1.2	0.0105
	6			0.0087
	7			0.0077
	9			0.0073
	12			0.0057
	13			0.0046
	15			0.0039
	18			0.0035
	30			0.0025
	37			0.0019
	58			0.0000

Table 14 Hydraulic jump tests; duration of air circulation period

Test	Slope (degrees)	Q (m ³ /s)	Period (s)		
			minimum	average	maximum
HJ5.2	3.4	0.01415	5	18	69
HJ5.3	3.4	0.01158	3	7	12
HJ6.1	2.5	0.00886	4	10	20
HJ6.2	2.5	0.01211	7	41	115

Table 15 Average air pocket velocities measured in the tests

Angle (degrees)	average ratios air pocket velocity / flow velocity
0	0.46
0.8	0.19
2.5	0.13
3.4	0.07
6	0.07
11.5	0.03

Table 16 Details of the Pipeline Profile – CASES 13 and 15

Chainage (m)	Elevation (m)	
	CASE 13	CASE 15
0.0	17.6	17.6
32.0	19.7	20.0
53.0	21.1	20.0
168.0	25.9	20.0
229.0	28.9	20.0
341.0	36.3	20.0
459.0	38.4	20.0
471.0	40.6	20.0
536.0	42.4	20.0
595.0	35.2	20.0
683.0	40.3	20.0
732.0	45.9	20.0
777.0	46.2	20.0
837.0	48.7	20.0
917.0	49.0	20.0
1045.0	49.6	20.0
1089.0	50.6	50.6

Table 17 Characteristic pump curve data

Flow (m ³ /s)	Head (m)	Power (kW)
0.000	54.3	29.8
0.019	50.3	34.3
0.038	46.9	40.3
0.060	44.5	49.2
0.076	42.4	58.2
0.095	39.6	64.9
0.114	36.3	74.6
0.321	0.0	165.0

Table 18 Critical Locations for Various Volumes of Air Pocket – Showing Overall Maximum Total Head Values (At Pump Exit)

Air Pocket Volume (m ³)	CASE 13			CASE 15		
	Total Head (m)	Time of Peak (s)	Location of Air Pocket	Total Head (m)	Time of Peak (s)	Location of Air Pocket
0.001	148	6	Junction 2	106	4 - 5	Junction 1
0.010	150	6	Junction 1	164	12 - 13	Junction 1
0.025	148	7	Junction 1	148	6	Junction 1
0.050	156	8	Junction 1	150	7	Junction 1
0.1	157	10	Junction 1	148	9	Junction 1
1.0	114	5	Junction 6	107	24	Junction 1

Table 19 Air Pocket Volumes and Locations to give Peak Surges at Sequential Locations along the Pipeline Profile

Peak Pressure given With Air Located at Junction No.	Air Pocket Volume (m ³)					
	Pump Exit		Junction 1		Junction 2	
	CASE 13	CASE 15	CASE 13	CASE 15	CASE 13	CASE 15
1	0.100	0.010	0.025	0.010	0.025	0.010
2	0.010	0.010	0.025	0.010	0.010	0.025
3	0.025	0.050	0.025	0.050	0.010	0.050
4	0.000	0.050	0.000	0.050	0.000	0.050
5	0.000	0.100	0.000	0.100	0.000	0.100
6	0.000	All (Equal Values)	0.000	All (Equal Values)	0.000	All (Equal Values)

Peak Pressure given With Air Located at Junction No.	Air Pocket Volume (m ³)					
	Junction 3		Junction 4		Junction 5	
	CASE 13	CASE 15	CASE 13	CASE 15	CASE 13	CASE 15
1	0.025	0.010	0.000	0.010	0.000	0.010
2	0.010	0.025	0.000	0.025	0.000	0.001
3	0.000	0.050	0.000	0.025	0.000	0.001
4	0.000	0.100	0.000	0.100	0.000	0.001
5	0.000	0.100	0.000	0.100	0.000	0.025
6	0.000	All (Equal Values)	0.000	All (Equal Values)	0.000	All (Equal Values)

Table 20 Locations of Air Pocket to give Peak Surges at Sequential Locations along the Pipeline Profile

Air Pocket Volume (m ³)	Pocket Location for Max. Head Results					
	Pump Exit		Junction 1		Junction 2	
	CASE 13	CASE 15	CASE 13	CASE 15	CASE 13	CASE 15
0.001	J2	J1	J2	J2	J2	J1
0.010	J1	J1	J2	J1	J2	J1
0.025	J1	J1	J1	J1	J1	J1
0.050	J1	J1	J1	J1	J1	J1
0.100	J1	J1	J1	J1	J1	J1
1.000	J6	J1	J6	J2	J6	J3

Air Pocket Volume (m ³)	Pocket Location for Max. Head Results					
	Junction 3		Junction 4		Junction 5	
	CASE 13	CASE 15	CASE 13	CASE 15	CASE 13	CASE 15
0.001	J2	J2	J2	J1	J3	J1
0.010	J2	J1	J1	J1	J1	J1
0.025	J1	J1	J1	J1	J3	J1
0.050	J1	J1	J1	J1	J5	J1
0.100	J1	J1	J6	J1	J6	J6
1.000	J6	J4	J6	J5	J6	J6

Table 21 CASE 13 - Peak Pressure Enhancement Factors at Sequential Locations along the Pipeline Profile**(a), 'Pump Exit'**

Pressure Head at Pump Exit - Chainage 0m												
No Air Present = 129.735 m												
Volume of Air (m ³)	Pressure Head (m)						Relative to Volume Zero					
	Air @ J1	Air @ J2	Air @ J3	Air @ J4	Air @ J5	Air @ J6	Air @ J1	Air @ J2	Air @ J3	Air @ J4	Air @ J5	Air @ J6
0.000	129.735	129.735	129.735	129.735	129.74	129.735	1.000	1.000	1.000	1.000	1.000	1.000
0.001	91.607	129.023	119.413	102.927	98.244	97.073	0.706	0.995	0.920	0.793	0.757	0.748
0.010	133.443	132.456	126.305	121.328	97.107	97.073	1.029	1.021	0.974	0.935	0.749	0.748
0.025	133.879	131.290	132.603	124.520	120.033	97.073	1.032	1.012	1.022	0.960	0.925	0.748
0.050	135.349	123.526	121.766	120.922	107.054	97.073	1.043	0.952	0.939	0.932	0.825	0.748
0.100	138.486	114.778	101.803	97.133	93.209	97.073	1.067	0.885	0.785	0.749	0.718	0.748
1.000	85.187	80.535	70.527	72.019	87.189	97.073	0.657	0.621	0.544	0.555	0.672	0.748

(b), 'Junction 1'

Pressure Head at Junction 1 - Chainage 168m												
No Air Present = 115.354 m												
Volume of Air [m ³]	Pressure Head [m]						Relative to Volume Zero					
	Air @ J1	Air @ J2	Air @ J3	Air @ J4	Air @ J5	Air @ J6	Air @ J1	Air @ J2	Air @ J3	Air @ J4	Air @ J5	Air @ J6
0.000	115.354	115.354	115.354	115.354	115.35	115.354	1.000	1.000	1.000	1.000	1.000	1.000
0.001	73.945	116.729	108.479	83.058	82.389	86.597	0.641	1.012	0.940	0.720	0.714	0.751
0.010	117.105	119.571	114.212	108.170	83.511	86.597	1.015	1.037	0.990	0.938	0.724	0.751
0.025	119.166	118.649	118.186	107.905	90.618	86.597	1.033	1.029	1.025	0.935	0.786	0.751
0.050	116.325	108.700	106.264	106.624	89.131	86.597	1.008	0.942	0.921	0.924	0.773	0.751
0.100	105.507	101.652	87.113	82.051	78.286	86.597	0.915	0.881	0.755	0.711	0.679	0.751
1.000	43.959	64.173	56.043	60.717	68.280	86.597	0.381	0.556	0.486	0.526	0.592	0.751

(c), 'Junction 2'

Pressure Head at Junction 2 - Chainage 341m												
No Air Present = 100.719 m												
Volume of Air [m ³]	Pressure Head [m]						Relative to Volume Zero					
	Air @ J1	Air @ J2	Air @ J3	Air @ J4	Air @ J5	Air @ J6	Air @ J1	Air @ J2	Air @ J3	Air @ J4	Air @ J5	Air @ J6
0.000	100.719	100.719	100.719	100.719	100.72	100.719	1.000	1.000	1.000	1.000	1.000	1.000
0.001	65.793	100.690	96.031	68.199	66.069	68.238	0.653	1.000	0.953	0.677	0.656	0.678
0.010	99.976	103.048	101.826	74.826	67.897	68.238	0.993	1.023	1.011	0.743	0.674	0.678
0.025	104.762	102.286	97.979	83.724	71.239	68.238	1.040	1.016	0.973	0.831	0.707	0.678
0.050	102.303	98.013	88.552	82.203	72.803	68.238	1.016	0.973	0.879	0.816	0.723	0.678
0.100	84.230	79.639	72.024	61.119	64.771	68.238	0.836	0.791	0.715	0.607	0.643	0.678
1.000	30.844	29.519	47.071	46.658	50.409	68.238	0.306	0.293	0.467	0.463	0.500	0.678

Table 21 CASE 13 - Peak Pressure Enhancement Factors at Sequential Locations along the Pipeline Profile (continued)

(d), 'Junction 3'

Pressure Head at Junction 3 - Chainage 536m												
No Air Present = 89.072 m												
Volume of Air [m ³]	Pressure Head						Relative to Volume Zero					
	[m]											
	Air @ J1	Air @ J2	Air @ J3	Air @ J4	Air @ J5	Air @ J6	Air @ J1	Air @ J2	Air @ J3	Air @ J4	Air @ J5	Air @ J6
0.000	89.072	89.072	89.072	89.072	89.072	89.072	1.000	1.000	1.000	1.000	1.000	1.000
0.001	61.101	86.349	79.354	63.884	58.761	53.266	0.686	0.969	0.891	0.717	0.660	0.598
0.010	82.882	93.227	68.854	56.922	57.414	53.266	0.931	1.047	0.773	0.639	0.645	0.598
0.025	89.262	84.090	62.316	58.064	65.777	53.266	1.002	0.944	0.700	0.652	0.738	0.598
0.050	79.595	74.388	63.200	53.916	57.195	53.266	0.894	0.835	0.710	0.605	0.642	0.598
0.100	62.734	60.492	57.699	50.729	53.773	53.266	0.704	0.679	0.648	0.570	0.604	0.598
1.000	21.193	20.177	20.270	33.206	44.996	53.266	0.238	0.227	0.228	0.373	0.505	0.598

Table 22 CASE 15 - Peak Pressure Enhancement Factors at Sequential Locations along the Pipeline Profile**(a), 'Pump Exit'**

Pressure Head at Pump Exit - Chainage 0m												
No Air Present = 69.429 m												
Volume of Air [m ³]	Pressure Head [m]						Relative to Volume Zero					
	Air @ J1	Air @ J2	Air @ J3	Air @ J4	Air @ J5	Air @ J6	Air @ J1	Air @ J2	Air @ J3	Air @ J4	Air @ J5	Air @ J6
0.000	69.429	69.429	69.429	69.429	69.429	69.429	1.000	1.000	1.000	1.000	1.000	1.000
0.001	89.481	88.072	77.041	71.528	69.600	69.429	1.289	1.269	1.110	1.030	1.002	1.000
0.010	146.382	128.540	97.025	78.288	86.941	69.429	2.108	1.851	1.397	1.128	1.252	1.000
0.025	132.633	120.202	109.578	92.952	96.624	69.429	1.910	1.731	1.578	1.339	1.392	1.000
0.050	134.138	119.898	116.299	100.952	89.887	69.429	1.932	1.727	1.675	1.454	1.295	1.000
0.100	131.541	111.345	103.595	91.222	111.619	69.429	1.895	1.604	1.492	1.314	1.608	1.000
1.000	85.717	76.746	82.253	78.867	78.811	69.429	1.235	1.105	1.185	1.136	1.135	1.000

(b), 'Junction 1'

Pressure Head at Junction 1 - Chainage 168m												
No Air Present = 54.992 m												
Volume of Air [m ³]	Pressure Head [m]						Relative to Volume Zero					
	Air @ J1	Air @ J2	Air @ J3	Air @ J4	Air @ J5	Air @ J6	Air @ J1	Air @ J2	Air @ J3	Air @ J4	Air @ J5	Air @ J6
0.000	54.992	54.992	54.992	54.992	54.992	54.992	1.000	1.000	1.000	1.000	1.000	1.000
0.001	56.233	63.553	60.839	61.376	59.672	54.992	1.023	1.156	1.106	1.116	1.085	1.000
0.010	135.840	117.539	81.381	63.492	72.444	54.992	2.470	2.137	1.480	1.155	1.317	1.000
0.025	128.481	115.872	103.701	84.419	72.058	54.992	2.336	2.107	1.886	1.535	1.310	1.000
0.050	124.575	115.838	109.344	95.775	80.926	54.992	2.265	2.106	1.988	1.742	1.472	1.000
0.100	108.836	107.786	96.470	87.813	83.723	54.992	1.979	1.960	1.754	1.597	1.522	1.000
1.000	51.213	73.278	66.168	65.408	65.005	54.992	0.931	1.333	1.203	1.189	1.182	1.000

(c), 'Junction 2'

Pressure Head at Junction 2 - Chainage 341m												
No Air Present = 56.365 m												
Volume of Air [m ³]	Pressure Head [m]						Relative to Volume Zero					
	Air @ J1	Air @ J2	Air @ J3	Air @ J4	Air @ J5	Air @ J6	Air @ J1	Air @ J2	Air @ J3	Air @ J4	Air @ J5	Air @ J6
0.000	56.365	56.365	56.365	56.365	56.365	56.365	1.000	1.000	1.000	1.000	1.000	1.000
0.001	67.083	57.960	61.992	59.167	60.909	56.365	1.190	1.028	1.100	1.050	1.081	1.000
0.010	126.989	99.810	80.427	68.385	60.091	56.365	2.253	1.771	1.427	1.213	1.066	1.000
0.025	122.688	114.867	99.569	83.916	63.518	56.365	2.177	2.038	1.767	1.489	1.127	1.000
0.050	114.043	108.502	99.778	85.341	74.173	56.365	2.023	1.925	1.770	1.514	1.316	1.000
0.100	103.054	97.932	91.786	83.786	80.187	56.365	1.828	1.737	1.628	1.486	1.423	1.000
1.000	48.308	49.536	67.015	66.476	65.442	56.365	0.857	0.879	1.189	1.179	1.161	1.000

Table 22 CASE 15 - Peak Pressure Enhancement Factors at Sequential Locations along the Pipeline Profile (continued)**(d), 'Junction 3'**

Pressure Head at Junction 3 - Chainage 536m												
No Air Present		=	57.145 m									
Volume of Air [m³]	Pressure Head						Relative to Volume Zero					
	[m]											
	Air @ J1	Air @ J2	Air @ J3	Air @ J4	Air @ J5	Air @ J6	Air @ J1	Air @ J2	Air @ J3	Air @ J4	Air @ J5	Air @ J6
0.000	57.145	57.145	57.145	57.145	57.145	57.145	1.000	1.000	1.000	1.000	1.000	1.000
0.001	66.229	67.318	59.666	62.053	58.614	57.145	1.159	1.178	1.044	1.086	1.026	1.000
0.010	127.925	95.492	76.490	59.623	59.996	57.145	2.239	1.671	1.339	1.043	1.050	1.000
0.025	111.062	108.435	82.831	71.931	70.940	57.145	1.944	1.898	1.449	1.259	1.241	1.000
0.050	105.168	91.463	84.502	75.533	70.813	57.145	1.840	1.601	1.479	1.322	1.239	1.000
0.100	91.429	81.939	83.469	78.580	80.736	57.145	1.600	1.434	1.461	1.375	1.413	1.000
1.000	44.376	45.484	46.911	65.957	65.026	57.145	0.777	0.796	0.821	1.154	1.138	1.000

(e), 'Junction 4'

Pressure Head at Junction 4 - Chainage 732m													
No Air Present		=	56.848		m								
Volume of Air [m³]	Pressure Head						Relative to Volume Zero						
	[m]												
	Air @ J1	Air @ J2	Air @ J3	Air @ J4	Air @ J5	Air @ J6	Air @ J1	Air @ J2	Air @ J3	Air @ J4	Air @ J5	Air @ J6	
0.000	56.848	56.848	56.848	56.848	56.848	56.848	1.000	1.000	1.000	1.000	1.000	1.000	
0.001	65.189	64.148	61.714	55.462	58.831	56.848	1.147	1.128	1.086	0.976	1.035	1.000	
0.010	106.221	73.166	67.752	54.011	69.055	56.848	1.869	1.287	1.192	0.950	1.215	1.000	
0.025	98.336	82.566	75.514	57.333	69.268	56.848	1.730	1.452	1.328	1.009	1.218	1.000	
0.050	86.509	73.733	73.245	59.153	75.813	56.848	1.522	1.297	1.288	1.041	1.334	1.000	
0.100	73.128	69.140	67.060	66.107	76.574	56.848	1.286	1.216	1.180	1.163	1.347	1.000	
1.000	40.251	41.538	42.251	43.959	63.700	56.848	0.708	0.731	0.743	0.773	1.121	1.000	

(f), 'Junction 5'

Pressure Head at Junction 5 - Chainage 917m												
No Air Present		=	55.525		m							
Volume of Air [m³]	Pressure Head [m]						Relative to Volume Zero					
	Air @ J1	Air @ J2	Air @ J3	Air @ J4	Air @ J5	Air @ J6	Air @ J1	Air @ J2	Air @ J3	Air @ J4	Air @ J5	Air @ J6
0.000	55.525	55.525	55.525	55.525	55.525	55.525	1.000	1.000	1.000	1.000	1.000	1.000
0.001	66.252	63.262	60.553	62.257	51.651	55.525	1.193	1.139	1.091	1.121	0.930	1.000
0.010	73.240	62.765	61.657	54.013	60.318	55.525	1.319	1.130	1.110	0.973	1.086	1.000
0.025	69.327	60.635	60.272	51.470	68.036	55.525	1.249	1.092	1.085	0.927	1.225	1.000
0.050	58.831	55.131	58.125	49.951	55.275	55.525	1.060	0.993	1.047	0.900	0.995	1.000
0.100	55.270	53.069	52.488	50.468	54.384	55.525	0.995	0.956	0.945	0.909	0.979	1.000
1.000	36.603	37.079	37.266	38.311	40.241	55.525	0.659	0.668	0.671	0.690	0.725	1.000

Table 22 CASE 15 - Peak Pressure Enhancement Factors at Sequential Locations along the Pipeline Profile (continued)**(e), 'Junction 4'**

Pressure Head at Junction 4 - Chainage 732m												
No Air Present = 80.229 m												
Volume of Air [m ³]	Pressure Head						Relative to Volume Zero					
	[m]											
	Air @ J1	Air @ J2	Air @ J3	Air @ J4	Air @ J5	Air @ J6	Air @ J1	Air @ J2	Air @ J3	Air @ J4	Air @ J5	Air @ J6
0.000	80.229	80.229	80.229	80.229	80.229	80.229	1.000	1.000	1.000	1.000	1.000	1.000
0.001	47.481	64.921	57.460	42.315	45.112	45.070	0.592	0.809	0.716	0.527	0.562	0.562
0.010	74.690	57.542	56.008	56.973	48.682	45.070	0.931	0.717	0.698	0.710	0.607	0.562
0.025	66.075	53.207	54.295	48.661	61.191	45.070	0.824	0.663	0.677	0.607	0.763	0.562
0.050	57.430	52.698	48.334	39.238	45.683	45.070	0.716	0.657	0.602	0.489	0.569	0.562
0.100	42.649	43.471	41.336	44.498	40.481	45.070	0.532	0.542	0.515	0.555	0.505	0.562
1.000	13.791	13.705	13.292	14.152	32.280	45.070	0.172	0.171	0.166	0.176	0.402	0.562

(f), 'Junction 5'

Pressure Head at Junction 5 - Chainage 917m												
No Air Present = 74.244 m												
Volume of Air [m ³]	Pressure Head						Relative to Volume Zero					
	[m]											
	Air @ J1	Air @ J2	Air @ J3	Air @ J4	Air @ J5	Air @ J6	Air @ J1	Air @ J2	Air @ J3	Air @ J4	Air @ J5	Air @ J6
0.000	74.244	74.244	74.244	74.244	74.244	74.244	1.000	1.000	1.000	1.000	1.000	1.000
0.001	36.372	46.808	50.271	35.279	28.800	34.328	0.490	0.630	0.677	0.475	0.388	0.462
0.010	69.278	49.850	37.944	39.302	29.455	34.328	0.933	0.671	0.511	0.529	0.397	0.462
0.025	37.918	36.314	41.846	34.649	37.405	34.328	0.511	0.489	0.564	0.467	0.504	0.462
0.050	33.743	31.487	25.732	22.867	41.410	34.328	0.454	0.424	0.347	0.308	0.558	0.462
0.100	56.802	24.920	20.780	24.730	23.791	34.328	0.765	0.336	0.280	0.333	0.320	0.462
1.000	7.401	7.156	6.758	7.152	8.013	34.328	0.100	0.096	0.091	0.096	0.108	0.462

Table 23 CASE 1 - Peak Pressure Enhancement Factors at Sequential Locations along the Pipeline Profile**(a), 'Pump Exit'**

<u>Pressure Head at Pump Exit - Chainage 0m</u>						
No Air Present			= 34.78			
Volume of Air [m³]	Pressure Head [m]			Relative to Volume Zero		
	Air @ J1	Air @ J2	Air @ J3	Air @ J1	Air @ J2	Air @ J3
0.000	34.78	34.78	34.78	1.000	1.000	1.000
0.010	38.127	34.566	34.780	1.096	0.994	1.000
0.050	36.412	33.730	34.780	1.047	0.970	1.000
0.100	34.817	36.536	34.780	1.001	1.050	1.000
1.000	35.434	33.606	34.780	1.019	0.966	1.000

(b), 'Junction 1'

<u>Pressure Head at Junction 1 - Chainage 1180m</u>						
No Air Present			= 23.833			
Volume of Air [m³]	Pressure Head [m]			Relative to Volume Zero		
	Air @ J1	Air @ J2	Air @ J3	Air @ J1	Air @ J2	Air @ J3
0.000	23.833	23.833	23.833	1.000	1.000	1.000
0.010	30.047	23.162	23.833	1.261	0.972	1.000
0.050	26.024	24.918	23.833	1.092	1.046	1.000
0.100	22.972	24.335	23.833	0.964	1.021	1.000
1.000	15.751	20.297	23.833	0.661	0.852	1.000

(c), 'Junction 2'

<u>Pressure Head at Junction 2 - Chainage 2400m</u>						
No Air Present			= 19.608			
Volume of Air [m³]	Pressure Head [m]			Relative to Volume Zero		
	Air @ J1	Air @ J2	Air @ J3	Air @ J1	Air @ J2	Air @ J3
0.000	19.608	19.608	19.608	1.000	1.000	1.000
0.010	19.868	23.096	19.608	1.013	1.178	1.000
0.050	16.002	21.059	19.608	0.816	1.074	1.000
0.100	14.169	19.343	19.603	0.723	0.986	1.000
1.000	10.375	15.253	19.608	0.529	0.778	1.000

Table 24 CASE 2 - Peak Pressure Enhancement Factors at Sequential Locations along the Pipeline Profile**(a), 'Pump Exit'**

Pressure Head at Pump Exit - Chainage 0m								
No Air Present		=	25.53 m					
Volume of Air [m³]	Pressure Head [m]				Relative to Volume Zero			
	Air @ J1	Air @ J2	Air @ J3	Air @ J4	Air @ J1	Air @ J2	Air @ J3	Air @ J4
0.000	25.53	25.53	25.53	25.53	1.000	1.000	1.000	1.000
0.010	27.331	27.710	23.614	23.530	1.071	1.085	0.925	0.922
0.050	28.968	32.371	31.896	23.530	1.135	1.268	1.249	0.922
0.100	32.761	29.842	28.438	23.530	1.283	1.169	1.114	0.922
1.000	22.775	22.343	22.224	23.530	0.892	0.875	0.871	0.922

(b), 'Junction 1'

Pressure Head at Junction 1 - Chainage 374m								
No Air Present		=	13.123 m					
Volume of Air [m³]	Pressure Head [m]				Relative to Volume Zero			
	Air @ J1	Air @ J2	Air @ J3	Air @ J4	Air @ J1	Air @ J2	Air @ J3	Air @ J4
0.000	13.123	13.123	13.123	13.123	1.000	1.000	1.000	1.000
0.010	16.918	20.957	16.346	13.123	1.289	1.597	1.246	1.000
0.050	22.401	25.359	21.050	13.123	1.707	1.932	1.604	1.000
0.100	24.311	22.965	22.244	13.123	1.853	1.750	1.695	1.000
1.000	12.239	15.743	15.005	13.123	0.933	1.200	1.143	1.000

(c), 'Junction 2'

(c), Junction 2								
Pressure Head at Junction 2 - Chainage 622m								
No Air Present		=	10.035 m					
Volume of Air [m³]	Pressure Head [m]				Relative to Volume Zero			
	Air @ J1	Air @ J2	Air @ J3	Air @ J4	Air @ J1	Air @ J2	Air @ J3	Air @ J4
0.000	10.035	10.035	10.035	10.035	1.000	1.000	1.000	1.000
0.010	12.734	17.294	12.015	10.035	1.269	1.723	1.197	1.000
0.050	19.328	18.889	15.434	10.035	1.926	1.882	1.538	1.000
0.100	16.685	17.493	15.720	10.035	1.663	1.743	1.567	1.000
1.000	7.222	7.196	10.761	10.035	0.720	0.717	1.072	1.000

Table 24 CASE 2 - Peak Pressure Enhancement Factors at Sequential Locations along the Pipeline Profile (continued)

(d), 'Junction 3'

Pressure Head at Junction 3 - Chainage 930m								
No Air Present = 14.059 m								
Volume of Air [m ³]	Pressure Head [m]				Relative to Volume Zero			
	Air @ J1	Air @ J2	Air @ J3	Air @ J4	Air @ J1	Air @ J2	Air @ J3	Air @ J4
0.000	14.059	14.059	14.059	14.059	1.000	1.000	1.000	1.000
0.010	14.863	19.585	16.370	14.059	1.057	1.393	1.164	1.000
0.050	19.708	17.351	17.504	14.059	1.402	1.234	1.245	1.000
0.100	17.009	16.799	14.912	14.059	1.210	1.195	1.061	1.000
1.000	9.783	10.025	11.520	14.059	0.696	0.713	0.819	1.000

Table 25 CASE 3 - Peak Pressure Enhancement Factors at Sequential Locations along the Pipeline Profile**(a), 'Pump Exit'**

<u>Pressure Head at Pump Exit - Chainage 0m</u>												
No Air Present		=	25.03		m							
Volume of Air [m³]	Pressure Head						Relative to Volume Zero					
	[m]											
	Air @ J1	Air @ J2	Air @ J3	Air @ J4	Air @ J5	Air @ J6	Air @ J1	Air @ J2	Air @ J3	Air @ J4	Air @ J5	Air @ J6
0.000	25.03	25.03	25.03	25.03	25.03	25.03	1.000	1.000	1.000	1.000	1.000	1.000
0.010	29.364	32.252	26.857	30.474	27.610	32.775	1.173	1.289	1.073	1.217	1.103	1.309
0.050	36.773	37.836	34.420	36.325	31.300	29.378	1.469	1.512	1.375	1.451	1.250	1.174
0.100	35.640	35.579	34.544	35.560	30.369	31.066	1.424	1.421	1.380	1.421	1.213	1.241
1.000	32.673	50.502	29.364	31.517	32.132	30.203	1.305	2.018	1.173	1.259	1.284	1.207

(b), 'Junction 1'

</

(c), 'Junction 2'

Pressure Head at Junction 2 - Chainage 912m												
No Air Present		=	13.925		m							
Volume of Air [m³]	Pressure Head [m]						Relative to Volume Zero					
	Air @ J1	Air @ J2	Air @ J3	Air @ J4	Air @ J5	Air @ J6	Air @ J1	Air @ J2	Air @ J3	Air @ J4	Air @ J5	Air @ J6
0.000	13.925	13.925	13.925	13.925	13.925	13.925	1.000	1.000	1.000	1.000	1.000	1.000
0.010	21.510	19.055	15.976	18.005	15.981	18.129	1.545	1.368	1.147	1.293	1.148	1.302
0.050	20.366	22.260	19.172	20.125	18.191	17.209	1.463	1.599	1.377	1.445	1.306	1.236
0.100	26.209	21.254	21.327	19.273	19.512	19.364	1.882	1.526	1.532	1.384	1.401	1.391
1.000	20.666	20.813	21.510	23.470	20.342	20.448	1.484	1.495	1.545	1.685	1.461	1.468

Table 25 CASE 3 - Peak Pressure Enhancement Factors at Sequential Locations along the Pipeline Profile (continued)**(d), 'Junction 3'**

Pressure Head at Junction 3 - Chainage 1157m												
No Air Present = 16.276 m												
Volume of Air [m ³]	Pressure Head [m]						Relative to Volume Zero					
	Air @ J1	Air @ J2	Air @ J3	Air @ J4	Air @ J5	Air @ J6	Air @ J1	Air @ J2	Air @ J3	Air @ J4	Air @ J5	Air @ J6
0.000	16.276	16.276	16.276	16.276	16.276	16.276	1.000	1.000	1.000	1.000	1.000	1.000
0.010	22.116	20.954	18.700	20.017	17.182	19.912	1.359	1.287	1.149	1.230	1.056	1.223
0.050	22.725	25.159	21.587	23.059	20.392	20.176	1.396	1.546	1.326	1.417	1.253	1.240
0.100	26.244	24.215	21.561	24.379	20.563	19.774	1.612	1.488	1.325	1.498	1.263	1.215
1.000	21.807	21.560	22.116	23.108	21.732	21.233	1.340	1.325	1.359	1.420	1.335	1.305

(e), 'Junction 4'

Pressure Head at Junction 4 - Chainage 1402m												
No Air Present = 16.295 m												
Volume of Air [m ³]	Pressure Head [m]						Relative to Volume Zero					
	Air @ J1	Air @ J2	Air @ J3	Air @ J4	Air @ J5	Air @ J6	Air @ J1	Air @ J2	Air @ J3	Air @ J4	Air @ J5	Air @ J6
0.000	16.295	16.295	16.295	16.295	16.295	16.295	1.000	1.000	1.000	1.000	1.000	1.000
0.010	19.504	20.756	17.945	20.346	16.354	19.572	1.197	1.274	1.101	1.249	1.004	1.201
0.050	22.942	22.220	22.236	25.092	18.058	17.668	1.408	1.364	1.365	1.540	1.108	1.084
0.100	23.600	24.096	23.560	25.091	19.203	21.406	1.448	1.479	1.446	1.540	1.178	1.314
1.000	20.659	20.214	19.504	20.682	21.351	19.308	1.268	1.241	1.197	1.269	1.310	1.185

(f), 'Junction 5'

Pressure Head at Junction 5 - Chainage 1767m												
No Air Present = 17.553 m												
Volume of Air [m ³]	Pressure Head [m]						Relative to Volume Zero					
	Air @ J1	Air @ J2	Air @ J3	Air @ J4	Air @ J5	Air @ J6	Air @ J1	Air @ J2	Air @ J3	Air @ J4	Air @ J5	Air @ J6
0.000	17.553	17.553	17.553	17.553	17.553	17.553	1.000	1.000	1.000	1.000	1.000	1.000
0.010	18.944	20.864	17.759	17.946	19.867	19.938	1.079	1.189	1.012	1.022	1.132	1.136
0.050	23.934	21.047	19.629	19.233	21.632	21.489	1.364	1.199	1.118	1.096	1.232	1.224
0.100	22.713	23.869	19.701	23.275	21.426	23.648	1.294	1.360	1.122	1.326	1.221	1.347
1.000	19.327	18.523	18.944	18.702	17.852	17.702	1.101	1.055	1.079	1.065	1.017	1.008

Table 25 CASE 3 - Peak Pressure Enhancement Factors at Sequential Locations along the Pipeline Profile (continued)

(g), 'Junction 6'

<u>Pressure Head at Junction 6 - Chainage 2427m</u>												
No Air Present = 14.616 m												
Volume of Air [m ³]	Pressure Head [m]						Relative to Volume Zero					
	Air @ J1	Air @ J2	Air @ J3	Air @ J4	Air @ J5	Air @ J6	Air @ J1	Air @ J2	Air @ J3	Air @ J4	Air @ J5	Air @ J6
0.000	14.616	14.616	14.616	14.616	14.616	14.616	1.000	1.000	1.000	1.000	1.000	1.000
0.010	11.182	15.411	13.738	13.672	13.716	19.130	0.765	1.054	0.940	0.935	0.938	1.309
0.050	19.141	16.735	14.032	16.020	13.843	18.542	1.310	1.145	0.960	1.096	0.947	1.269
0.100	16.848	16.852	13.986	16.343	13.402	19.233	1.153	1.153	0.957	1.118	0.917	1.316
1.000	10.874	10.193	11.182	11.423	10.642	13.179	0.744	0.697	0.765	0.782	0.728	0.902

Table 26 Summary of Peak Pressure Enhancement Factors

Case Study	Approximate Peak Enhancement Factor	Location of Peak Pressure	Air Pocket	
			Size [m ³]	Location
CASE 13	1.10	Pump Exit	0.1	Junction 1
CASE 15	2.60	Junction 1	0.01	Junction 1
CASE 1	1.30	Junction 1	0.01	Junction 1
CASE 2	2.00	Junction 1	0.05	Junction 2
CASE 3	2.60	Junction 1	0.05	Junction 2

NB. Peak Enhancement being the factor relating the results to that achieved at the same location, under the same simulation conditions, with no air present in the model.

Plates

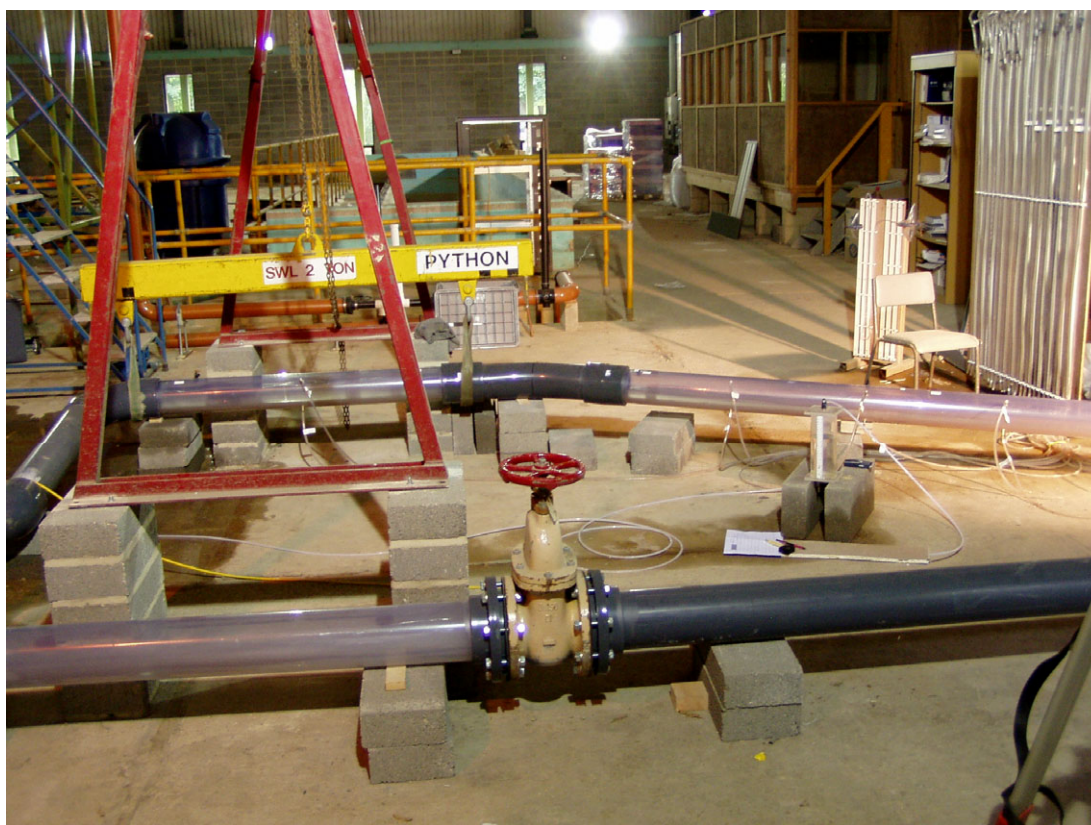


Plate 1 *Test section with a flat set-up viewed from downstream*



Plate 2 *Test section at a 22.5 degree slope*

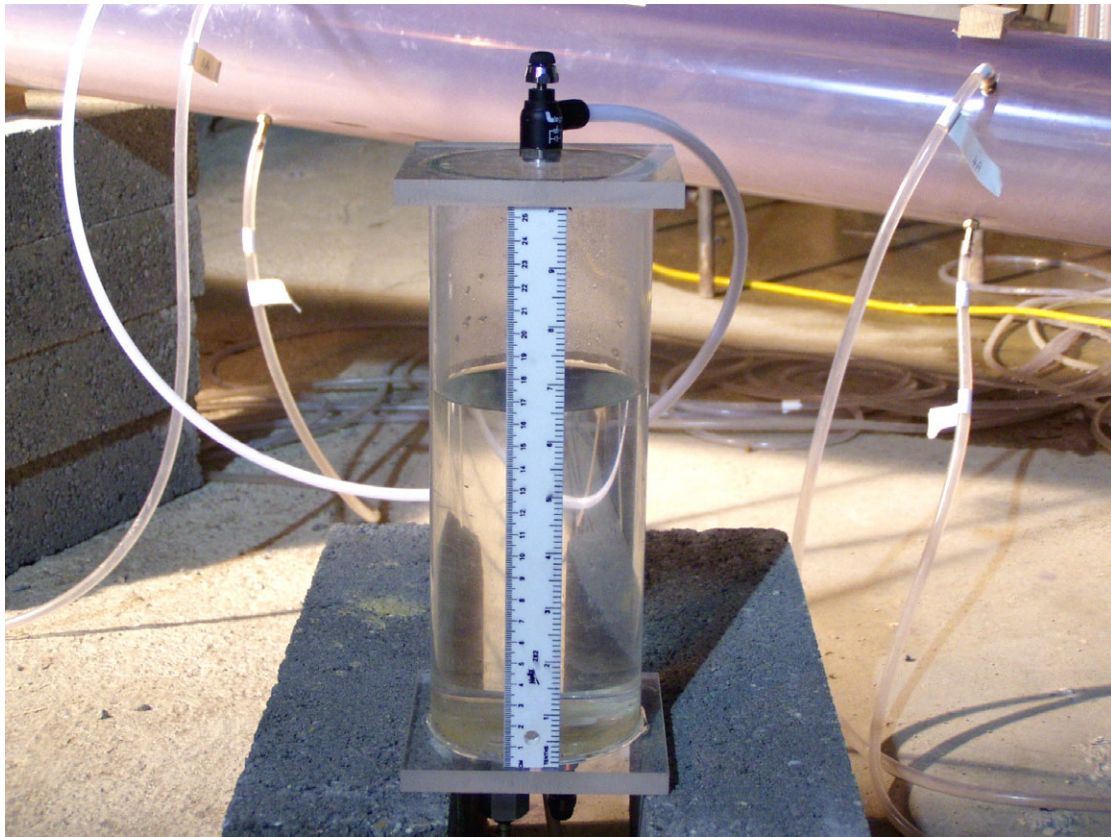


Plate 3 ***Air injection system***

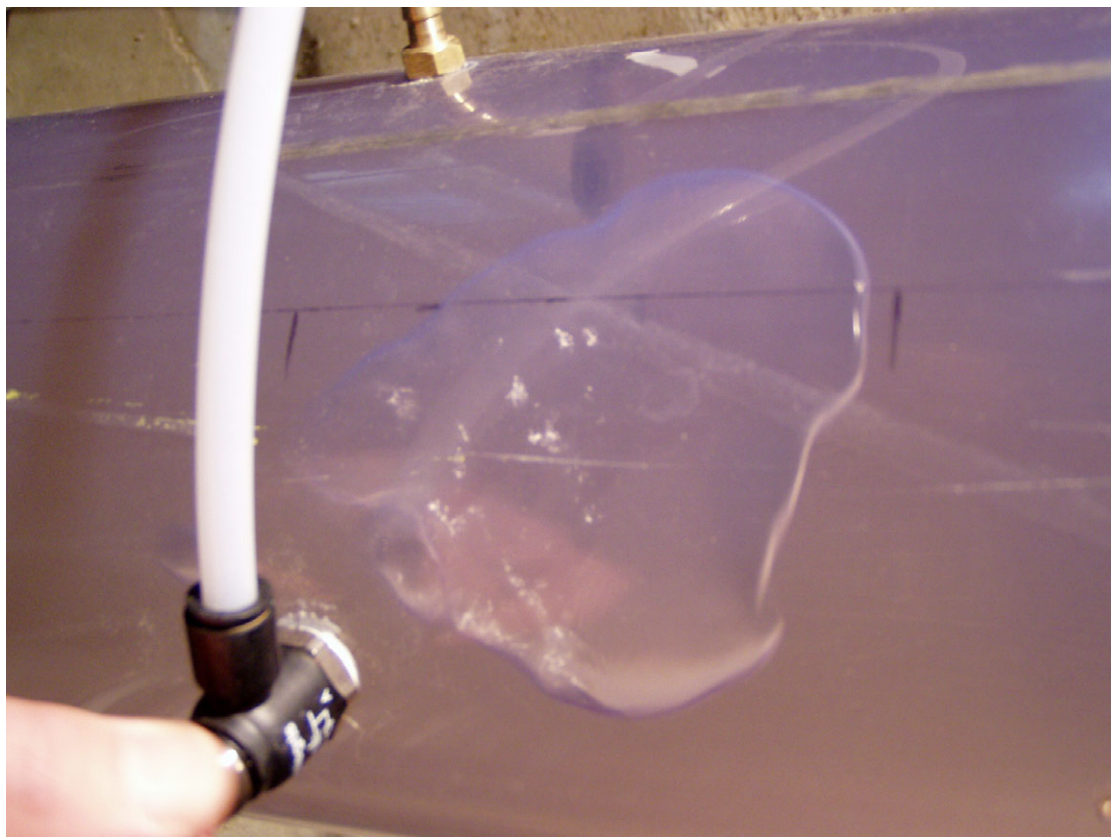


Plate 4 ***Injecting air into the test section***

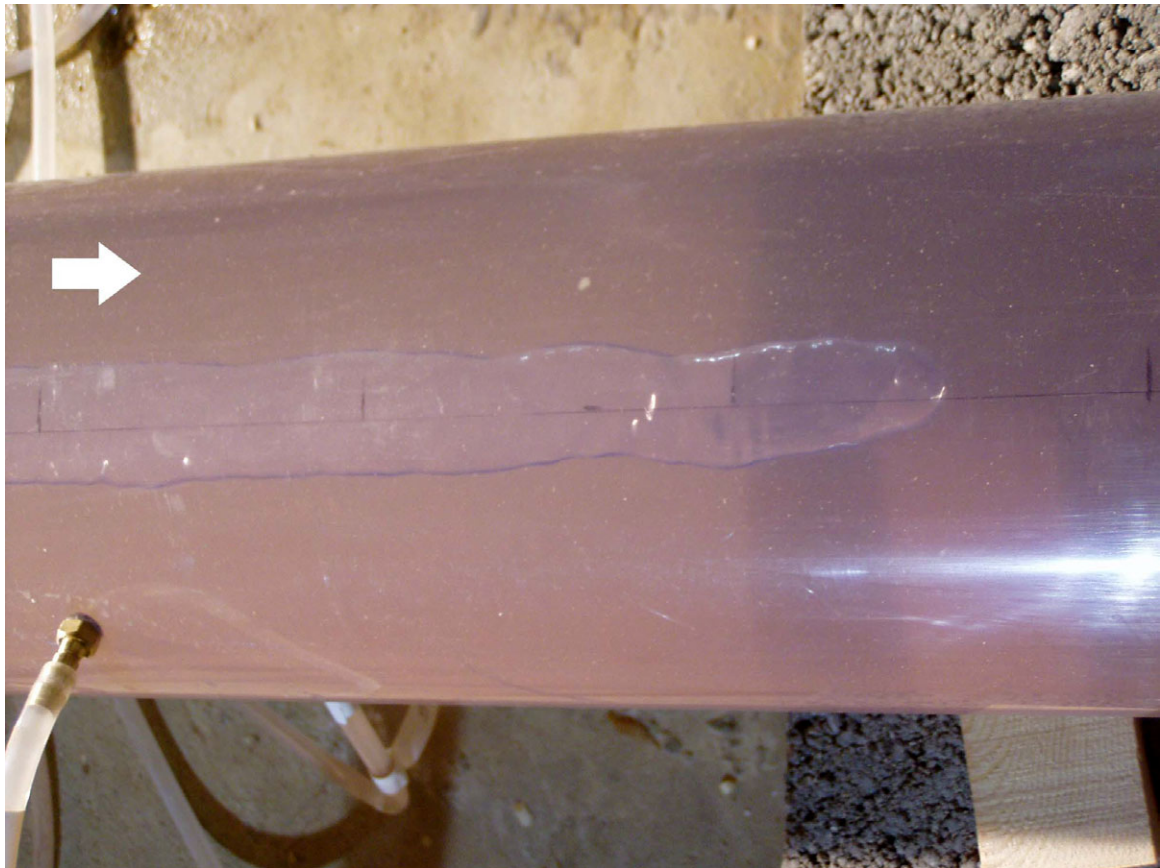


Plate 5 ***Example of elongated air pocket on flat slope***



Plate 6 ***Example of wedge-like air pocket***

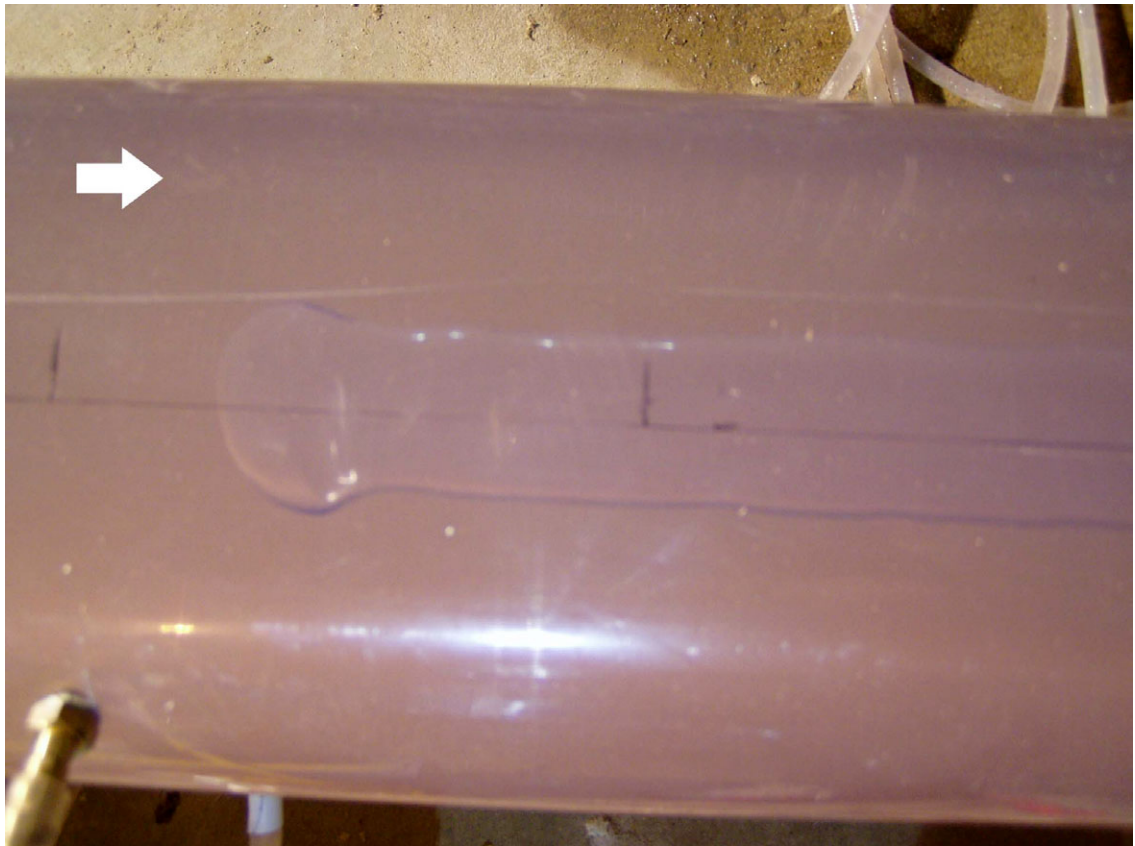


Plate 7 *Flat slope; upstream end of air pocket; top view*

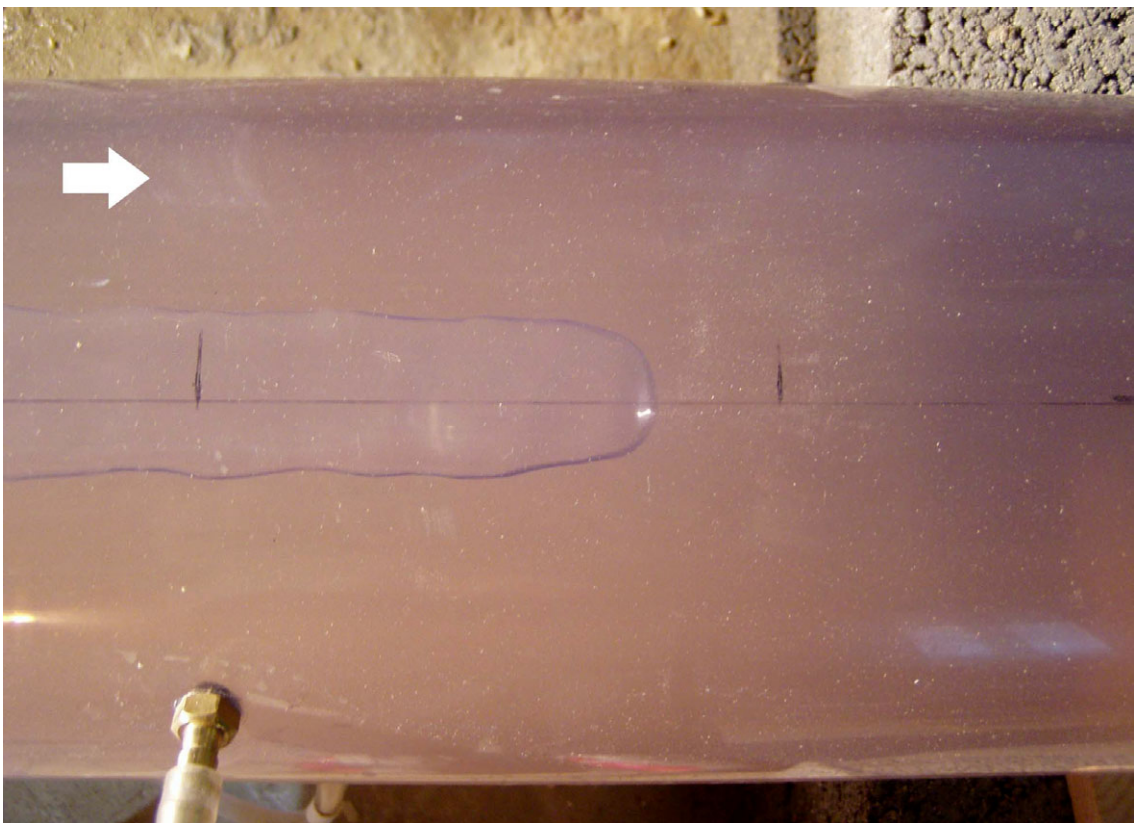


Plate 8 *Flat slope; downstream end; top view*

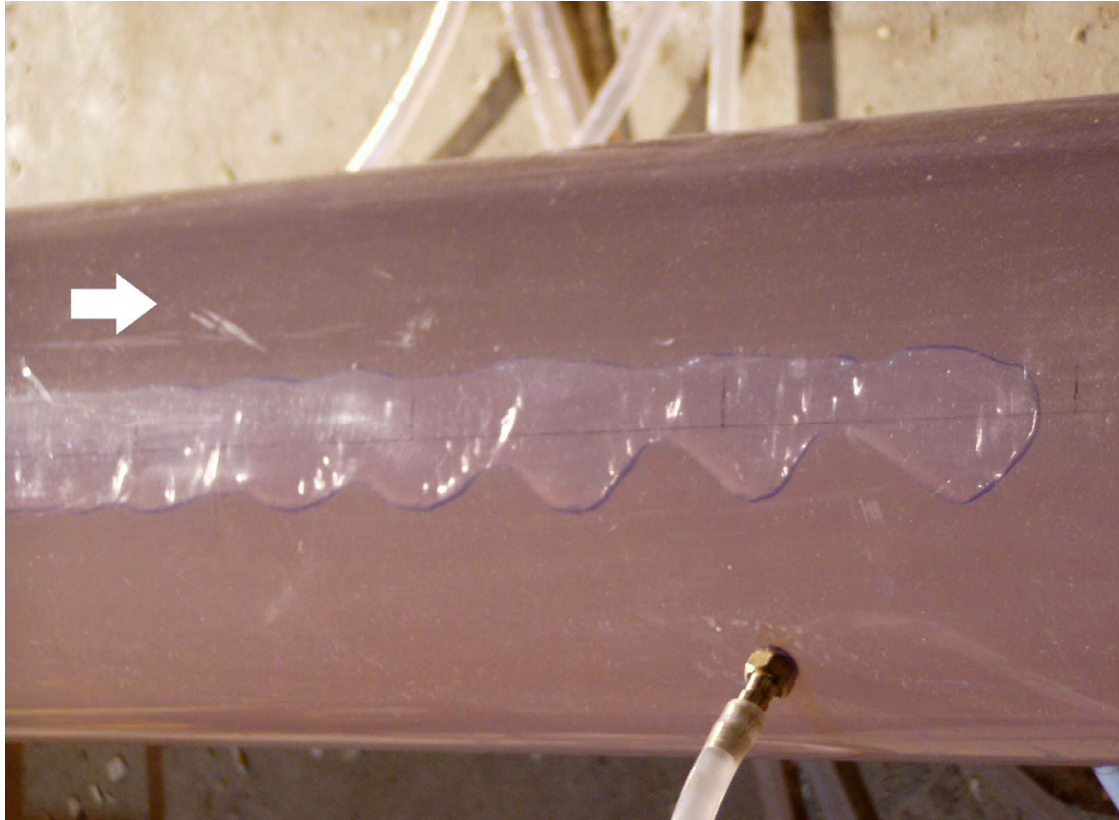


Plate 9 *Flat slope; air pocket at increasing velocity; top view*

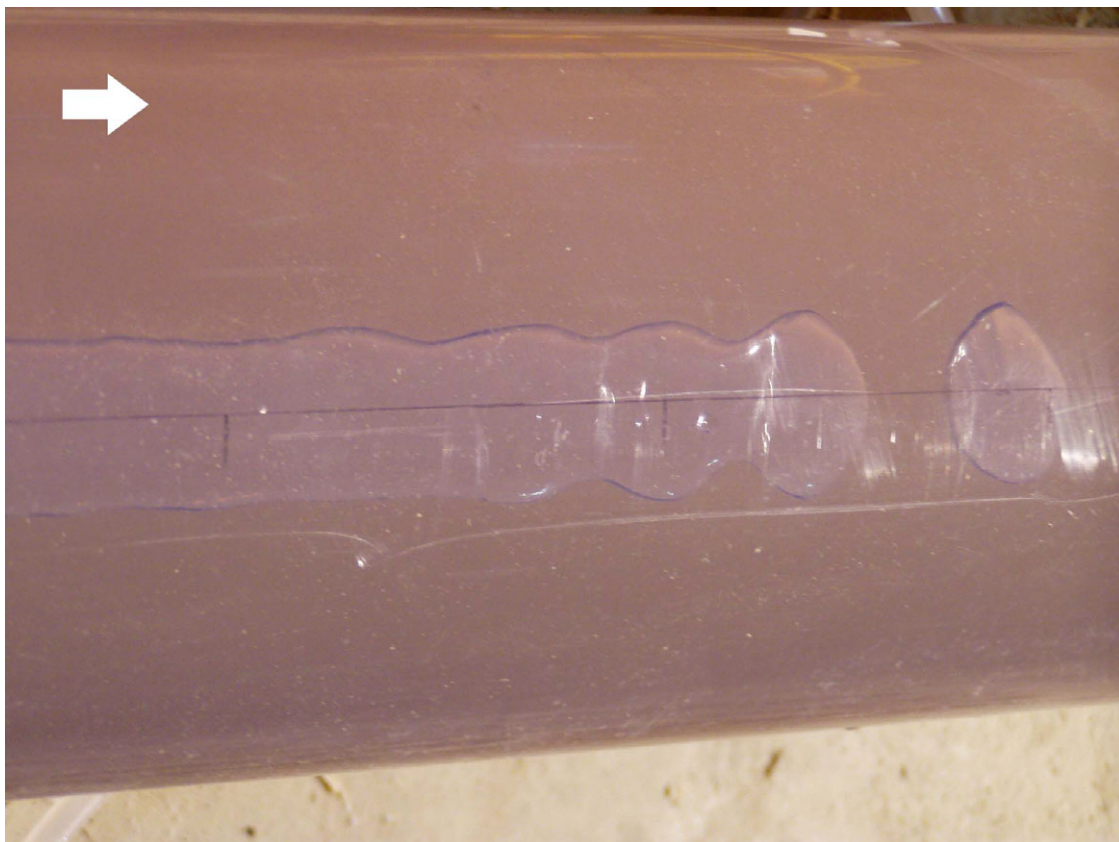


Plate 10 *Flat slope; breaking of air pocket; top view*

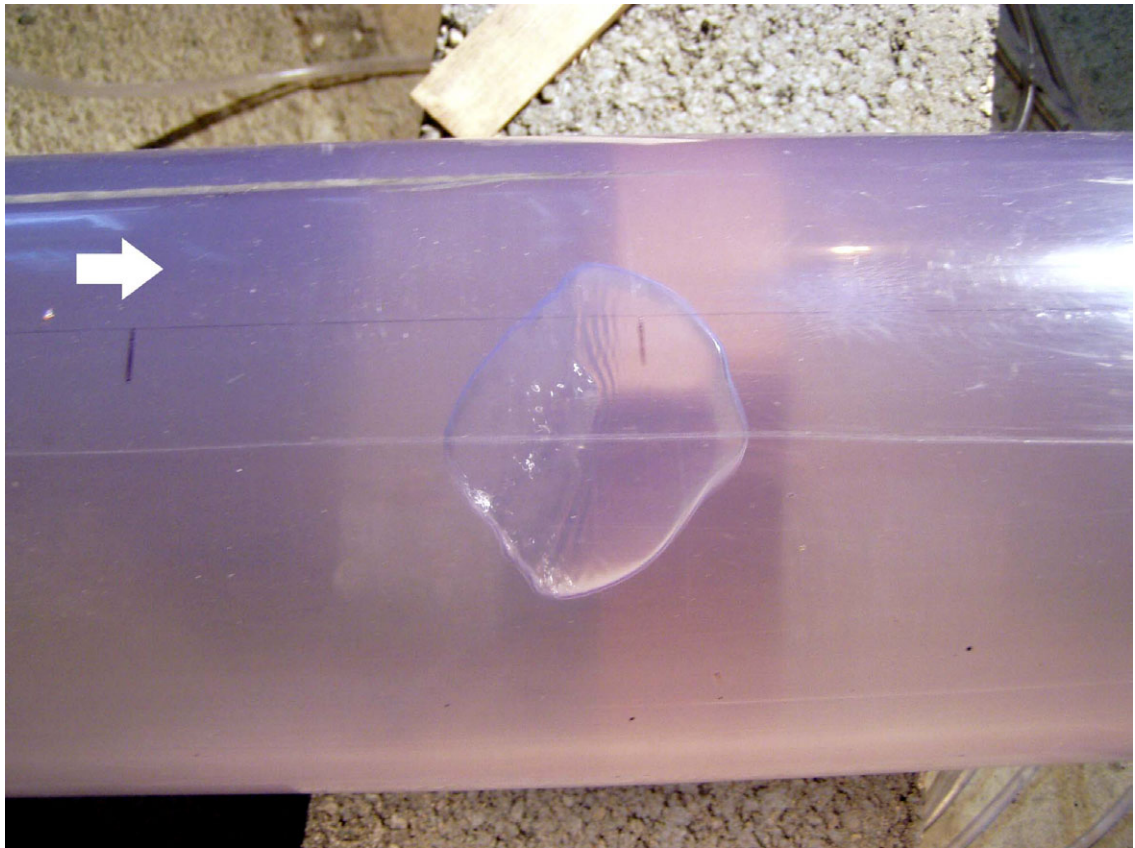


Plate 11 ***6 degree slope; wedge-shape pocket; top view***

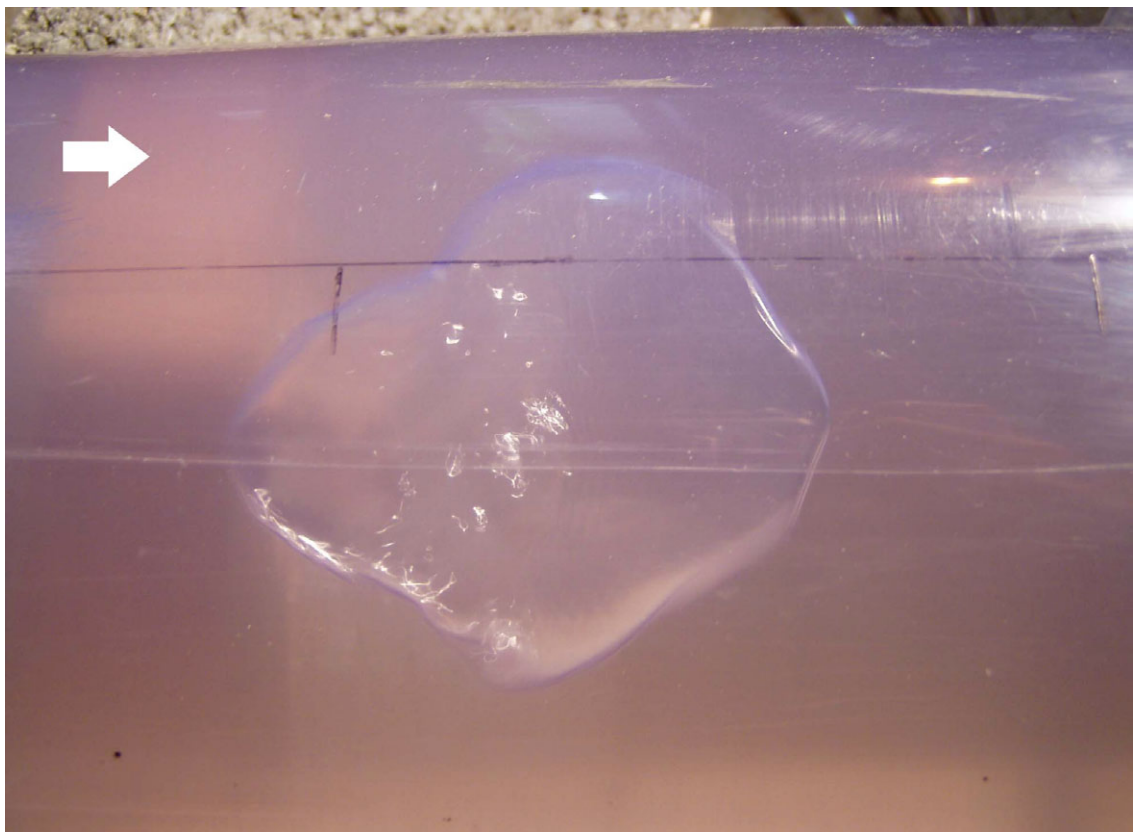


Plate 12 ***6 degree slope; air pocket; top view***



Plate 13 *6 degree slope; air pocket increasing flow*

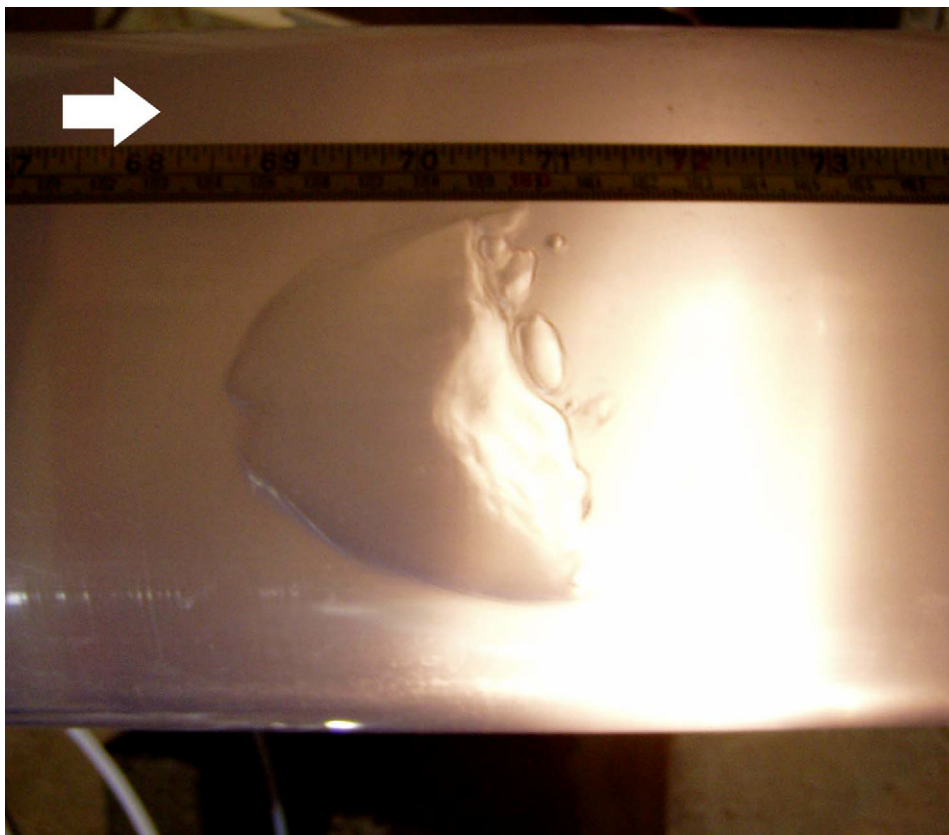


Plate 14 *22.5 degree slope; air pocket*

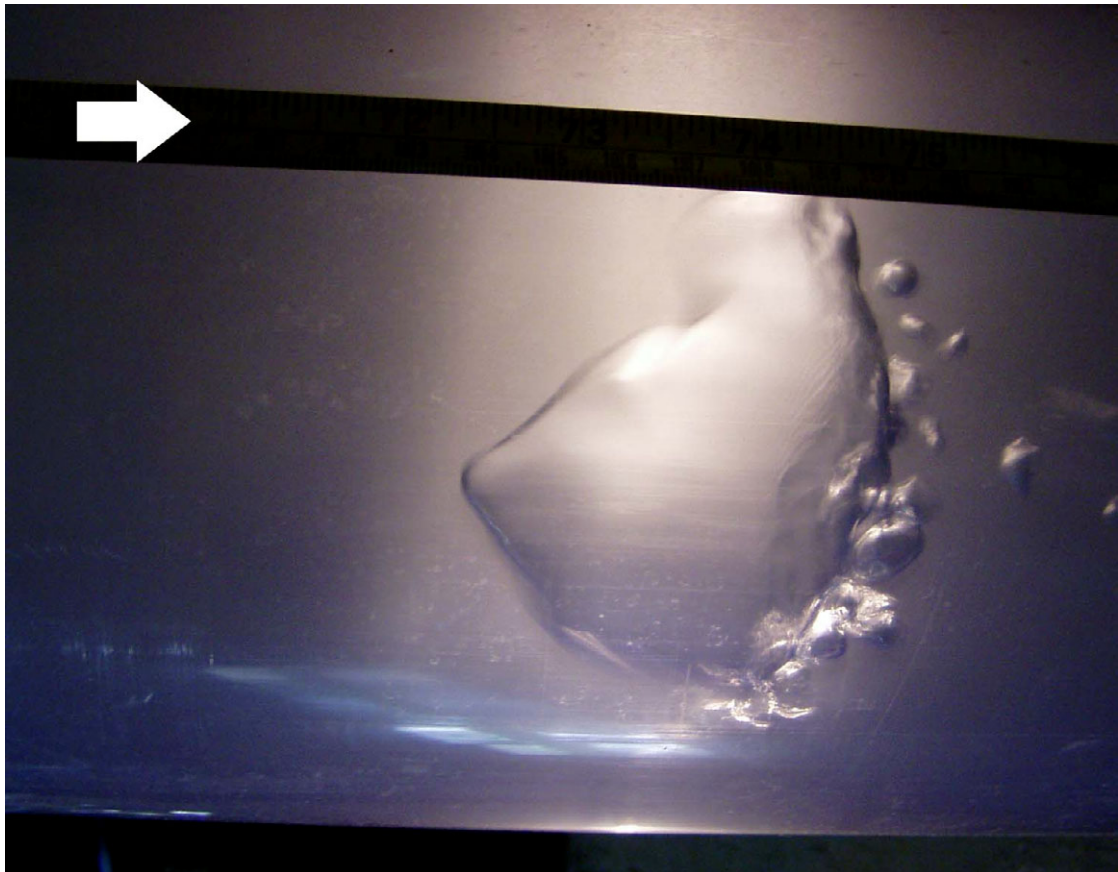


Plate 15 *22.5 degree slope; air pocket breaking*

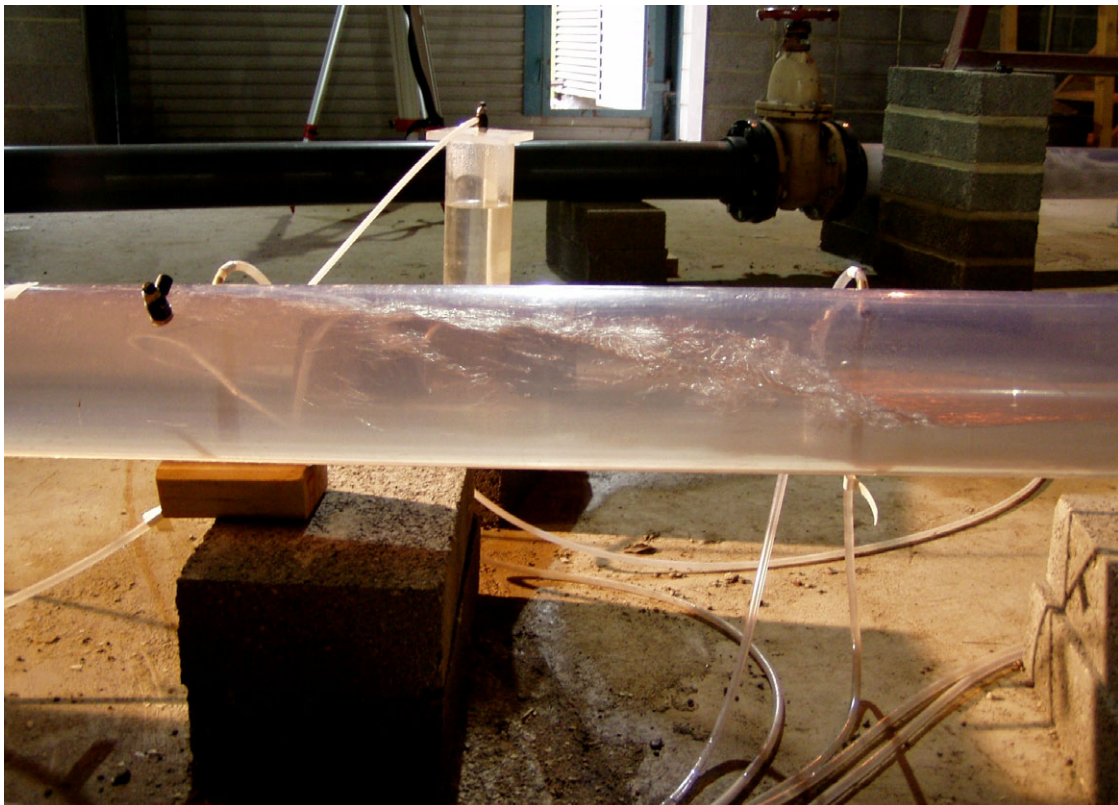


Plate 16 *Test HJ6, 2.5 degrees, side view*

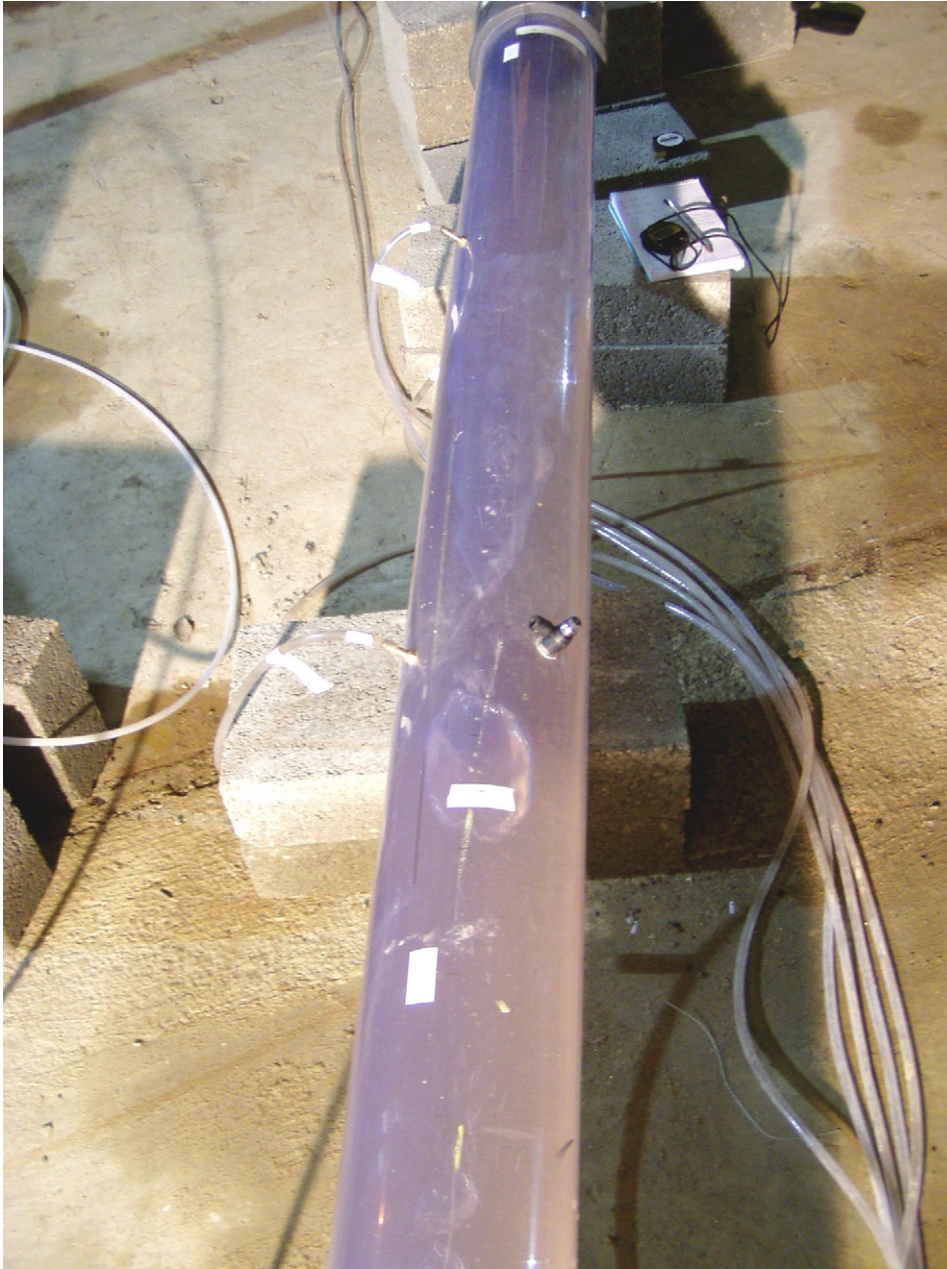


Plate 17 Test HJ6, 2.5 degrees, bubbles coalescing; view from top

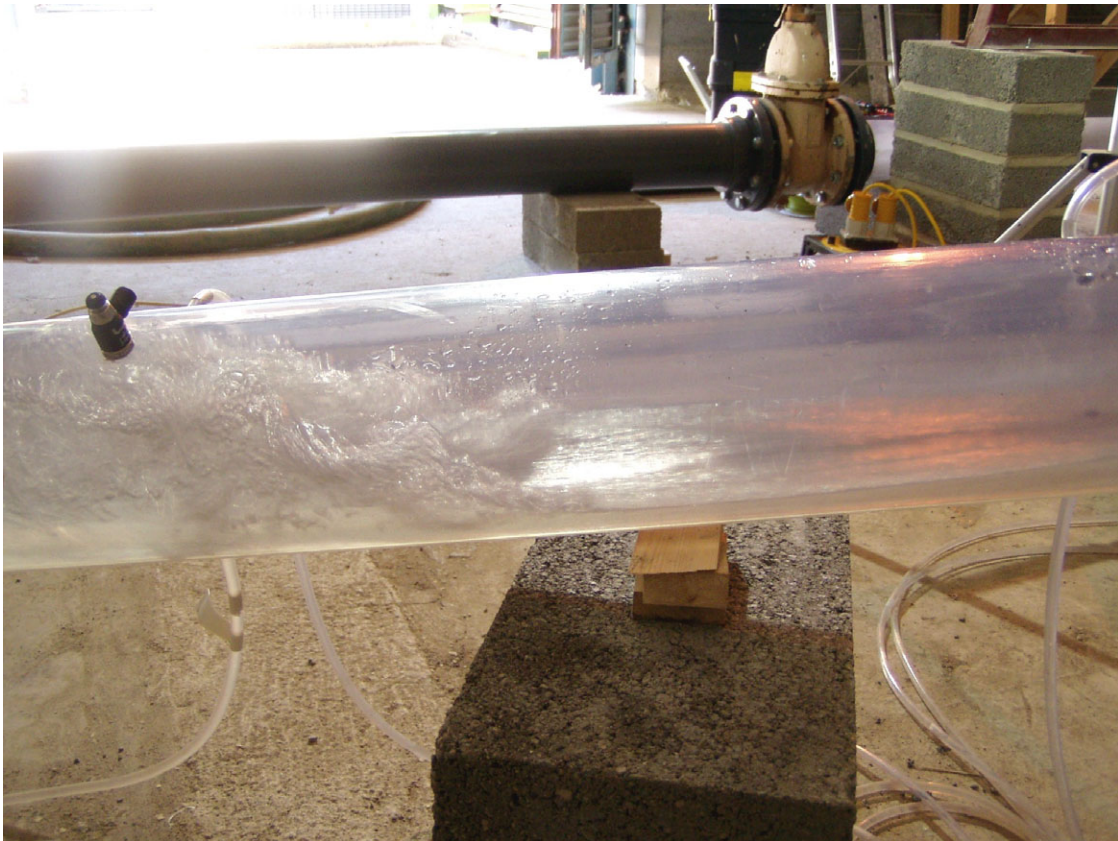


Plate 18 ***Test HJ, 6 degrees; flow 6 l per sec***

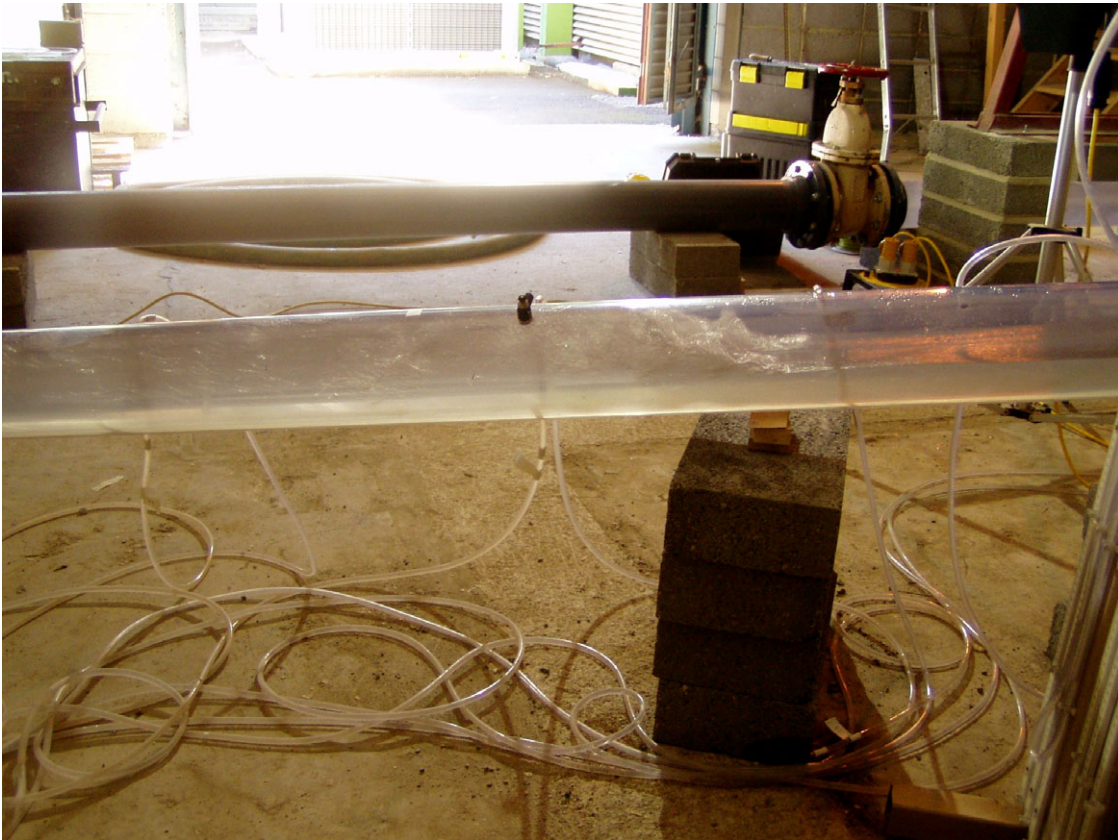


Plate 19 ***Test HJ, 6 degrees; flow 15 l per sec***



Plate 20 Hydraulic jump; 11 degree slope; 18 l per sec